2017

# Understanding patterns and drivers of Alaskan fire-regime variability across spatial and temporal scales

Tyler J. Hoecker
*University of Montana*

# UNDERSTANDING PATTERNS AND DRIVERS OF ALASKAN FIRE-REGIME VARIABILITY ACROSS SPATIAL AND TEMPORAL SCALES

By
TYLER JOHN HOECKER
Bachelor of Arts, Willamette University, Salem, OR, 2011

Thesis
presented in partial fulfillment of the requirements
for the degree of

Master of Science
in Systems Ecology

The University of Montana
Missoula, MT

May 2017

Approved by:

Scott Whittenburg, Dean of The Graduate School

Dr. Philip E. Higuera, Chair
Department of Ecosystem and Conservation Sciences

Dr. Ashley P. Ballantyne
Department of Ecosystem and Conservation Sciences

Dr. Solomon Z. Dobrowski
Department of Forest Management

Dr. Ryan Kelly
Neptune and Company, Inc.

Dr. Carl A. Seielstad
Department of Forest Management

Hoecker, Tyler, M.S., Spring 2017 Systems Ecology

Understanding patterns and drivers of Alaskan fire-regime variability across spatial and temporal scales

Chairperson: Dr. Philip E. Higuera

Boreal forest and tundra ecosystems are globally important because the mobilization of large carbon stocks and changes in energy balance could act as positive feedbacks to ongoing climate warming. In Alaska, wildfire is a key driver of ecosystem structure and function, and therefore fire strongly determines the feedbacks between high-latitude ecosystems and the larger Earth system. The paleoecological record from Alaska reveals the sensitivity of fire regimes to climatic and vegetation change over centennial to millennial time scales, highlighting increased burning with warming and/or increased landscape flammability associated with large-scale vegetation changes.

This thesis focuses on two studies aimed at advancing our understanding of the history and spatiotemporal patterns of fire in Alaskan ecosystems over Holocene time scales (i.e., the past 10,000 years). In Chapter 1, I developed seven lake-sediment records of fire history spanning the past 465 years from CE 1550 to 2015. In Chapter 2 I synthesized 27 published sediment-charcoal records from four Alaskan ecoregions to evaluate variability and synchrony in fire activity over the past 10,000 years. In both chapters, fire history was inferred from interpretations of macroscopic charcoal records from lake sediments.

Biomass burning varied over centennial and millennial time scales within each of the four Alaskan ecoregions. Both biomass burning and fire frequency increased significantly with the expansion of black spruce, c. 4-6 thousand years ago. Biomass burning also increased during the Medieval Climate Anomaly (MCA) in some regions, but results do not indicate prolonged periods of synchronous fire activity among regions. Upper limits to fire synchrony suggest fire-vegetation interaction may provide a negative feedbacks to increased burning. Increases in biomass burning with non-varying fire return intervals suggests an increase in fire severity during warm periods. Over the last century, our records also reveal significant increases in biomass burning.

This research highlights the sensitivity of fire activity to broad-scale environmental change, including climate warming and major shifts in vegetation flammability. The lack of prolonged synchrony and apparent tradeoffs between tree recruitment and biomass burning indicate important vegetation feedbacks that may confer resilience of boreal forests to increased warming and fire activity.

**Acknowledgements**

I would like to acknowledge, with deep gratitude, the guidance, support, and contributions of many individuals and organizations that made this thesis possible. This work was supported by the Paleoecological Observatory Network (PalEON), a multi-institutional program funded by the U.S. National Science Foundation, including grant EF-1241846 to Dr. Philip Higuera. Dr. Higuera supervised the design and implementation of the research, and contributed significantly to the analysis, interpretation, and writing of the manuscripts. Committee members Drs. Ashley Ballantyne, Solomon Dobrowski, Ryan Kelly, and Carl Seielstad significantly improved the work with their feedback during the project proposal and defense. Dr. Ryan Kelly contributed significantly to statistical analyses and interpretation.

The research was conducted at the University of Montana's PaleoEcology and Fire Ecology Lab with assistance from research technicians Andrew Neumann, Kerry Sullivan and Camie Westfall. Field sampling was conducted with Dr. Philip Higuera, Meghan Foard of the University of Idaho, and Alex Shapiro of Alaska Land Exploration. Travel and laboratory support was provided by a graduate research award from the University of Minnesota's National Lacustrine Core Facility. Lab members Kimberley Davis, Lacey Hankin, and Adam Young provided support during analysis and contributed to the interpretation of results. Both chapters relied heavily on data provided by collaborators. Drs. Paul Duffy and Daniel Mann produced the tree demography data used in Chapter 1. Drs. Feng Sheng Hu, Philip Higuera, Ryan Kelly, Melissa Chipman, and Carolyn Barrett-Dash led studies that produced the lake-sediment based fire history data used in Chapter 2.

Dr. Philip Higuera advised my academic program and provided significant personal and professional support throughout. W. A. Franke College of Forestry and Conservation faculty members Drs. Ben Colman and Cory Cleveland provided professional guidance and support. Fellow graduate students in the College and the Systems Ecology Program provided personal and intellectual support. Finally, my family members Jay, Jeanne and Heather Hoecker, and my partner Mathilda Hendin, provided unwavering personal support throughout my program.

## Table of Contents

## List of Figures



## List of Tables

Chapter 2

**Chapter 1**

# Interactions among climate, fire, and vegetation over the last four centuries in an Alaskan interior boreal forest landscape*

**This chapter is written for publication with co-author P.E. Higuera.*

## 1.1 Abstract

The Alaskan boreal forest is part of a globally extensive biome that can significantly influence Earth's climate through changes in carbon storage and large-scale surface energy balance. Understanding the ecological significance of recent changes in the characteristic frequency, extent, and severity of wildfires in the boreal forest requires broader temporal context than observational records can provide. We developed seven fire history records spanning the 465 years (CE 1550-2015) to characterize fire activity in a boreal forest landscape near the Nowitna National Wildlife Refuge in Alaska, USA. We compared patterns in fire timing and biomass burning to existing climate and vegetation datasets from the area to infer how climate and landscape flammability interacted as drivers of past fire activity.

Biomass burning was highest ca. 1625, from 1750-1875, and at present. Fire frequency was also higher over the past 50 years than during any other 50-yr period over the 465-yr record. Mean fire return intervals (mFRI) at individual sites ranged from 25-405 years, with a study-wide average was 120 years. Pulses in tree recruitment ca. 1800, 1850, 1900, and 1950 generally corresponded with low fire activity, and were preceded by high fire activity. Proxies of fire, climate, and vegetation were only weakly correlated before 1900, but after 1900, biomass burning (50-yr trend) was positively correlated with summer temperature ($r = 0.69$, $p < 0.01$, in 50-yr bins), and negatively correlated with black spruce tree establishment ($r = -0.58$, $p < 0.01$).

These results indicate that fire-conducive climatic conditions alone did not appear to facilitate high fire activity. Instead, fire activity was highest when black spruce stands exceeded 100 years old across the landscape and fire-year-mean temperatures were above average. These results support other evidence of that fire-vegetation feedbacks can limit the frequency of fire in high-severity regimes, and they imply that at intermediate spatial scales (100's $km^2$) fire activity is controlled by the combination of landscape flammability and climatic conditions.

**1.2 Introduction**

In Alaskan boreal forests, fire is a primary control of carbon (C) cycling and vegetation dynamics, which in turn drive important feedbacks to the climate system through changes in atmospheric greenhouse gas concentrations and radiative balance (Bonan et al. 1992, Payette 1992, Chapin et al. 2000, Randerson et al. 2006, Bond-Lamberty et al. 2007). Furthermore, by altering soil properties, nutrient cycling and microclimates, and initiating primary succession, high-severity fires drive structural patterns and ecosystem function across North American boreal forests (Johnson 1996, Johnstone et al. 2010a). Evidence of increasing frequency, extent, and severity of wildfire in North American boreal forests has motivated investigation into the relative importance of broad climatic forcing and local ecosystem properties in driving fire activity across the biome (Duffy et al. 2005, Hu et al. 2006, Parisien et al. 2011, Mann et al. 2012). Although the Alaskan boreal forest has sustained high-severity fire regimes for millennia (Lynch et al. 2002, 2004, Hu et al. 2006, Higuera et al. 2009), under directional climate change, fire can catalyze abrupt ecosystem shifts (Crausbay et al. In Press), which in turn could have significant consequences for the resilience of boreal forests to future climate change (Chapin et al. 2004, Johnstone and Chapin 2006, Johnstone et al. 2010b, 2016).

The important role of fire in structuring ecosystem processes in the boreal forest necessitates an accurate characterization of the frequency, severity, and spatial patterning of fire activity over centuries to millennia, and across the biome. Fire activity in the observational record (1950 to present) varies widely across Alaskan boreal forests, with fire rotation periods (FRP, the time to burn an area equal in size to the landscape of interest) ranging from 80 years (yr) in the Yukon Flats region to more than 2000 yr in the Copper River Basin (Kasischke et al. 2002, Young et al. 2017). Evidence also suggests that the extent, frequency, and severity of burning across the boreal forest has generally increased over the past several decades (Kasischke and Turetsky 2006, Kasischke et al. 2010), with statistical models predicting this trend will continue over the coming century in response to projected warming (Balshi et al. 2009, Mann et al. 2012, Young et al. 2017).

Annual area burned in the North American boreal forest is tightly linked to the frequency and duration of blocking high-pressure ridges during summer months, which in turn are linked to atmospheric teleconnections that vary over multi-annual to decadal time scales (e.g., El Nino Southern Oscilllation, Pacific Decadal Oscillation). These climate dynamics control seasonal fuel moisture and fire weather, and thus have strong statistical and mechanistic links to annual area burned (Duffy et al. 2005, Macias Fauria and Johnson 2008). In addition to direct coupling of fire and climate through changes in fuel moisture and ignitions, multi-decadal scale climate impacts fire activity indirectly across a productivity gradient, by determining the abundance of flammable biomass across the landscape (Krawchuk and Moritz 2011, Pausas and Ribeiro 2013). Paleoecological records likewise highlight the importance of vegetation flammability to determine fire activity, highlighted in Alaska by increased fire activity that occurred distinctly with the expansion of flammable black spruce, despite long-term climatic cooling (Lynch et al.

2002, 2004, Higuera et al. 2009). In the eastern Canadian boreal forest, regions with a high proportion of deciduous species burned with less frequency than regions with low proportions of deciduous species, even under the warm conditions that prevailed 6000-3000 yr before present (Girardin et al. 2013). Analyses of more recent fire activity also show complex interactions (feedbacks) between vegetation and fire, where high-severity fires limited subsequent fire activity for decades (Héon et al. 2014, Parks et al. 2015).

Because both climate and vegetation change are slowly varying processes that unfold over decades to centuries, quantifying and understanding fire-regime change requires datasets that encompass appropriately broad temporal scales (Whitlock et al., 2010). Macroscopic charcoal preserved in lake sediment can supplement tree-ring based methods of reconstructing fire history by extending fire reconstructions further into the past. Fire history reconstructions from lake-sediment charcoal ("paleofire records") are particularly well suited to study fire in systems characterized by infrequent, stand-replacing fire-regimes (e.g., boreal forests).

Here, we improve the scope and resolution of fire history in interior Alaskan boreal forests by quantifying fire activity in an approximately 900 $km^2$ landscape over the past 465 years. We compare fire, climate, and vegetation datasets to test two main hypotheses: i) fire activity was positively correlated to summer temperatures, over decadal time scales, because of direct climatic controls on fire activity, including fire-conducive weather and low fuel moisture; ii) periods of widespread burning at the landscape scale drive spatial patterns in vegetation, and are inherently followed by periods of reduced fire activity due to lower fuel connectivity and flammability, irrespective of climate. Our results inform our understanding of the drivers of fire activity at landscape to regional scales, and have important implications for anticipating future fire activity under climate warming.

## 1.3 Methods

To test our hypotheses about the interactions among climate, fire, and vegetation, and characterize the frequency of extensive and synchronous fire activity, we developed seven paleofire records and compared them to stand age reconstructions from 58 forest plots (c. 0.1 ha, Duffy, 2006), reconstructed growing season temperatures from the Gulf of Alaska (Wiles et al. 2014), and modeled summer temperatures at our study sites (SNAP 2015). Our fire-history, tree-ring inferred temperature, and tree-demography data sets span the past 465 and 365 years, respectively, while the modeled summer temperature datasets spans 1900-2005.

### 1.3.1 Study area

Our study area is a boreal forest landscape in interior Alaska, USA, within and around the Nowitna National Wildlife Refuge (NNWR). The NNWR is an 8,500 $km^2$ area approximately 320 km west of Fairbanks, surrounding the Nowitna River, a tributary of the Yukon River to the north, and its adjacent forests, lakes, bogs and floodplains. The study area is in the Kuskokwim Mountains ecoregion (Nowacki et al. 2003); beyond the Nowitna River and floodplain, highly weathered, undulating uplands rise southward towards the Kuskokwim Range. The region experiences a highly continental climate, characterized by long cold winters and short, relatively warm summers. Air temperatures have an average maximum of 19.9° C (min. 11.1° C) in July, and -18.8° C (min. -27.7° C) in January (1942-1993, Galena Airport, 64.733 N, 156.928 W, WRCC).

Vegetation in the region is comprised of both spruce- (*Picea mariana* and *Picea glauca*) and deciduous-dominated (*Populus tremuloides, Betula papyrifera*) forest stands. Tall willow (*Salix* spp.) and *Betula* thrive in recently burned areas, while *Populus* are common on well-drained upland sites. Black spruce thrive in cool, wet low-lying areas, and white spruce form

galleries along riparian corridors. Extensive areas of peat form in poorly drained areas, surrounding lakes, and in river floodplains. The mean fire rotation period from 1950-2009 in Kuskokwim Mountains ecoregion is 191 years, indicating less fire activity in the Kuskokwim Mountains than in the highly flammable Yukon Flats ecoregion (FRP = 82 years), but more than the boreal forest average (FRP = 276 years; Young et al. 2017).

### 1.3.2 Lake-sediment charcoal sampling

We characterized the past 465 yr of fire activity in our study area using a network of seven high-resolution lake-sediment cores collected during a week-long field campaign in June 2015 (Fig. 1). Candidate lakes were identified prior to the field campaign using satellite imagery based on surface area (1-10 ha) and landscape position (upland of the Yukon and Nowitna River floodplains). Candidate lakes were further evaluated in the field from an aircraft for simple, consistent shorelines, and minimal inlet or outlet streams. Lakes were selected for sampling after bathymetric measurements, made with a portable acoustic bathometer, confirmed simple subsurface basin shapes, and water depths of 5-10 m (Table 1).

Surface cores were collected using a 7.6-cm diameter polycarbonate tube fitted with a piston, and the sediment-water interface was preserved by adding sodium polyacrylate prior to shipping. Deeper cores were co-located with (i.e., within several meters of) surface cores and collected with a 5-cm diameter modified Livingstone piston corer. Each sediment core was divided lengthwise and imaged at the University of Minnesota's National Lacustrine Core Facility (LacCore), where one third of each core remains archived. Lake sediments were characterized by alternating laminations of light grey allochthonous silacious silt and dark highly decomposed organic sapropel (gyttja). Laminations approximately 1-5 mm thick were visible in the upper 15-40 cm of sediment before being transitioning to >10 cm-layers of undecomposed

peat and woody organic material mixed with silt and sand. Where peat layers occurred mid-core, the cores terminated with unlaminated silt layers.

Working sections were transported to the University of Montana's PaleoEcology and Fire Ecology Lab, where each core was sliced into continuous 0.25-cm thick sections. Prior to slicing, magnetic susceptibility was measured at 0.25-cm resolution, corresponding to sliced sections, with a MS3 meter and handheld MS2 sensor (Bartington Instruments Ltd., Witney, UK). To quantify macroscopic charcoal concentration, 1-3 $cm^3$ subsamples were taken from each 0.25-cm section and treated with a solution of equal parts 5% sodium metaphosphate and 5% sodium hypochlorite for 24 hours to loosen the sediment and bleach non-charcoal organic material. Each subsample was sieved through a 150-µm sieve, and pieces of macroscopic charcoal were individually identified and counted under a Nikon SMZ645 stereomicroscope at 10-40x magnification (Nikon Instruments Inc. Melville, NY).

### 1.3.3 Chronological control

We developed age-depth models for each core based on radiometrically estimated ages of core sections. Sediment ages for the top 15 cm of each core were estimated from measurements of $^{210}$Pb-activity using the constant-rate-of-supply model (Binford 1990). In some cores, our estimates of background $^{210}$Pb activity (by direct measurement of $^{210}$Po) were corroborated with measurements of $^{226}$Ra, a parent isotope to $^{210}$Pb. Measurements of $^{210}$Pb and $^{226}$Ra activity were obtained from Flett Research Ltd. (Manitoba, Canada; *http://www.flettresearch.ca*). The age of material below 15 cm (approximately >150 yr old) was estimated from accelerated mass spectrometer (AMS) measurements of $^{14}$C in terrestrial macrofossils, bulk sediments, or concentrated charcoal spanning 0.25-1 cm of core. Radiocarbon measurements were made at the Lawrence Livermore National Laboratory's Center for AMS.

The $^{210}$Pb- $^{14}$C-estimated ages were used to develop a model of sediment accumulation rates over the entire length of the core (Fig. 2). We developed age-depth models using the Bacon v2.2 program in R, which uses sample ages and their corresponding depths to model sediment accumulation as a semi-parametric autoregressive gamma process (Blaauw and Christeny 2011, R Core Team 2016). All $^{14}$C ages were converted to calibrated yr before present ("cal yr BP", before CE 1950) in Bacon using the IntCal 13 dataset (Reimer et al. 2013), and are presented in cal yr BP (Fig. 2, Appendix Fig. 1).

We used weak prior distributions of sediment accumulation and segment autocorrelation parameters to inform the age-depth models (Table 2). We constrained sediment accumulation rates to a gamma distribution with a mean of 10 (yr cm$^{-1}$) and a shape (i.e., variance) parameter of 1, and assumed low, positive autocorrelation between discrete 0.5 cm core sections with a memory parameter of 0.1 and memory strength (variance) parameter of 10. We identified depths in each core where distinct changes in a combinations of sediment type, stratigraphy, $^{14}$C dates, and/or charcoal concentration suggested abrupt down-core transitions to high or nearly instantaneous sediment accumulation rates. We modeled these points of transition using the hiatus functionality in Bacon, with a mean length prior of 1 yr, although we do not interpret the transitions themselves as hiatuses.

Bacon uses an MCMC routine to generate thousands of potential distributions of sediment accumulation and sample autocorrelation, and fits age-depth models based on these parameters to dated samples. The estimated (interpolated) age of the core in continuous 0.25-cm segments is derived from the 50$^{th}$ percentile of the simulated ages, and 90% confidence intervals are derived from the 5$^{th}$ and 95$^{th}$ percentiles. We estimated the sediment accumulation rates

associated with every core sample by dividing the difference in each sample's top and bottom depths by the difference in its top and bottom age (cm $yr^{-1}$).

### 1.3.4 Quantifying fire activity

We estimated the charcoal accumulation rate ("CHAR", pieces $cm^{-2}$ $year^{-1}$) of each sample by taking the product of charcoal concentration (pieces $cm^{-3}$) and the estimated sediment accumulation rate (cm $year^{-1}$). CHARs represent variability in the influx of burned organic material to a lake through time, and simulations of charcoal dispersal and comparisons of lake-sediment charcoal to observed fire history indicate that variability in CHAR represents area burned within several km of a lake, while peaks in macroscopic CHAR represent fire occurrence within approximately 500-1000 m of a lake (Higuera et al. 2007, 2011c, Kelly et al. 2013).

CHAR time series that met a minimum ratio of high-frequency "signal" to low-frequency "noise" (Kelly et al. 2011) were statistically decomposed using the CharAnalysis program (version 1.1, *https://github.com/phiguera/CharAnalysis*; Higuera *et al.*, 2009, 2010). Each record was interpolated to a common resolution of 5 yr $sample^{-1}$. Low-frequency ("background") trends were estimated using a 200- or 250-year LOESS regression robust to outliers, and background CHAR was removed by subtraction to obtain a "peak" series, interpreted to represent high-frequency variability due to local fire occurrence and natural variability in charcoal deposition ("noise"). We modeled the noise component of the peak CHAR series using a globally fit Guassian mixture model, and we used the $95^{th}$ or $99^{th}$ percentile of this distribution to identify statistically significant peaks in CHAR. Finally, to avoid identifying peaks based on insignificant changes in charcoal counts, we removed any peaks where charcoal counts had > 5-25% probability of being drawn from the same Poisson distribution as the

minimum count from samples in the preceding 150 yr (Higuera et al. 2010). All parameters are listed in Table 2.

The procedures outlined above produce two forms of fire history information from individual charcoal records: time series of charcoal influx, reflecting trends in biomass burning ("biomass burning") within approximately 10 km of a lake, and a binary time series of charcoal peaks, used to estimate the timing local fire events ("fires"). For each individual record, we calculated fire return intervals ("FRI", the time between consecutive fires at a given lake), the mean FRI ("mFRI"), and fire frequency ("FF"), the total number of fires divided by the length of the record multiplied by 100 (fires per 100 yr). To quantify the degree of synchrony in the timing of fires among records, we calculated the percentage of sites that recorded fire in continuous 50-year windows as the sum of fires in the window divided by the total number of sites recording in that window.

### 1.3.5 Composite record of fire activity

We developed composite records of fire activity from our network of seven lakes, to represent biomass burning and fire occurrence at the scale of our entire study area (c. 900 $km^2$) (Higuera et al. 2011c, Kelly et al. 2013, Calder et al. 2015). For biomass burning, we used the method introduced by Kelly *et al.* (2013), which models CHAR at individual lakes as a zero-inflated log-normal process ("ZIL method"). The ZIL method avoids the Box-Cox transformation of CHAR, and the associated addition of an arbitrary constant to zero values, used by other approaches. The ZIL method thereby reduces the introduction of bias that can accompany these transformation and preserves the natural distribution of CHAR data (log-normal with a high proportion of zero values, Fig. 2). To account for systematic differences in CHAR among individual sites, non-zero accumulation rates were log-transformed, rescaled

within each site to a z-score (mean = 0, standard deviation = 1), and then returned to their original domain through exponentiation. We estimated the parameters of ZIL distributions centered at continuous 5-year time steps using a Gaussian kernel-weighted smoothing function with 5-year and 50-year windows. The index of biomass burning at each time step was the mean of 1000 bootstrapped mean parameter estimates, and 90% confidence intervals were derived from the $5^{th}$ and $95^{th}$ percentiles. The resultant values are a unitless index of landscape-scale biomass burning. In the Yukon Flats region (c. 450 km NE of our study area) empirical evidence indicates that such a composite biomass burning records is well correlated with modern observational record of area burned at distances <10 km from sampled lakes, with maximum agreement within 5 km (Kelly et al. 2013).

### 1.3.6 Tree demography records

We compared composite records of fire history (standardized CHAR and percent of sites burned) to stand-age reconstructions spanning the past 365 yr based on tree-ring records collected near our lake-sediment sites. We used pith dates from 1139 tree cross sections collected in 55 different plots from transects along the Nowitna River in 2002 and 2003 (Duffy 2006), and 66 tree cores from three plots collected during the 2015 field campaign. Tree-ring data are annually resolved in both datasets, but are presented here in five year bins (summarized as the mean count of each species within 5-year intervals from 1550 to 2015).

Records from Duffy (2006) were collected in transects along the Nowitna River, each containing five "nodes." Within each node, cross sections from 3-6 of the largest trees were collected from five plots at the corners and center of a square with 100 m sides. Species were identified in the field, and where multiple species cohorts were present, samples were collected from each species. Cross sections were sanded and annual rings were counted under a 10-40x

stereomicroscope. Pith dates for each sample were estimated from annual ring counts, but were not cross-dated. Records collected in 2015 were taken from variable-radius plots adjacent to sampled lakes. Exact plot locations were randomly located within representative forest patches, and sized such that 20 or more adult trees were sampled. In total, 66 tree cores from three plots were collected, and species were identified in the field. Cores were sanded and annual rings were counted as with the cross sections, but all tree-core samples were visually and statistically cross dated with the computer program COFECHA (Grissino-Mayer 2001).

### 1.3.7 Climate records

To evaluate fire-climate relationships, we compared our fire-history records to empirical and a modeled climate data. Our empirical dataset was a composite reconstruction of annual growing-season air temperature for the past 1200 yr, based on living and subfossil mountain hemlock tree-ring widths near the Gulf of Alaska ("GOA") (Wiles et al. 2014). We selected this dataset because it is an annually resolved temperature record spanning the entirety of our fire-history records. Although dendrochronological records have exhibited non-stationarity in growth-climate relationships under modern warming, the mid-elevation position of these records minimizes this potential divergence of tree-ring response to temperature (Wiles et al. 2014). We converted the original dataset from Wiles et al. (2014) to anomalies relative to the 20$^{th}$ century, in degrees C, to facilitate comparison with other proxies. Because of relatively frequent disturbances and tree mortality in interior Alaska, annually resolved dendrochronological climate records are not available in closer proximity to our sites, and other proxies (i.e., midges) do not provide appropriately fine temporal resolution for this analysis.

We used an additional modeled temperature and precipitation dataset for the 20$^{th}$ century from the Climate Research Unit (Harris et al. 2014), which were statistically downscaled to 2-km

resolution and made publicly available by the Scenarios Network for Alaska and Arctic Planning (SNAP, 2015). We relied on these data for the 20th century because they are from downscaled units that encompass our study area, and are also annually resolved. These data are rigorously validated for accuracy in interior Alaska, but are subject to the potential biases of their modeling and downscaling approaches. Here we present the 5-year anomaly of mean June, July and August temperature, averaged over all of the units covering our study area.

### 1.3.8 Evaluating relationships among proxies

To test our hypotheses about the relationships among fire, climate, and vegetation, we quantified correlations between fire history and tree demography, and between fire history and temperature records before and after 1900. All sources of tree and temperature data were summarized into 5-year mean values for continuous, non-overlapping time steps corresponding to interpolated fire history data. We calculated pairwise Pearson product-moment correlation coefficients and associated measures of significance (p-values) among biomass burning, percent of sites burned, tree establishment (75% *Picea mariana*), and temperature anomalies from the GOA for the period 1550 – 1895, and among biomass burning, percent of sites burned, tree establishment, and modeled temperature and precipitation records between 1900 and 2005.

## 1.4 Results

### 1.4.1 Chronological control

Background $^{210}$Pb activity was reached in the upper 3-10 cm of sediment in all cores, except for Nodwell Lake (where above-background decay was sufficient to estimate sample ages). Radiocarbon ages of bulk sediments were generally thousands of yr older than of terrestrial macrofossils or concentrated charcoal, suggesting the incorporation of "ancient" carbon into the lake sediments; thus, these samples were not used in our age-depth models. (Fig.

2). Complex down-core sedimentation prevented us from developing robust chronologies for the entire length of sampled material collected, but high-resolution records were obtained from the upper 16-40 cm of material. Multiple sources of evidence, including $^{14}C$ dates, visible changes in sedimentation, and abrupt changes in proxies allowed us to confidently identify abrupt transitions in sedimentation rates, and model them with separate sediment accumulation-rate parameters above and below the transition (Appendix Figs. 1-7). The median sample resolution of our records ranged from 2-15 cm $year^{-1}$, yielding seven high-resolution records extending to 222-1046 yr BP (Table 2). Uncertainty around age estimates (i.e., 90% confidence intervals) ranged from 4 yr in the upper portion of cores to >300 yr for some ages older than 400 yr BP (prior to 1550 CE). The median range of the 90% confidence interval from among all samples and all cores was 95 yr.

**1.3.2 Fire history**

Here we present records from CE 1550-2015, a period covered by a majority of the records we developed in the study area, and where chronological uncertainty is relatively low (Fig. 3). Charcoal concentrations and charcoal accumulation rates (CHAR) from 1550-2015 ranged (mean, standard deviation) from 0 – 41.67 pieces $cm^{-3}$ (2.40, 4.54), and 0 – 3.82 pieces $cm^{-2}$ $yr^{-1}$ (0.11, 0.27) among all lakes, respectively (Fig. 3). The signal-to-noise index for the period of analysis in all seven records averaged 9.8 (range 3.3-14.2), indicating their suitability for charcoal peak analysis (Kelly et al. 2011). Peak analysis revealed 1 – 6 statistically significant CHAR peaks at each site since 1550 CE. Fire return intervals (FRI) varied substantially within and among sites, ranging from 25 – 405 yr (Table 3). The site-specific mFRI (standard deviation) ranged from 50 – 265 yr (10 – 85; Fig. 3). The overall mFRI when pooling FRIs from all sites was 116 yr (37). The percentage of sites burned in any 50-year period ranged

from 0 – 100%, with maxima centered around ca. CE 1665, 1710, 1800, 1855, 1985 and 1990. The highest percentage of sites burned since 1550, 100%, was in the 50-yr period centered on 1985 (i.e., 1965-2015).

Our composite biomass burning record (standardized CHAR) displays substantial variability over the last 475 yr, with maxima in the 100-year mean ca. CE 1640, 1785, 1865 and 2015, and relatively distinct peaks in the 5-yr mean centered at ca. CE 1640, 1765, 1845, 1945 and 2005. The average (standard deviation) time between these maxima in the 5-yr mean was 91 (27) yr.

### 1.4.3 Tree demography

Estimated tree pith dates ranged from 1650 – 1996 CE, and include five species (number, % of total) (*Picea mariana* (788, 65%)*, Picea glauca* (151, 13%)*, Larix laricina* (50, 4%), *Betula papyrifera* (215, 18%)*,* and *Populus tremuloides* (1, 0.1%)). Over 65% of the trees sampled had pith dates between 1900 and 1975. The combined age structure contains seven relatively distinct modes, interpreted as pulses of tree recruitment, ca. CE 1650, 1720, 1800, 1840, 1900, 1950, and 1990 (Fig. 4C). The average interval between these modes was 57 yr (standard deviation 16 yr). We interpret the tree-ring record cautiously, assuming that tree mortality limits our ability to directly compare the magnitude of distinct pulses in tree recruitment, particularly prior to ca. 1900.

### 1.4.4 Comparison among proxies

The relationships among fire, vegetation, and climate proxies differed between time periods. Measures of fire activity were positively correlated with tree establishment before 1900, but had negative or insignificant relationships after 1900. Measures of fire activity and temperature had insignificant relationships before 1900, but were positively correlated after

1900. For the period 1650-1895, 50-year mean composite biomass burning and percent sites burned were both positively correlated with tree establishment ($r = 0.58$, $p = <0.00001$ and $r = 0.44$, $p = 0.001$, respectively) (Table 4). During the 20th century (1900-2005), however, all measures of fire activity were positively correlated with modeled temperature, but there was a negative correlation between fire activity and tree establishment (Table 5). There was a strong positive relationship between modeled temperature and 50-year mean composite biomass burning ($r = 0.69$ at $p < 0.001$), and between 5-year mean composite biomass burning and CRU temperature ($r = 0.43$ and $p = 0.05$). The relationship between 50-year mean composite biomass burning and tree establishment from 1900-2005 was strongly negative ($r = -0.58$, $p < 0.00001$).

In addition to significant correlations among measures of fire activity, temperature, and tree establishment during the 20th century, there were clear qualitative relationships between fire, climate, and vegetation proxies. Periods of high fire activity, reflected in 5- and 50-year mean composite biomass burning and high percent sites burned, appear to proceed pulses in tree establishment. In particular, the nadir in percent sites burned and biomass burning from ca. 1900-1950 corresponds with the most clearly detected pulse in tree establishment in our record ca. 1950.

**1.5 Discussion**

The relationship between climate and fire activity varied over the past 465 years, and was likely mediated by landscape-scale changes in flammability resulting from black spruce dominance and succession. Our records showed tighter coupling between fire activity and temperature after ca. 1900 than in the preceding 350 years, increased burning under warm 20th-century temperatures, and elevated fire activity following landscape-scale black spruce dominance. High agreement between our lake-sediment fire history records and observed fire

events since 1950 further validate the ability of high-resolution proxy fire history records to accurately characterize fire activity over centennial timescales.

Our records document coupling between climate and fire activity throughout the study period, but the relationship between high rates of burning and warm temperatures was strongest after 1900. Periods of elevated biomass burning ca. 1625, 1725, 1800, and 1850 coincided with positive temperature anomalies, consistent with the expectation that warm temperatures would facilitate burning through low fuel moisture (Duffy et al. 2005, Flannigan et al. 2009, Parisien et al. 2011). Although these short periods of high fire activity before 1900 appear to correspond with relatively warm temperatures, the link between climate and fire activity was not consistent through time: temperatures were cooler than average during a peak in biomass burning ca. 1750, and the relationship between fire activity and temperature was statistically insignificant from 1550-1895. However, the lack of correlation between the paleoclimate record and our composite record of biomass burning does not necessarily imply individual years with high fire activity were not facilitated by warm, dry conditions. By averaging the paleoclimate record over five-year periods to align with lake-sediment fire history records, we inherently smooth over annual variability, thus reducing the ability to detect annual-scale relationships.

The strongest evidence for tight coupling between climate and fire activity comes after 1900, when both fire activity and summer temperatures increased distinctly, and were thus positively correlated. The significant increases in biomass burning and percent of sites burned that began ca. 1900 coincides with an increase in local modeled temperatures, which were above average for much of the 20$^{th}$ century, particularly after 1975. Biomass burning and percent sites burned both reached their highest points of the last 465 years in the decades since 1980, consistent with other evidence of recent increases in fire activity based on shorter observational

records (Kasischke and Turetsky 2006, Kasischke et al. 2010). The peak in fire activity ca. 1800 was characterized by a percent sites burned similar to the peak in fire activity ca. 1980 (80% ca. 1800 vs. 100% ca. 1980), but with significantly lower biomass burning. Greater biomass burning per fire event could indicate an increase in fire severity under warm 20th century conditions, which has been documented elsewhere in the boreal forest (Shenoy et al. 2011, Mann et al. 2012), and during the warm Medieval Climate Anomaly ca. CE 1000 – 1500 (Kelly et al. 2013).

The widespread burning we observed under average and above-average temperatures was likely mediated by the landscape-scale dominance and succession of black spruce during the 20th century. Even after 1900, when the fire-climate relationship in our study area was strongest, significant relationships between fire activity and vegetation suggest that variability in landscape-scale fire activity was driven by complex interactions with climate and vegetation, rather than unidirectional forcing by either independently. Periods of elevated biomass burning and high fire synchrony (high percent sites burned) generally preceded pulses in tree establishment, and establishment was likewise highest during periods with low fire activity (Fig. 4). At multi-decadal, landscape scales, fire activity is facilitated and attenuated by variability in fire-conducive climatic conditions as well as the structure and flammability of vegetation on the landscape (Girardin et al. 2013, Héon et al. 2014). The substantial increase in fire activity since 1950 documented here was likely facilitated by the large pulse in black spruce establishment ca. 1900-1950, creating a mosaic of late-successional, highly flammable fuels suitable for widespread burning. The late 20th century increase in fire activity in this study area were, therefore, probably the result of vegetation dynamics and climate variability operating synergistically to promote extensive fire activity. Empirical and model-based evidence from elsewhere in the boreal forest document a similar pattern, where the combination of late-

successional black spruce dominance and consistently warm 20th-century temperatures have resulted in increased fire frequency and severity (Mann et al. 2012), with subsequent impacts on successional trajectories and species composition (Johnstone and Chapin 2006, Johnstone et al. 2010b, Shenoy et al. 2011, Brown and Johnstone 2012). If these widespread fire-regime changes continue to be observed across the boreal forest, they could initiate an ecosystem state transition from a black spruce-dominated to a deciduous-dominated forest in interior Alaska.

These connections between the timing of widespread fire activity and landscape-scale tree recruitment also support modern observations of the bi-directional feedbacks between fire activity, post-fire vegetation, and subsequent fire activity. Fires not only drive landscape-scale heterogeneity in stand ages, but because boreal forest species vary widely in their flammability, their relative proportions and arrangement on the landscape modify the impact of climate (Dash et al. 2016). Particularly when climatic conditions are not extreme, the spatial patterning of vegetation can have a large impact on fire spread (Turner and Romme 1994). Elevated landscape-scale fire activity can reset successional trajectories (i.e., initiating a shift from black spruce to deciduous species) and stand ages, thereby reducing landscape flammability (Parks et al. 2015, 2016). Post-fire vegetation patterns and composition can limit the extent and magnitude of fire activity in the proceeding centuries (Ali et al. 2009, Girardin et al. 2013, Héon et al. 2014). Although such a shift would reduce fire activity in the near term (decades to centuries), it could promote synchronous fire activity in the future, if large areas of deciduous-dominated stands follow a trajectory or relay succession and transition back to black spruce dominance.

The potentially self-limiting nature of fire through negative feedbacks with vegetation may explain the weak correlation between fire and climate in our study area before 1900. These results do not contradict evidence of strong climatic control of fire at inter-annual, biome-wide

scales (Duffy et al. 2005). Instead, they provide additional evidence that fire-climatic relationships are mediated by landscape-scale patterns of vegetation. Our study does not predict how these feedbacks scale to the larger boreal forest, which has yet to exhibit broad-scale fuel limitation. However, it supports the notion that forested landscapes are a dynamic mosaic of vegetation states with components that do not move uniformly in response to climatic forcing.

## 1.6 References


Ali, A. A., C. Carcaillet, and Y. Bergeron. 2009. Long-term fire frequency variability in the eastern Canadian boreal forest: The influences of climate vs. local factors. Global Change Biology 15:1230–1241.

Balshi, M. S., A. D. McGuire, P. Duffy, M. Flannigan, J. Walsh, and J. Melillo. 2009. Assessing the response of area burned to changing climate in western boreal North America using a Multivariate Adaptive Regression Splines (MARS) approach. Global Change Biology 15:578–600.

Binford, M. W. 1990. Calculation and uncertainty analysis of 210Pb dates for PIRLA project lake sediment cores. Journal of Paleolimnology 3:253–267.

Blaauw, M., and J. A. Christeny. 2011. Flexible paleoclimate age-depth models using an autoregressive gamma process. Bayesian Analysis 6:457–474.

Bonan, G. B., D. Pollard, and S. L. Thompson. 1992. Effects of boreal forest vegetation on global climate. Nature 359:716–718.

Bond-Lamberty, B., S. D. Peckham, D. E. Ahl, and S. T. Gower. 2007. Fire as the dominant driver of central Canadian boreal forest carbon balance. Nature 450:89.

Brown, C. D., and J. F. Johnstone. 2012. Once burned, twice shy: Repeat fires reduce seed availability and alter substrate constraints on Picea mariana regeneration. Forest Ecology and Management 266:34–41.

Calder, W. J., D. Parker, C. J. Stopka, G. Jiménez-Moreno, and B. N. Shuman. 2015. Medieval warming initiated exceptionally large wildfire outbreaks in the Rocky Mountains. Proceedings of the National Academy of Sciences of the United States of America 112:13261–13266.

Chapin, F. S., T. V Callaghan, Y. Bergeron, M. Fukuda, J. F. Johnstone, G. Juday, and S. A. Zimov. 2004. Global Change and the Boreal Forest: Thresholds, Shifting States or Gradual Change? AMBIO: A Journal of the Human Environment 33:361–365.

Chapin, F. S., A. D. Mcguire, J. Randerson, R. Pielke, D. Baldocchi, S. E. Hobbie, N. Roulet, W. Eugster, E. Kasischke, E. B. Rastetter, S. A. Zimov, and S. W. Running. 2000. Arctic and boreal ecosystems of western North America as components of the climate system. Global Change Biology 6:211–223.

Crausbay, S. D., P. E. Higuera, D. G. Sprugel, and L. B. Brubaker. 2017. Fire catalyzed rapid ecological change in lowland coniferous forests of the Pacific Northwest over the past 14,000 years. Ecology:doi:10.1002/ecy.1897.

Dash, C. B., J. M. Fraterrigo, and F. S. Hu. 2016. Land cover influences boreal-forest fire responses to climate change: geospatial analysis of historical records from Alaska. Landscape Ecology 31:1781–1793.

Duffy, P. A. 2006. Interactions among climate, fire, and vegetation in the Alaskan boreal forest. Department of Forest Sciences, University of Alaska, Fairbanks:Ph.D. Dissertation 143 pp.

Duffy, P. A., J. E. Walsh, J. M. Graham, D. H. Mann, and T. S. Rupp. 2005. Imapcts of Lage-Scale Atmospheric–Ocean Variability on Alaskan Fire Season Severity. Ecological Applications 15:1317–1330.

Flannigan, M., B. Stocks, M. Turetsky, and M. Wotton. 2009. Impacts of climate change on fire activity and fire management in the circumboreal forest. Global Change Biology 15:549–560.

Girardin, M. P., A. A. Ali, C. Carcaillet, O. Blarquez, C. Hély, A. Terrier, A. Genries, and Y. Bergeron. 2013. Vegetation limits the impact of a warm climate on boreal wildfires. New Phytologist 199:1001–1011.

Grissino-Mayer, H. D. 2001. Evaluating crossdating accuracy: a manual and tutorial for the computer program COFECHA. Tree-ring research 57:205–221.

Harris, I., P. D. Jones, T. J. Osborn, and D. H. Lister. 2014. Updated high-resolution grids of monthly climatic observations–the CRU TS3. 10 Dataset. International Journal of Climatology 34:623–642.

Héon, J., D. Arseneault, and M.-A. Parisien. 2014. Resistance of the boreal forest to high burn rates. Proceedings of the National Academy of Sciences of the United States of America 111:13888–13893.

Higuera, P. E., L. B. Brubaker, P. M. Anderson, F. S. Hu, and T. A. Brown. 2009. Vegetation mediated the impacts of postglacial climate change on fire regimes in the south-central Brooks Range, Alaska. Ecological Monographs 79:201–219.

Higuera, P. E., D. G. Gavin, P. J. Bartlein, and D. J. Hallett. 2010. Peak detection in sediment-charcoal records: Impacts of alternative data analysis methods on fire-history interpretations. International Journal of Wildland Fire 19:996–1014.

Higuera, P. E., M. E. Peters, L. B. Brubaker, and D. G. Gavin. 2007. Understanding the origin and analysis of sediment-charcoal records with a simulation model. Quaternary Science Reviews 26:1790–1809.

Higuera, P. E., C. Whitlock, and J. A. Gage. 2011. Linking tree-ring and sediment-charcoal records to reconstruct fire occurrence and area burned in subalpine forests of Yellowstone National Park, USA. The Holocene 21:327–341.

Hu, F. S., L. B. Brubaker, D. G. Gavin, P. E. Higuera, J. A. Lynch, T. S. Rupp, and W. Tinner. 2006. How Climate and Vegetation Influence the fire Regime of the Alaskan Boreal Biome: The Holocene Perspective. Mitigation and Adaptation Strategies for Global Change 11:829–846.

Johnson, E. A. 1996. Fire and vegetation dynamics: studies from the North American boreal forest. Cambridge University Press.

Johnstone, J. F., C. D. Allen, J. F. Franklin, L. E. Frelich, B. J. Harvey, P. E. Higuera, M. C. Mack, R. K. Meentemeyer, M. R. Metz, G. L. W. Perry, T. Schoennagel, and M. G. Turner. 2016. Changing disturbance regimes, ecological memory, and forest resilience. Frontiers in Ecology and the Environment 14:369–378.

Johnstone, J. F., and F. S. Chapin. 2006. Fire interval effects on successional trajectory in boreal forests of northwest Canada. Ecosystems 9:268–277.

Johnstone, J. F., F. S. Chapin, T. N. Hollingsworth, M. C. Mack, V. Romanovsky, and M. Turetsky. 2010a. Fire, climate change, and forest resilience in interior Alaska. Canadian Journal of Forest Research 40:1302–1312.

Johnstone, J. F., T. N. Hollingsworth, F. S. Chapin, and M. C. Mack. 2010b. Changes in fire regime break the legacy lock on successional trajectories in Alaskan boreal forest. Global Change Biology 16:1281–1295.

Kasischke, E. S., and M. R. Turetsky. 2006. Recent changes in the fire regime across the North American boreal region—spatial and temporal patterns of burning across Canada and Alaska. Geophysical Research Letters 33:doi:10.1029/2006GL025677.

Kasischke, E. S., D. L. Verbyla, T. S. Rupp, A. D. McGuire, K. A. Murphy, R. Jandt, J. L.

Barnes, E. E. Hoy, P. A. Duffy, M. Calef, and M. R. Turetsky. 2010. Alaska's changing fire regime — implications for the vulnerability of its boreal forests. Canadian Journal of Forest Research 40:1313–1324.
Kasischke, E. S., D. Williams, and D. Barry. 2002. Analysis of the patterns of large fires in the boreal forest region of Alaska. International Journal of Wildland Fire 11:131–144.
Kelly, R., M. L. Chipman, P. E. Higuera, I. Stefanova, L. B. Brubaker, and F. S. Hu. 2013. Recent burning of boreal forests exceeds fire regime limits of the past 10,000 years. Proceedings of the National Academy of Sciences of the United States of America 110:13055–13060.
Kelly, R. F., P. E. Higuera, C. M. Barrett, and F. S. Hu. 2011. A signal-to-noise index to quantify the potential for peak detection in sediment–charcoal records. Quaternary Research 75:11–17.
Krawchuk, M. A., and M. A. Moritz. 2011. Constraints on global fire activity vary across a resource gradient. Ecology 92:121–132.
Lynch, J. A., J. S. Clark, N. H. Bigelow, M. E. Edwards, and B. P. Finney. 2002. Geographic and temporal variations in fire history in boreal ecosystems of Alaska. Journal of Geophysical Research 108:1–17.
Lynch, J. A., J. L. Hollis, and F. S. Hu. 2004. Climatic and landscape controls of the boreal forest fire regime: Holocene records from Alaska. Journal of Ecology 92:477–489.
Macias Fauria, M., and E. . Johnson. 2008. Climate and wildfires in the North American boreal forest. Philosophical Transactions of the Royal Society B: Biological Sciences 363:2315–2327.
Mann, D. H., T. Scott Rupp, M. A. Olson, and P. A. Duffy. 2012. Is Alaska's boreal forest now crossing a major ecological threshold? Arctic, Antarctic, and Alpine Research 44:319–331.
Nowacki, G. J., P. Spencer, M. Fleming, T. Brock, T. Jorgenson, and S. Geological. 2003. Unified Ecoregions of Alaska: 2001. Page Open-File Report. No. 2002-2.
Parisien, M. A., S. A. Parks, M. A. Krawchuk, M. D. Flannigan, L. M. Bowman, and M. A. Moritz. 2011. Scale-dependent controls on the area burned in the boreal forest of Canada, 1980-2005. Ecological Applications 21:789–805.
Parks, S. A., L. M. Holsinger, C. Miller, and C. R. Nelson. 2015. Wildland fire as a self-regulating mechanism: The role of previous burns and weather in limiting fire progression. Ecological Applications 25:1478–1492.
Parks, S. A., C. Miller, L. M. Holsinger, L. S. Baggett, and B. J. Bird. 2016. Wildland fire limits subsequent fire occurrence. International Journal of Wildland Fire 25:182–190.
Pausas, J. G., and E. Ribeiro. 2013. The global fire-productivity relationship. Global Ecology and Biogeography 22:728–736.
Payette, S. 1992. Fire as a controlling process in the North American boreal forest. A systems analysis of the global boreal forest:144–169.
R Core Team. 2016. R: A language and environment for statistical computing. R Foundation for Statistical Computing, Vienna, Austria, 2012. ISBN 3-900051-07-0.
Randerson, J. T., H. Liu, M. G. Flanner, S. D. Chambers, Y. Jin, P. G. Hess, G. Pfister, M. C. Mack, K. K. Treseder, L. R. Welp, F. S. Chapin, J. W. Harden, M. L. Goulden, E. Lyons, J. C. Neff, E. a G. Schuur, and C. S. Zender. 2006. The impact of boreal forest fire on climate warming. Science 314:1130–1132.
Reimer, P. J., E. Bard, A. Bayliss, J. W. Beck, P. G. Blackwell, C. B. Ramsey, C. E. Buck, H.

Cheng, R. L. Edwards, M. Friedrich, P. M. Grootes, T. P. Guilderson, H. Haflidason, I. Hajdas, C. Hatté, T. J. Heaton, D. L. Hoffmann, A. G. Hogg, K. A. Hughen, K. F. Kaiser, B. Kromer, S. W. Manning, M. Niu, R. W. Reimer, D. A. Richards, E. M. Scott, J. R. Southon, R. A. Staff, C. S. M. Turney, and J. van der Plicht. 2013. IntCal13 and Marine13 Radiocarbon Age Calibration Curves 0–50,000 Years cal BP. Radiocarbon 55:1869–1887.

Shenoy, A., J. F. Johnstone, E. S. Kasischke, and K. Kielland. 2011. Persistent effects of fire severity on early successional forests in interior Alaska. Forest Ecology and Management 261:381–390.

SNAP. 2015. Projected monthly and derived temperature products – 2 km CMIP5/AR5. Scenarios Network for Alaska and Arctic Planning, Fairbanks.

Turner, M., and W. Romme. 1994. Landscape dynamics in crown fire ecosystems. Landscape Ecology 9:59–77.

Wiles, G. C., R. D. D'Arrigo, D. Barclay, R. S. Wilson, S. K. Jarvis, L. Vargo, and D. Frank. 2014. Surface air temperature variability reconstructed with tree rings for the Gulf of Alaska over the past 1200 years. The Holocene 24:198–208.

Young, A. M., P. E. Higuera, P. A. Duffy, and F. S. Hu. 2017. Climatic thresholds shape northern high-latitude fire regimes and imply vulnerability to future climate change. Ecography 40:606–617.

## 1.7 Tables and Figures

**Table 1**. Sampled lakes and associated information. The year when fires burned within 1 km of the lake are listed as "Fires < 1 km."

| Lake name | Site code | Latitude | Longitude | Depth (m) | Area (ha) | Record length (cm) | Fires < 1 km |
|---|---|---|---|---|---|---|---|
| Buster Brown | BB15 | 64.156 | -154.301 | 4.7 | 2 | 30 | 1991 |
| Duffy | DU15 | 64.137 | -154.221 | 7.5 | 10 | 40 | 1991 |
| Macchiato | MA15 | 64.302 | -154.518 | 17.3 | 4 | 16 | 2013 |
| Nodwell | NW15 | 64.312 | -154.530 | 16.0 | 8 | 40 | 1953 |
| Shapiro | SH15 | 64.286 | -154.663 | 7.1 | 3 | 18 | 1953 |
| Three Lodge | TL15 | 64.267 | -154.545 | 10.0 | 5 | 39 | 2013 |
| Ursa | UR15 | 64.170 | -154.249 | 5.7 | 1 | 15 | 1991 |

**Table 2.** Parameters used in Bacon and CharAnalysis for age-depth modeling and charcoal peak analysis. Multiple values for parameter priors refer to values above and below a change-point in the age-depth model, respectively.

| | Parameter | BB15 | DU15 | MA15 | NW15 | SH15 | TL15 | UR15 |
|---|---|---|---|---|---|---|---|---|
| Age-depth modeling (Bacon) | Acc. rate prior (yr $cm^{-1}$) | 10, 0.5 | 10, 10 | 20, 0.5 | 20, 0.5 | 20, 0.5 | 20, 0.5 | 50 |
| | Acc. rate shape prior | 1, 1 | 1, 1 | 1, 1 | 1, 1 | 1, 1 | 1, 1 | 1 |
| | AR memory prior | 0.1 | 0.1 | 0.1 | 0.1 | 0.1 | 0.1 | 0.1 |
| | Memory strength prior | 10 | 10 | 10 | 10 | 10 | 10 | 10 |
| Charcoal peak analysis (CharAnalysis) | Record end (yr BP) | -65 | -65 | -65 | -65 | -65 | -65 | -65 |
| | Record start (yr BP) | 222 | 302 | 323 | 1046 | 228 | 469 | 610 |
| | Interpolation (yr) | 5 | 5 | 5 | 5 | 5 | 5 | 5 |
| | Smoothing (yr) | 250 | 250 | 200 | 250 | 250 | 250 | 250 |
| | Threshold percentile | 0.99 | 0.99 | 0.95 | 0.99 | 0.99 | 0.99 | 0.99 |
| | Min. count p-value | 0.15 | 0.25 | 0.15 | 0.15 | 0.05 | 0.05 | 0.10 |
| Native median resolution (cm $yr^{-1}$) | | 2 | 3 | 6 | 11 | 9 | 4 | 15 |

**Table 3.** Summary of peak analysis results.

| Site | Record length (yr) | Total fires recorded | Mean fire return interval (SD) (yr) | Fire frequency ( # 100 $yr^{-1}$) |
|---|---|---|---|---|
| BB15 | 285 | 4 | 90 (60) | 1.4 |
| DU15 | 360 | 6 | 50 (25) | 1.67 |
| MA15 | 385 | 3 | 115 (85) | 0.78 |
| NW15 | 1080 | 4 | 265 (170) | 0.37 |
| SH15 | 575 | 5 | 110 (75) | 0.87 |
| TL15 | 525 | 4 | 115 (85) | 0.76 |
| UR15 | 570 | 3 | 65 (10) | 0.53 |

**Table 4.** Pearson product-moment correlation coefficients (r) between all proxies from 1550-1895 (fire history and climate data) and 1650-1895 (fire history and tree establishment data), and their significance. Bold and italicized values are significant at α = 0.01, bold values are significant at α = 0.05, and values with an asterisk are significant at α = 0.10. "CRU precip." refers to downscaled, modeled annual precipitation (mm), "CRU temp." refers to downscaled, modeled temperature (deg. C), "GOA temperature" refers to tree-ring based growing season temperature anomalies (deg. C), and "tree establishment" refers to total tree count of all species.

| | 50-year mean CHAR | 5-year mean CHAR | Percent burned | GOA temp. |
|---|---|---|---|---|
| GOA temperature | 0.09 | 0.07 | 0.13 | |
| Tree establishment | ***0.58*** | 0.23 | ***0.44*** | ***0.40*** |

**Table 5.** Pearson product-moment correlation coefficients (r) between all proxies from 1900-2005, and their significance. Bold and italicized values are significant at $\alpha = 0.01$, bold values are significant at $\alpha = 0.05$, and values with an asterisk are significant at $\alpha = 0.10$. "CRU precip." refers to downscaled, modeled annual precipitation (mm), "CRU temp." refers to downscaled, modeled temperature (deg. C), "GOA temp." refers to tree-ring based growing season temperature, and "tree est." refers to tree establishment in all species.

| | 50-year mean CHAR | 5-year mean CHAR | Percent burned | CRU precip. | CRU temp. | GOA temp. |
|---|---|---|---|---|---|---|
| CRU precip. | 0.02 | 0.09 | 0.28 | | | |
| CRU temp. | ***0.69*** | **0.43** | 0.42* | 0.13 | | |
| GOA temp. | 0.14 | -0.02 | 0.19 | **0.48** | 0.34 | |
| Tree est. | ***-0.58*** | -0.26 | -0.07 | **0.44** | -0.41* | -0.21 |

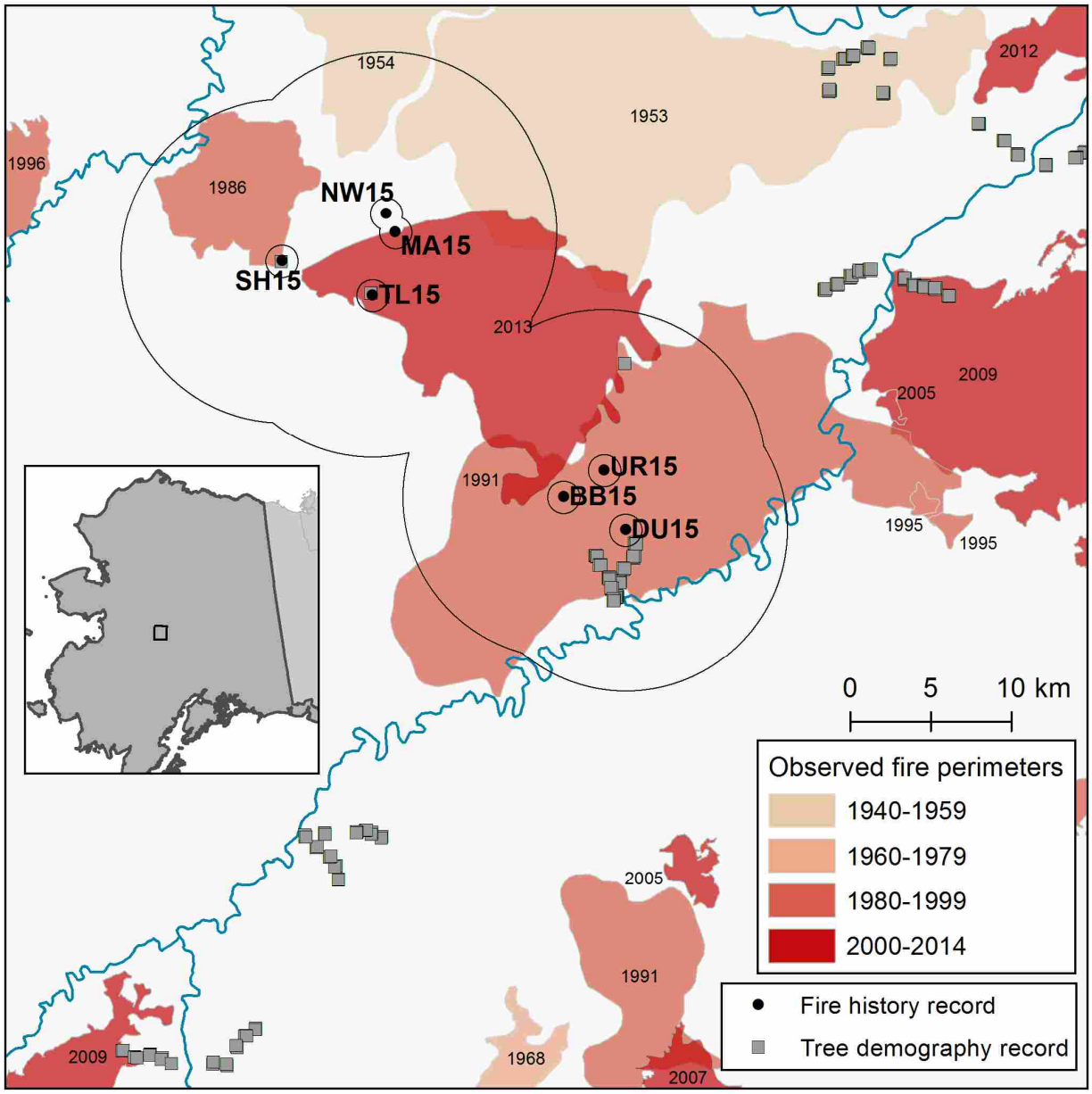


**Figure 1.** Map of study area. Colored polygons are observed fire perimeters since 1940, black circles are locations of lake-sediment cores, and grey squares are locations of tree cross-sections, blue lines are major river channels. Small black dots cover a 500-m radius, while the black circles show 1- and 10-km radii around each lake. Note: two tree demography records are immediately adjacent to SH15 and TL15 fire history records.

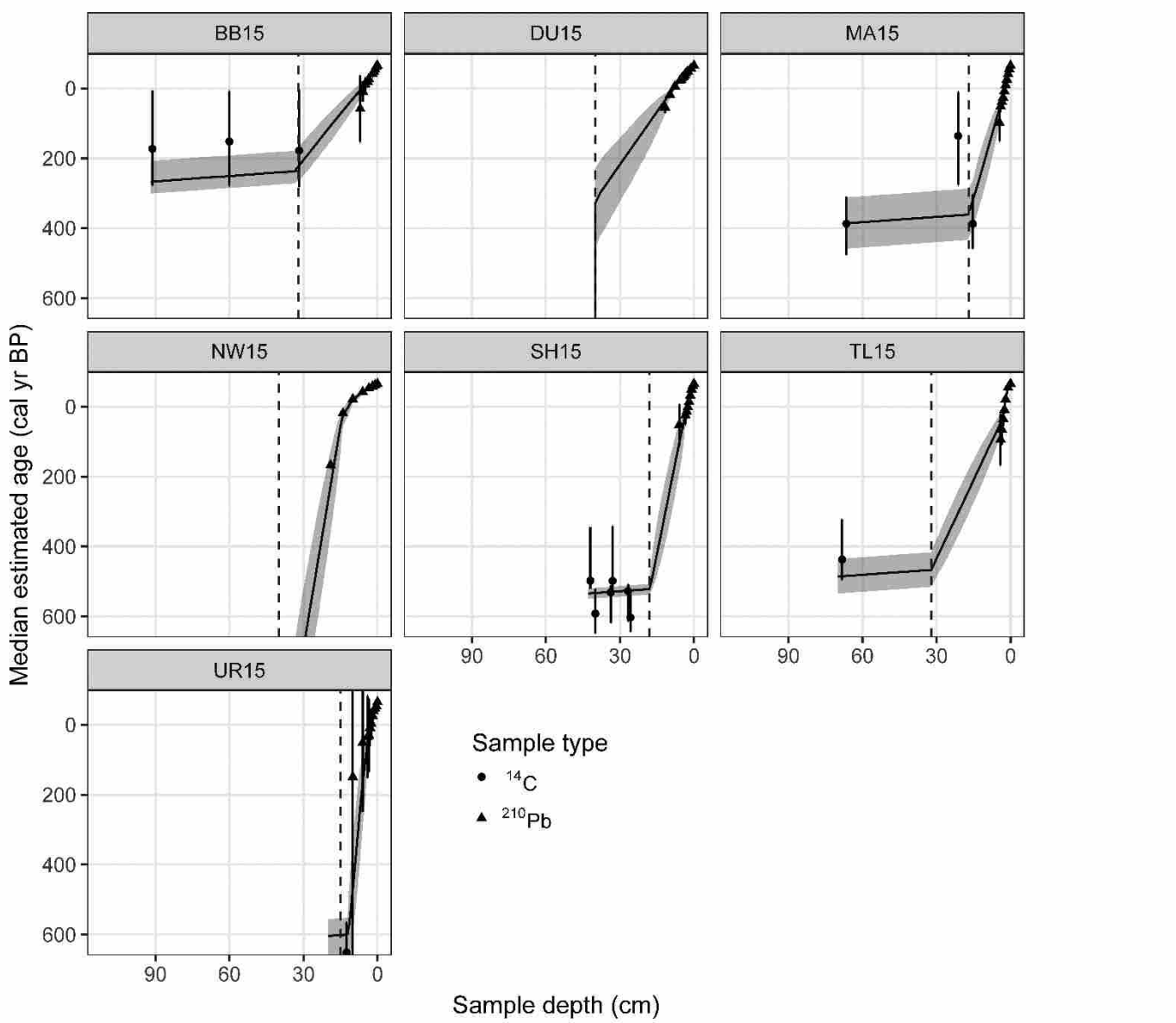


**Figure 2.** Age-depth models for lake-sediment records. Triangles indicate age estimates from $^{210}$Pb-based models, and points indicate age estimates from calibrated $^{14}$C-dated terrestrial macrofossils and concentrated charcoal. Black lines indicate the median sediment age modeled as an auto-regressive gamma process with prior constraints on sediment accumulation and sample memory. Vertical dashed lines indicate the transition to near-instantaneous sedimentation (from top to bottom), as described in the text. Note: BB15, DU15, and NW15 are constrained by dates outside the (uniform) plotting window; see appendix for complete models alongside core images.

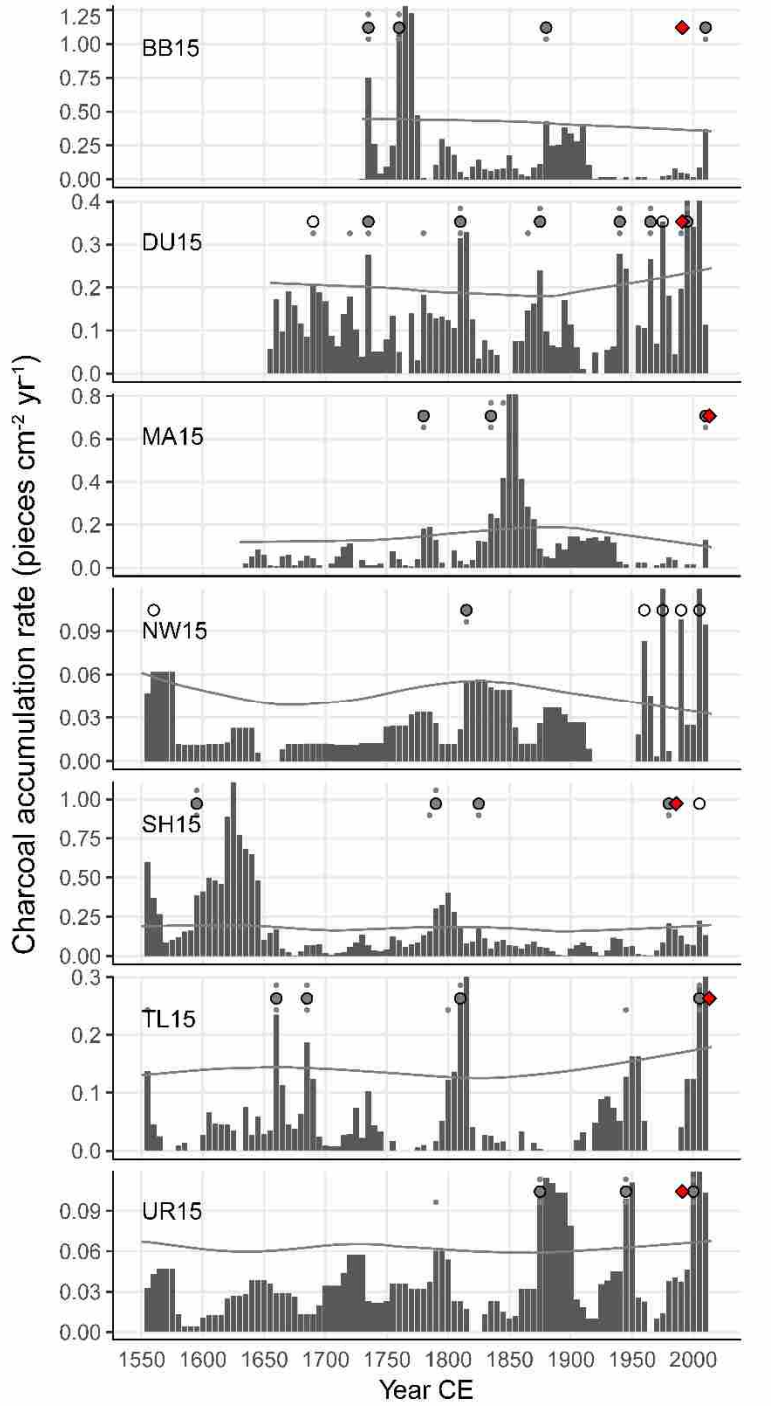


**Figure 3.** Charcoal records and inferred fire history. Vertical black bars are 5-yr interpolated charcoal accumulation rates (CHAR), and grey lines are thresholds (99$^{th}$ percentile) used to identify charcoal peaks; filled circles are significant CHAR peaks, and small circles are peaks exceeding higher (99.9$^{th}$ percentile) and lower (95$^{th}$ percentile) thresholds. Open circles failed minimum-count test for significance. Red diamonds are fires from the observed record (1950-2014) that occurred within 1 km of a given lake.

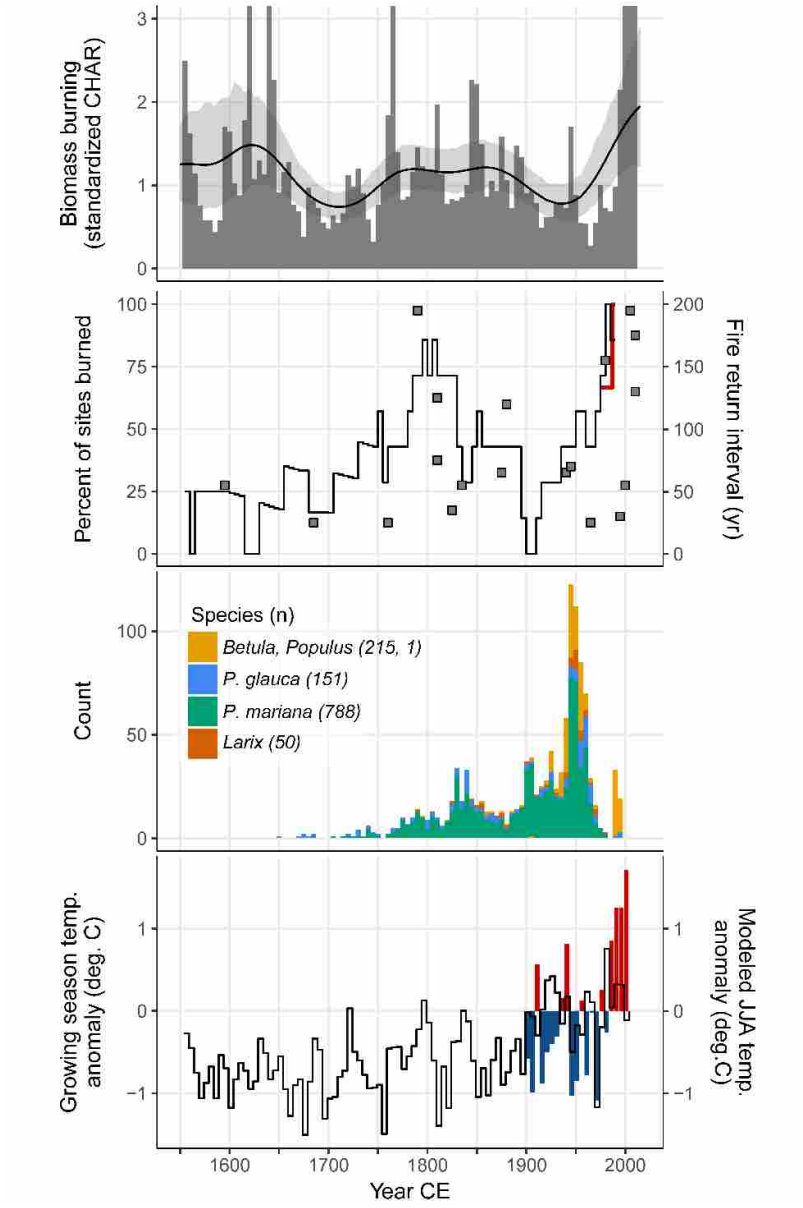


**Figure 4.** Comparison of composite fire history, percent of sites burned, tree demography, and climate reconstructions. First row: Grey bars are the 5-yr composite mean of biomass burning (standardized CHAR), the black curve is the 100-yr mean, and the grey shading is the bootstrapped 90% confidence interval. Second row: circles are fire return intervals (FRI, yr) at the year they were observed, black stepped line is the percent of sites burned in 50-yr periods, plotted in 5-yr overlapping increments; the dashed step line is the percent of sites burned in the past 50 years, based on the observational record (1950-present). Third row: histogram of pith dates with color representing genus. Fourth row: the black stepped line is tree-ring-based growing season temperature anomaly from the Gulf of Alaska (Wiles et al. 2014), while colored bars are modeled June, July, August mean temperature anomalies from downscaled climate data (SNAP, 2015).

**Table S1.** Radiometric dates ($^{14}C$ and $^{210}Pb$) from all lakes. Asterisks (*) after lab ID indicate dates not used in the age-depth model, mainly bulk $^{14}C$ dates which were deemed systematically older than $^{14}C$ dates based on macrofossils from nearby sediment depths.

| Site code | Top depth (cm) | Bottom depth (cm) | Material | $^{14}C$ or $^{210}Pb$ activity | $^{14}C$ age or $^{210}Pb$ activity st. dev. | Age (cal yr BP) | Age 5th | Age 95th | Lab ID |
|---|---|---|---|---|---|---|---|---|---|
| BB15 | 0.00 | 0.50 | bulk sediment | 2.9753 | 0.1964 | -65.00 | -71.02 | -58.98 | Flett-75911 |
| BB15 | 0.50 | 1.00 | bulk sediment | 5.0651 | 0.2537 | -62.35 | -68.59 | -56.11 | Flett-75912 |
| BB15 | 1.00 | 1.50 | bulk sediment | 3.6862 | 0.1906 | -54.12 | -61.26 | -46.99 | Flett-75913 |
| BB15 | 1.50 | 2.00 | bulk sediment | 3.2887 | 0.2267 | -48.48 | -56.44 | -40.53 | Flett-75914 |
| BB15 | 2.00 | 2.50 | bulk sediment | 2.1192 | 0.1446 | -41.90 | -50.99 | -32.81 | Flett-75915 |
| BB15 | 2.00 | 2.50 | bulk sediment | 1.3187 | 0.0398 | - | - | - | Flett-75915* |
| BB15 | 3.50 | 4.00 | bulk sediment | 2.2746 | 0.1511 | -26.94 | -39.87 | -14.01 | Flett-75918 |
| BB15 | 4.00 | 4.50 | bulk sediment | 1.4966 | 0.1808 | -19.05 | -34.85 | -3.25 | Flett-75919 |
| BB15 | 5.00 | 6.00 | bulk sediment | 1.8436 | 0.1397 | -11.87 | -30.56 | 6.82 | Flett-75921 |
| BB15 | 6.00 | 7.00 | bulk sediment | 1.7069 | 0.1509 | 8.91 | -20.78 | 38.61 | Flett-75922 |
| BB15 | 7.00 | 8.00 | bulk sediment | 1.3622 | 0.1632 | 58.28 | -36.14 | 152.71 | Flett-75923* |
| BB15 | 8.00 | 9.00 | bulk sediment | 1.2045 | 0.1213 | - | - | - | Flett-75924* |
| BB15 | 9.00 | 10.00 | bulk sediment | 1.1596 | 0.1126 | - | - | - | Flett-75925* |
| BB15 | 9.00 | 10.00 | bulk sediment | 1.1130 | 0.0371 | - | - | - | Flett-75925* |
| BB15 | 14.00 | 15.00 | bulk sediment | 1.5079 | 0.1234 | - | - | - | Flett-75930* |
| BB15 | 31.75 | 32.00 | wood macrofossil | 0.9795 | 0.0036 | 178.00 | 5.00 | 281.00 | CAMS-175825 |
| BB15 | 39.50 | 39.75 | bulk sediment | 0.3299 | 0.0012 | 10036.00 | 9919.00 | 10176.00 | CAMS-176589* |
| BB15 | 60.00 | 60.25 | wood macrofossil | 0.9817 | 0.0041 | 152.00 | 8.00 | 278.00 | CAMS-175826 |
| BB15 | 72.00 | 72.25 | wood macrofossil | 0.8782 | 0.0030 | 952.00 | 926.00 | 1042.00 | CAMS-175827 |
| BB15 | 91.25 | 91.50 | wood macrofossil | 0.9809 | 0.0035 | 173.00 | 7.00 | 278.00 | CAMS-175828 |
| DU15 | 0.00 | 0.75 | bulk sediment | 14.2798 | 0.5899 | -65.00 | -66.86 | -63.14 | Flett-75931 |
| DU15 | 1.25 | 1.75 | bulk sediment | 11.8882 | 0.4025 | -56.80 | -58.87 | -54.73 | Flett-75933 |
| DU15 | 2.50 | 3.25 | bulk sediment | 12.2693 | 0.4961 | -48.17 | -50.60 | -45.74 | Flett-75935 |
| DU15 | 2.50 | 3.25 | bulk sediment | 1.2595 | 0.0400 | - | - | - | Flett-75935* |
| DU15 | 3.25 | 3.75 | bulk sediment | 10.8727 | 0.4196 | -42.95 | -45.65 | -40.25 | Flett-75936 |
| DU15 | 3.75 | 4.25 | bulk sediment | 5.9687 | 0.3280 | -37.77 | -40.79 | -34.74 | Flett-75937 |
| DU15 | 4.25 | 4.75 | bulk sediment | 4.8331 | 0.2980 | -33.66 | -36.97 | -30.35 | Flett-75938 |
| DU15 | 4.75 | 5.25 | bulk sediment | 4.3575 | 0.2734 | -30.07 | -33.66 | -26.49 | Flett-75939 |
| DU15 | 5.25 | 5.75 | bulk sediment | 3.1513 | 0.2199 | -25.41 | -29.39 | -21.43 | Flett-75940 |
| DU15 | 5.75 | 6.75 | bulk sediment | 2.8402 | 0.2034 | -21.96 | -26.26 | -17.67 | Flett-75941 |
| DU15 | 7.75 | 8.75 | bulk sediment | 2.9789 | 0.2531 | -5.86 | -11.47 | -0.26 | Flett-75943 |
| DU15 | 9.75 | 10.75 | bulk sediment | 2.7243 | 0.2509 | 18.72 | 10.80 | 26.64 | Flett-75945 |
| DU15 | 11.75 | 12.75 | bulk sediment | 2.1053 | 0.2042 | 54.83 | 39.59 | 70.07 | Flett-75947* |
| DU15 | 13.75 | 15.00 | bulk sediment | 1.4379 | 0.2030 | - | - | - | Flett-75949* |

| | | | | | | | | | |
|---|---|---|---|---|---|---|---|---|---|
| DU15 | 13.75 | 15.00 | bulk sediment wood | 1.3232 | 0.0400 | - | - | - | Flett-75949* |
| DU15 | 50.00 | 50.25 | macrofossil | 0.0935 | 0.0006 | 22916.00 | 22768.00 | 23034.00 | CAMS-175829 |
| DU15 | 55.75 | 56.00 | bulk sediment wood | 0.2805 | 0.0011 | 11786.00 | 11922.00 | 12038.00 | CAMS-176590* |
| DU15 | 73.75 | 74.00 | macrofossil wood | 0.0835 | 0.0006 | 24006.00 | 23882.00 | 24128.03 | CAMS-175830 |
| DU15 | 106.50 | 106.75 | macrofossil wood | 0.0771 | 0.0006 | 24783.00 | 24551.00 | 25031.00 | CAMS-175831 |
| DU15 | 111.00 | 111.25 | macrofossil | 0.0784 | 0.0006 | 24546.00 | 24396.00 | 24856.00 | CAMS-175832 |
| MA15 | 0.00 | 0.50 | bulk sediment | 19.2996 | 0.5822 | -65.00 | -67.11 | -62.89 | Flett-77259 |
| MA15 | 0.50 | 1.00 | bulk sediment | 19.4721 | 0.6275 | -55.21 | -57.58 | -52.85 | Flett-77260 |
| MA15 | 1.00 | 1.50 | bulk sediment | 14.0752 | 0.4909 | -41.48 | -44.35 | -38.61 | Flett-77261 |
| MA15 | 1.50 | 2.00 | bulk sediment | 9.8065 | 0.3865 | -25.48 | -29.29 | -21.67 | Flett-77262 |
| MA15 | 2.00 | 2.50 | bulk sediment | 6.5494 | 0.3677 | -9.18 | -14.55 | -3.81 | Flett-77263 |
| MA15 | 2.50 | 3.00 | bulk sediment | 4.7233 | 0.2818 | 7.99 | 0.30 | 15.69 | Flett-77264 |
| MA15 | 3.00 | 3.50 | bulk sediment | 2.7286 | 0.1968 | 26.18 | 14.61 | 37.76 | Flett-77265 |
| MA15 | 3.50 | 4.00 | bulk sediment | 2.4020 | 0.1792 | 38.23 | 23.81 | 52.65 | Flett-77266 |
| MA15 | 4.00 | 4.50 | bulk sediment | 2.9280 | 0.2283 | 51.21 | 33.21 | 69.21 | Flett-77267 |
| MA15 | 4.50 | 5.00 | bulk sediment | 1.7636 | 0.1658 | 98.21 | 45.58 | 150.85 | Flett-77268* |
| MA15 | 5.00 | 6.00 | bulk sediment | 1.2095 | 0.1451 | - | - | - | Flett-77269* |
| MA15 | 5.00 | 6.00 | bulk sediment | 0.9711 | 0.0337 | - | - | - | Flett-77269* |
| MA15 | 9.00 | 10.00 | bulk sediment | 2.0659 | 0.1934 | - | - | - | Flett-77273* |
| MA15 | 14.00 | 15.00 | bulk sediment | 1.1827 | 0.1582 | - | - | - | Flett-77278* |
| MA15 | 14.00 | 15.00 | bulk sediment wood | 1.5298 | 0.0412 | - | - | - | Flett-77278* |
| MA15 | 15.25 | 15.50 | macrofossil | 0.9627 | 0.0031 | 387.00 | 303.00 | 458.00 | CAMS-176005 |
| MA15 | 15.25 | 15.50 | bulk sediment wood | 0.4877 | 0.0018 | 6574.00 | 6497.00 | 6646.00 | CAMS-176591* |
| MA15 | 21.25 | 22.00 | macrofossil wood | 0.9833 | 0.0050 | 136.00 | 10.00 | 276.00 | CAMS-176006 |
| MA15 | 66.50 | 66.75 | macrofossil | 0.9595 | 0.0035 | 387.00 | 311.00 | 476.00 | CAMS-176007 |
| NW15 | 0.00 | 0.50 | bulk sediment | 14.9582 | 0.8668 | -65.00 | -62.64 | -67.36 | Flett-77219 |
| NW15 | 1.00 | 1.50 | bulk sediment | 15.9483 | 0.7607 | -61.77 | -59.30 | -64.25 | Flett-77221 |
| NW15 | 2.00 | 2.50 | bulk sediment | 14.0353 | 0.7528 | -57.96 | -55.32 | -60.60 | Flett-77223 |
| NW15 | 3.00 | 3.50 | bulk sediment | 1.6614 | 0.1745 | - | - | - | Flett-77225* |
| NW15 | 3.50 | 4.00 | bulk sediment | 12.4801 | 0.6748 | -52.29 | -49.35 | -55.22 | Flett-77226 |
| NW15 | 6.00 | 7.00 | bulk sediment | 9.2710 | 0.5594 | -42.05 | -38.41 | -45.69 | Flett-77230 |
| NW15 | 10.00 | 11.00 | bulk sediment | 8.0172 | 0.4285 | -21.24 | -16.17 | -26.30 | Flett-77234 |
| NW15 | 13.00 | 14.00 | bulk sediment | 1.3217 | 0.0687 | - | - | - | Flett-77237* |
| NW15 | 14.00 | 15.00 | bulk sediment | 6.6813 | 0.4205 | 19.09 | 32.60 | 5.58 | Flett-77238 |
| NW15 | 19.00 | 20.00 | bulk sediment | 4.5611 | 0.2171 | 167.51 | 176.45 | 158.56 | Flett-78515* |
| NW15 | 23.50 | 24.50 | bulk sediment | 6.0981 | 0.3346 | - | - | - | Flett-78517* |
| NW15 | 25.50 | 26.50 | bulk sediment | 0.7275 | 0.0030 | 2705.00 | 2507.00 | 2747.00 | CAMS-176228* |
| NW15 | 46.50 | 47.25 | bulk sediment | 0.5679 | 0.0165 | 5192.00 | 4571.00 | 5759.00 | CAMS-176229* |

| | | | | | | | | | |
|---|---|---|---|---|---|---|---|---|---|
| NW15 | 72.75 | 74.25 | concentrated charcoal | 0.8571 | 0.0031 | 1195.00 | 1079.00 | 1263.00 | CAMS-176230 |
| SH15 | 0.00 | 0.50 | bulk sediment | 5.5858 | 0.3015 | -65.00 | -68.18 | -61.82 | Flett-77239 |
| SH15 | 0.50 | 1.00 | bulk sediment | 8.6176 | 0.3667 | -59.72 | -63.09 | -56.35 | Flett-77240 |
| SH15 | 1.00 | 1.50 | bulk sediment | 9.2358 | 0.3783 | -49.31 | -53.27 | -45.35 | Flett-77241 |
| SH15 | 1.50 | 2.00 | bulk sediment | 6.1228 | 0.2767 | -32.09 | -37.69 | -26.48 | Flett-77242 |
| SH15 | 2.00 | 2.50 | bulk sediment | 3.7203 | 0.2324 | -13.72 | -22.65 | -4.79 | Flett-77243 |
| SH15 | 2.50 | 3.00 | bulk sediment | 2.7599 | 0.1888 | 1.49 | -12.03 | 15.02 | Flett-77244 |
| SH15 | 3.00 | 3.50 | bulk sediment | 2.2555 | 0.1800 | 14.27 | -5.24 | 33.77 | Flett-77245 |
| SH15 | 3.50 | 4.00 | bulk sediment | 1.7370 | 0.1415 | 24.68 | -1.71 | 51.07 | Flett-77246 |
| SH15 | 3.50 | 4.00 | bulk sediment | 1.4222 | 0.0374 | - | - | - | Flett-77246* |
| SH15 | 6.00 | 7.00 | bulk sediment | 1.5947 | 0.1372 | 52.72 | -6.76 | 112.20 | Flett-77250* |
| SH15 | 10.00 | 11.00 | bulk sediment | 1.2459 | 0.1151 | - | - | - | Flett-77254* |
| SH15 | 10.00 | 11.00 | bulk sediment | 1.4033 | 0.0383 | - | - | - | Flett-77254* |
| SH15 | 14.00 | 15.00 | bulk sediment | 1.4609 | 0.1581 | - | - | - | Flett-77258 |
| SH15 | 15.75 | 16.00 | bulk sediment | 0.7310 | 0.0026 | 2588.00 | 2496.00 | 2732.00 | CAMS-176592* |
| SH15 | 25.75 | 26.00 | concentrated charcoal | 0.9302 | 0.0034 | 603.00 | 537.00 | 644.00 | CAMS-176008 |
| SH15 | 26.75 | 27.00 | wood macrofossil | 0.9389 | 0.0029 | 527.00 | 508.00 | 614.00 | CAMS-176009 |
| SH15 | 33.00 | 33.25 | wood macrofossil | 0.9478 | 0.0034 | 498.00 | 342.00 | 521.00 | CAMS-176010 |
| SH15 | 33.75 | 34.00 | concentrated charcoal | 0.9378 | 0.0034 | 531.00 | 511.00 | 619.00 | CAMS-176011 |
| SH15 | 40.00 | 40.25 | concentrated charcoal | 0.9324 | 0.0052 | 592.00 | 522.00 | 648.00 | CAMS-176012 |
| SH15 | 42.00 | 42.25 | wood macrofossil | 0.9476 | 0.0033 | 498.00 | 344.00 | 520.00 | CAMS-176013 |
| TL15 | 0.00 | 1.00 | bulk sediment | 6.9937 | 0.3242 | -65.00 | -67.65 | -62.35 | Flett-75970 |
| TL15 | 1.00 | 2.00 | bulk sediment | 11.6154 | 0.3707 | -54.52 | -57.40 | -51.64 | Flett-75971 |
| TL15 | 2.00 | 2.50 | bulk sediment | 7.5257 | 0.2707 | -20.78 | -25.61 | -15.95 | Flett-75972 |
| TL15 | 2.50 | 3.00 | bulk sediment | 2.4663 | 0.1883 | 9.16 | -1.36 | 19.68 | Flett-75973 |
| TL15 | 3.00 | 3.50 | bulk sediment | 1.5936 | 0.1536 | 35.20 | 15.14 | 55.26 | Flett-75974 |
| TL15 | 3.50 | 4.00 | bulk sediment | 1.0888 | 0.1206 | 65.85 | 23.11 | 108.58 | Flett-75975 |
| TL15 | 4.00 | 4.50 | bulk sediment | 1.0064 | 0.1108 | 94.36 | 20.69 | 168.02 | Flett-75976 |
| TL15 | 4.50 | 5.00 | bulk sediment | 0.6937 | 0.0923 | - | - | - | Flett-75977* |
| TL15 | 7.00 | 8.00 | bulk sediment | 0.7313 | 0.0930 | - | - | - | Flett-75980* |
| TL15 | 10.00 | 11.00 | bulk sediment | 1.0085 | 0.1074 | - | - | - | Flett-75983* |
| TL15 | 14.00 | 15.00 | bulk sediment | 0.9544 | 0.0972 | - | - | - | Flett-75987* |
| TL15 | 29.25 | 29.50 | bulk sediment | 0.4823 | 0.0022 | 6646.00 | 6551.00 | 6720.00 | CAMS-176593* |
| TL15 | 68.25 | 68.50 | wood macrofossil | 0.9552 | 0.0034 | 437.00 | 322.00 | 496.00 | CAMS-175833 |
| UR15 | 0.00 | 0.50 | bulk sediment | 10.3464 | 0.4384 | -65.00 | -73.19 | -56.81 | Flett-77199 |
| UR15 | 0.50 | 1.00 | bulk sediment | 6.3729 | 0.3080 | -53.61 | -63.57 | -43.64 | Flett-77200 |
| UR15 | 1.00 | 1.50 | bulk sediment | 4.9635 | 0.2634 | -45.88 | -57.61 | -34.15 | Flett-77201 |

| | | | | | | | | | |
|---|---|---|---|---|---|---|---|---|---|
| UR15 | 1.50 | 2.00 | bulk sediment | 6.5949 | 0.3382 | -38.98 | -52.80 | -25.17 | Flett-77202 |
| UR15 | 2.00 | 2.50 | bulk sediment | 6.2717 | 0.3043 | -25.32 | -45.15 | -5.48 | Flett-77203 |
| UR15 | 2.50 | 3.00 | bulk sediment | 2.8435 | 0.2099 | -3.18 | -41.03 | 34.67 | Flett-77204 |
| UR15 | 2.50 | 3.00 | bulk sediment | 1.3108 | 0.0386 | - | - | - | Flett-77204* |
| UR15 | 3.00 | 3.50 | bulk sediment | 2.6720 | 0.2032 | 8.58 | -45.31 | 62.47 | Flett-77205 |
| UR15 | 3.50 | 4.00 | bulk sediment | 1.3147 | 0.1553 | 30.31 | -74.20 | 134.83 | Flett-77206 |
| UR15 | 4.00 | 4.50 | bulk sediment | 1.2320 | 0.1202 | 34.23 | -83.13 | 151.59 | Flett-77207 |
| UR15 | 6.00 | 7.00 | bulk sediment | 1.3342 | 0.1531 | 51.54 | -146.32 | 249.40 | Flett-77210 |
| UR15 | 10.00 | 11.00 | bulk sediment | 1.0823 | 0.1290 | 149.46 | -2739.93 | 3038.86 | Flett-77214* |
| UR15 | 12.50 | 12.75 | wood macrofossil | 0.9185 | 0.0035 | 651.00 | 565.00 | 680.00 | CAMS-176598 |
| UR15 | 14.00 | 15.00 | bulk sediment | 0.9530 | 0.1195 | - | - | - | Flett-77218* |
| UR15 | 14.00 | 15.00 | bulk sediment | 0.8339 | 0.0352 | - | - | - | Flett-77218* |
| UR15 | 29.00 | 29.25 | bulk sediment | 0.7070 | 0.0030 | 2883.00 | 2795.00 | 2964.00 | CAMS-176594* |
| UR15 | 52.00 | 52.25 | bulk sediment | 0.4841 | 0.0017 | 6646.00 | 6551.00 | 6720.00 | CAMS-176595* |

## Chapter 2

## Spatiotemporal variability in biomass burning reveals drivers of arctic and boreal fire regimes and limits to fire synchrony during the Holocene*

**This chapter is written for publication with co-authors including P.E. Higuera, R. Kelly, and F.S. Hu.*

### 2.1 Abstract

Boreal forest and tundra biomes are globally important because the mobilization of large carbon stocks and changes in energy balance could act as positive feedbacks to ongoing climate change. In Alaska, wildfire is a primary driver of ecosystem structure and function, and a key mechanism coupling high-latitude ecosystems to global climate. Paleoecological records reveal the sensitivity of fire regimes to climatic and vegetation change over centennial to millennial time scales, highlighting increased burning concurrent with warming or increased landscape flammability. To quantify spatiotemporal patterns in fire-regime variability, including simultaneous fire activity across disparate regions ("fire synchrony"), we analyzed 27 published sediment-charcoal records from four Alaskan ecoregions, and compared patterns to existing paleoclimate and paleovegetation records. The timing of individual fire events was estimated with a peak analysis, and the mean proportion of sites burned each century, integrating temporal uncertainty, was used to quantify fire synchrony; biomass burning was inferred form total charcoal accumulation in composite records, developed for both regional and Alaska-wide scales. Biomass burning and fire frequency increased significantly in boreal forest regions with the expansion of black spruce, ca. 6-4 thousand years before present (yr BP). Biomass burning also increased during warm periods in some regions, but was most pronounced in the Yukon Flats from ca. 1000-500 yr BP. Increases in biomass burning while fire return intervals remained

constant, particularly during warm periods, suggests increases in average fire severity (i.e., more biomass burning per fire. Finally, results also indicate significant increases in biomass burning over the last century across Alaska. Our analysis documents the sensitivity of fire activity to broad-scale environmental change, including climate warming and major shifts in vegetation. However, a lack of widespread, prolonged fire synchrony suggests regional heterogeneity limited simultaneous fire-regime change across Alaska, which may confer broad-scale resilience of the boreal forest to novel fire regimes in the future. In contrast, synchronous fire-regime change across Alaska in the future would be unprecedented in the last 4,000 years or more.

## 2.2 Introduction

Boreal forest and tundra regions are experiencing rapid environmental change, driven by the amplified effects of increasing atmospheric $CO_2$ concentrations on high-latitude ecosystems (Chapin et al. 2000, Hinzman et al. 2005, Miller et al. 2010). Disturbance by fire couples terrestrial and climate systems, and can serve as a positive feedback to climate warming by accelerating the movement of carbon stocks into the atmosphere and altering radiative balance through changes in albedo and energy partitioning (Randerson et al. 2006, Bond-Lamberty et al. 2007, Bonan 2008, Bowman et al. 2009). In addition to the significant feedbacks between fire and the climate system, fire has the potential to catalyze abrupt change in the structures and processes that have promoted the landscape-scale resilience of boreal ecosystems to repeated disturbance and climate variability for at least six millennia (Lynch et al. 2004, Hu et al. 2006, Higuera et al. 2009, Johnstone et al. 2016). Increases in the annual extent and severity of fire in the boreal forest (Kasischke and Turetsky 2006, Kasischke et al. 2010) and the occurrence of large, rare fire events in the Alaskan tundra (Hu et al. 2010, Chipman et al. 2015) have raised questions about the capacity for fire to initiate widespread ecosystem state change and impact the

trajectory of ecosystem properties (Kasischke and Johnstone 2005, Johnstone et al. 2010a, 2010b, Barrett et al. 2011, Mack et al. 2011, Grosse et al. 2011, Brown and Johnstone 2012, Genet et al. 2013). For example, increased fire severity and subsequently reduced organic-layer thickness may initiate post-fire shifts in species composition and promote permafrost thaw, with important consequences for radiative balance and the potential mobilization of large soil-carbon stocks (Barrett et al. 2011, O'Donnell et al. 2011, Shenoy et al. 2011, Pastick et al. 2014). The potential for fire to catalyze abrupt environmental change in boreal forest and tundra systems, with cascading feedbacks to global climate, motivates the need to quantify the sensitivity of fire regimes to climate forcing of the past, and the precedence of synchronous fire-regime change across broad regions.

Due to the temporally infrequent and spatially complex nature of fire and its effects, inferences about the causes and consequences of disturbance are scale-dependent (Johnstone et al. 2010a, Turner 2010). Reducing uncertainty around the sensitivity of fire activity to climate change, its future trajectory, and the impact of changing disturbance regimes on the properties and function of high-latitude ecosystems requires approaches that are appropriately broad in their spatial and temporal scope (Kasischke et al. 2002, 2010, Hu et al. 2015, Kelly et al. 2016). Paleoecological records are one way to provide broad-scale perspective, and a body of published records documents the relationships among climate, fire, and vegetation dynamics in boreal forest and tundra ecosystems over the Holocene (Hu et al. 2006, Whitlock et al. 2010, Marlon et al. 2013, 2016). These records point to the sensitivity of boreal forest and tundra fire regimes to climate variability, and the important role that vegetation plays in mediating the direct link between climate and fire (Lynch et al. 2002, 2004, Brubaker et al. 2009, Higuera et al. 2009, 2011a, 2011b, Barrett et al. 2013, Kelly et al. 2013). For example, fire activity in Alaska

increased markedly with the expansion of black spruce ca. 6000-4000 calibrated years before present (yr BP) (Lynch et al. 2002, Higuera et al. 2009, Kelly et al. 2013). In the boreal forest of the Copper River Basin, biomass burning and summer temperature varied independently of before ca. 3000 yr BP, but were positively correlated over the past three millennia (Barrett et al. 2013). Recent work from the Yukon Flats region, focused on the last 2000 years, documents strong links between centennial-scale climate warming during the Medieval Climate Anomaly (MCA, ca. 1000-500 yr BP) and subsequent cooling during the Little Ice Age (LIA, ca. 600-300 yr BP), and changes in biomass burning (Kelly et al. 2013). This work also identified potential negative feedbacks to burning after prolonged periods of elevated fire severity, whereby successional-scale vegetation changes eventually reduce landscape flammability, and subsequent fire frequency. Despite the importance of these finding for revealing region-specific fire-climate-vegetation dynamics, variability in fire-regime sensitivity to climate and the extent of synchrony in fire-regime change among regions remains unclear.

Understanding variability in fire activity over space and time is critical for understanding modern ecosystem states and anticipating fire-regime response to 21st-century warming. For example, incorporating paleoecological data into modeling frameworks can change predictions of the boreal forest as a net sink for atmospheric carbon to a net source (Kelly et al. 2016). Furthermore, predictions of future fire activity based on changes in fire-conducive weather and reduced fuel moisture with climate warming indicate widespread increases in fire activity in the boreal forest and tundra (Balshi et al. 2009, Flannigan et al. 2009). Fire-climate modeling shows nearly universal increases in fire frequency under median climate change scenarios, but highlights spatial variability in fire-regime changes across Alaska, particularly in areas near climatic thresholds to burning (Young et al. 2017). Although the implications of widespread

increases in fire activity for global climate and local ecosystems are significant, the magnitude of fire-regime sensitivity to climate warming during the Holocene remains uncertain, and the degree to which it occurred simultaneously across diverse Alaskan ecosystems is untested.

To identify the mechanisms that drive fire regimes at multiple spatiotemporal scales and quantify the degree of fire synchrony (i.e., simultaneous fire activity across broad regions) in fire-regime variability among regions, we characterized Holocene fire activity across flammable regions of Alaska by synthesizing datasets of previously published paleofire records. Using metrics of biomass burning and the timing of fire events, we investigated whether centennial- to millennial-scale, spatially broad forcing (e.g., climate change or biome shifts) promoted synchronous fire-regime change across flammable ecosystems, or if variations in vegetation, regional climate or other local factors limited widespread, concurrent changes in fire activity. Synchronous changes in biomass burning and fire occurrence among regions would provide evidence that broad-scale climatic variability and biome-scale changes in vegetation can act as dominant mechanisms driving fire-regime shifts, and homogenize fire activity across Alaska. Conversely, independent variability in biomass burning and fire occurrence across regions would indicate the importance of landscape-scale variation in ecosystem properties in controlling fire activity, or the importance of spatial variability in climate. Finally, limits to high fire activity at regional scales would suggest that fire-vegetation interactions may serve as negative feedbacks to widespread increases in fire activity through time.

We applied a robust method for estimating regional ("landscape-scale," $10^{1-3}$ $km^2$) and multi-region ("biome-scale," $10^{4-6}$ $km^2$) biomass burning to 27 lake-sediment charcoal records, and develop composite indices of biomass burning in Alaska's fire-prone boreal forest and tundra systems. To quantify concurrent fire activity among sites and regions, we estimate the

proportion of four regions individually, and collectively, affected by fire each century, and quantify the uncertainty around this metric by incorporating the uncertainty inherent to radiometric dating of lake sediments. Finally, we consider the implications of fire-regime sensitivity to climate and synchronous fire-regime change for species composition, carbon cycling, and radiative balance in high-latitude ecosystems.

## 2.3 Data and Methods

### 2.3.1 Study Area

Boreal forests occupy the vast expanse of floodplains and rolling hills of interior Alaska, bisected by the Yukon River, bounded to the north by the Brooks Range, and extending into the Copper River Basin south of the Alaska Range. Alaskan boreal forests consist of a patchwork of coniferous- (*Picea glauca* [white spruce]*, P. mariana* [black spruce]*, Larix laricina* [larch]), and deciduous-dominated (*Populus tremuloides* [quaking aspen], *Betula* [birch], *Alnus* [alder]*, Salix* [willow]) forest stands, and low-lying peatlands (*Sphagnum* [sphagnum moss]). Spruce and moss dominate on cool, moist sites over poorly drained and discontinuous permafrost soils, and co-exist with a regime of high-mortality crown fire (Johnson 1996, Hollingsworth et al. 2006). Broadleaf deciduous species thrive on well-drained upland sites and in recently burned areas with exposed mineral soils, and alongside white spruce in riparian corridors (Nowacki et al. 2003).

Tundra ecosystems characterized by cold arctic climates, but supporting vegetation types that overlap with those in the boreal forest, are found west of the interior boreal forest on the Seward Peninsula, and in the area of the Noatak River Watershed at the northwestern edge of the Brooks Range (Nowacki et al. 2003). These ecosystems are dominated by graminoids (*Cyperaceae* [sedges], *Poaceae* [grasses]) and woody shrubs (*Betula*, *Alnus*, and *Salix*, often

dwarf morphology), but also include patches of peatland, deciduous trees, and white spruce along river corridors.

We analyzed records from three boreal forest and one tundra region (n = 27 for biomass burning metric, and n = 25 for fire events) that are all fire-prone systems characterized by variation in climate, geology and vegetation (Nowacki et al. 2003). To study how landscape-scale variation in ecosystem properties mediate the impacts of broad-scale forcing on fire activity, our records span an order of magnitude range in modern fire rotation periods (60-1100 years; Table 1). We used records from the south-central Brooks Range in the Kobuk Ridges and Valleys ecoregion ("Kobuk"), the Copper River Basin ecoregion ("Copper River"), and the Yukon Flats area in the Yukon-Old Crow ecoregion ("Yukon Flats"), all considered part of the boreal forest biome. We also used records from the Noatak River Watershed ("Noatak"), located within the boundaries of the Kobuk Ridges and Valleys ecoregion, but considered ecologically distinct and part of the tundra biome. These study areas span a climatic and environmental gradient representing much of Alaska's fire-prone regions (Table 1), including the tundra systems of the Noatak, which experience frequent fire relative to graminoid-tundra systems further north and east (Rocha et al. 2012), and flammable boreal forest ecosystems. The boreal forest systems include regions near the northern extent of interior Alaska, characterized by a cold continental climate, and Alaska's most continental and flammable region, the Yukon Flats. In the most southern regions of the boreal forest, the Copper River Basin includes sites characterized by a cold, moderately wet climate.

### 2.3.2 Modern fire regimes and their controls

Fire regimes across North America's boreal forest and flammable tundra regions are tightly linked with weather and climate (Kasischke et al. 1995, 2002, Johnson 1996, Duffy et al.

2005, Hu et al. 2015, Young et al. 2017). The frequency and duration of blocking high-pressure ridges, which are in turn linked to teleconnections including the Pacific Decadal Oscillation (PDO) and El Nino Southern Oscillation (ENSO), strongly shape seasonal fuel moisture, fire-weather, and thus annual area burned (Johnson 1996, Hess et al. 2001, Duffy et al. 2005, Calef et al. 2015). In Alaska, the majority of area burned is from lightning-caused fires (Kasischke et al. 2002), with human ignitions quickly suppressed and thus contributing little to area burned relative to unmanaged fires (Kasischke and Turetsky 2006).

Climate drives fire activity through spatiotemporal variation in fuel abundance and fuel moisture, and through weather conditions conducive to ignitions and fire spread (Krawchuk et al. 2009, Moritz et al. 2012). Precipitation can regulate fire activity at multiple scales through its impacts both on fuel moisture and primary productivity, so it is important to characterize the interaction between precipitation and temperature to accurately characterize the influence of weather and climate on fire activity (Kasischke et al., 2002; Girardin et al., 2009; Krawchuk et al., 2009). Furthermore, empirical modeling of fire activity over annual to multi-decadal (i.e., 30-yr) timescales indicates that the relationship between climate and fire is strongly non-linear (Hu et al. 2015, Young et al. 2017). The probability of a region experiencing fire over multi-decadal time scales (e.g., similar to those resolved in lake-sediment records) can change abruptly over small variations in summer temperature and annual moisture availability when climate conditions are close to biophysical thresholds to burning (Young et al. 2017).

### 2.3.3 Paleoclimate

To evaluate potential relationships between fire activity and millennial-scale climatic change, we rely on a recent summary of Holocene climate in northwestern North America (Kaufman et al. 2016) based on the freely available circumpolar Arctic Holocene climate proxy

database (Sundqvist et al. 2014). We present the composite of 26 lake-sediment proxy temperature reconstructions from Kaufman *et al.* (2016), which includes midge-inferred July air temperature (Clegg et al. 2011, Irvine et al. 2012), pollen-inferred air temperature (Szeicz et al. 1995, Bunbury and Gajewski 2009, Viau and Gajewski 2009), and temperature anomalies from other proxies (McKay et al. 2008) (Fig. 1). Together these paleoclimate proxies document significant spatiotemporal variability in climate throughout the Holocene, with most records documenting temperature variability of 1-2°C. Records showed general agreement in a mid-Holocene thermal maximum centered around 6000 yr BP, with annual mean temperatures 0.2-0.5° C warmer than the most recent millennium. Temperature reconstructions had the greatest variability in the early Holocene, but generally document a warming trend through the mid-Holocene and a cooling trend after ca. 6000 yr BP, in agreement with results from a global Holocene temperature reconstruction for 30-90° N latitude (Marcott et al. 2013). Because the 500-year, subcontinental resolution of this composite paleoclimate record is lower than that of our paleofire records, we interpret it cautiously and present it as the best available proxy for the average climatic conditions at any given time and location in our study. We do not present the effective moisture proxy published by Kaufman et al. (2016) because the diversity of proxy types used results in wide uncertainty and limited temporal variability in the record. As a record of decadal- to centennial-scale climatic variability over the last 1200 years, we also call on a composite reconstruction of annual growing season air temperatures based on living and subfossil tree-ring widths from the Gulf of Alaska ("GOA") (Wiles et al. 2014). The GOA record provides a climate proxy with substantially higher temporal resolution for the most recent millennium (i.e., annual vs. 500-year mean).

Attributing changes in fire activity to climate variability is limited by the coarse spatiotemporal resolution of the climate proxy, in the case of the composite record from Kaufman *et al.* (2016). While the GOA record improves resolution, it may represent the climate at some of the paleofire record locations more accurately than others (e.g., in the Copper River Basin vs. the Noatak). However, understanding the degree of synchrony in fire activity among regions has significant implications even in the absence of clear attribution to a specific broad-scale forcing. We take advantage of the coarse-scale variability in climate, vegetation and biophysical properties among our study regions in the modern record to infer the relative importance of broad-scale forcing versus local heterogeneity as mechanisms controlling spatiotemporal patterns in fire activity.

**2.3.4 Records of biomass burning and fire occurrence**

We utilize two metrics of fire activity commonly derived from sediment-charcoal records: estimates of biomass burning based on a metric of standardized charcoal accumulation rates (CHAR), and estimates of the timing of past fire occurrence inferred from significant peaks in CHAR. All 27 records used in this study were developed with virtually identical methods (Table 1), briefly summarized here. Sediment cores were collected from small (< 10 ha), deep (> 5 m) lakes with simple basin shapes and minimal inlets or outlets, using polycarbonate tubes fitted with a piston and/or modified Livingstone coring devices. Core tops were sampled in the field at continuous 0.5-1.0 cm intervals, and in the laboratory, cores were sampled in contiguous 0.25-0.5 cm intervals, with 0.5-3.0 $cm^3$ samples taken for charcoal analysis. Samples were treated with sodium metaphosphate, oxidized with sodium hypochlorite or hydrogen peroxide, and sieved to isolate macroscopic charcoal (> 150-180 um). Charcoal particles were counted at 10-40x with a stereomicroscope, and CHAR (pieces $cm^{-2}$ $year^{-1}$) was derived as the product of

charcoal concentrations (pieces $cm^{-3}$) and sediment accumulation rates (cm $yr^{-1}$). Sediment accumulation rates were based on age-depth models, developed from $^{210}Pb$ (n = 26) and AMS $^{14}C$ dating of terrestrial macrofossils or concentrated charcoal particles. All records underwent a decomposition and peak analysis procedure by their original authors using the CharAnalysis software (github.com/phiguera/CharAnalysis), which separates background ("noise") from foreground ("signal") patterns in CHAR to identify statistically significant peaks. The estimated age of CHAR peaks is used to infer the timing of local fire events, interpreted as occurring within ~500-1000 m of a lake, based on simulation modeling and comparisons to modern fire activity (Higuera et al. 2007, Kelly et al. 2013). We made no changes to the chronologies or peak identification analysis from the original publications, and only used portions of the records from the past 10,000 years. As in the original publications, we also exclude (portions of) records with a signal-to-noise index < 3 from analyses calling upon peak identification (Kelly et al. 2011).

**2.3.5 Composite records of biomass burning**

We used CHAR data from multiple sites to develop an index of biomass burning at the landscape and biome scale. We produced composite records of biomass burning from networks of individual records using the method introduced by Kelly *et al.* (2013), which models CHAR as a zero-inflated log-normal process ("ZIL method"). The ZIL method avoids the Box-Cox transformation of CHAR, and the associated addition of an arbitrary constant to zero values, used by other approaches. The ZIL method thereby reduces the introduction of bias that can accompany these transformation, and preserves the natural distribution of CHAR data (log-normal with a high proportion of zero values, Fig. 2). To account for systematic differences in CHAR among individual sites, non-zero accumulation rates were temporarily log-transformed, rescaled within each site to a z-score (mean = 0, standard deviation = 1), and then returned to

their original domain through exponentiation. We estimated the parameters of ZIL distributions centered at continuous 10-year time steps using a Gaussian kernel-weighted smoothing function with 100-year and 500-year windows (overall median sample resolution = 9 yr). The index of biomass burning at each time step was the mean of 1000 bootstrapped mean parameter estimates, and 90% confidence intervals were derived from the $5^{th}$ and $95^{th}$ percentiles. We interpret changes in the 500-year mean estimate of biomass burning that exceed these confidence intervals to be statistically significant.

To quantify variability in biomass burning at the regional scale, we applied the ZIL method to networks of records within specific regions (Kobuk, n = 5; Copper River, n = 4; Yukon Flats, n = 14; and Noatak, n = 4). We developed an additional Alaska-wide composite record by applying the ZIL method to all the sites together (n = 27). Because the records contributing to our Alaska-wide composite were drawn from multiple regions containing different numbers of sites, we weighted every measure of charcoal accumulation such that each region contributed equally to the composite before estimating the mean of standardized CHAR using the ZIL method (Fig. 2).

**2.3.6 Fire event frequency**

To quantify synchrony in fire events within and among regions, we calculated the proportion of sites that recorded fire each century following the method presented by Calder *et al.* (2015). Within each region, we summed the number of fire events recorded in a 100-yr window, at continuous 10-year time steps, and divided that sum by the average number of sites recording within the window. This was done over all periods with at least two sites recording. There are a finite number of possible unique percentages with this metric, which is equivalent to

n sites + 1 if all records were of equal length; additionally, because a site can record more than one fire per century, the percentage of sites burned can exceed 100.

To account for the uncertainty in estimating the timing of fire events from CHAR, we resampled fire ages from a distribution of possible ages, based on the uncertainty associated with $^{210}$Pb and $^{14}$C dating. To quantify age uncertainty, but preserve the chronologies originally published with our records, we evaluated the age uncertainties in the published records and identified three modes in the standard deviation of all sample ages (Fig. S1). This analysis indicated a conservative estimate of age uncertainty would be a standard deviation of 25, 50 or 60 years for fires with estimated ages of 1000 – -50 yr BP, 4000 – 1000 yr BP, and 10,000 – 4000 yr BP, respectively. This estimate of chronological precision is conservative, because the uncertainty at any given depth in an age-depth model is constrained by age estimates for multiple samples. Here, we present the results of this analysis using a uniform standard deviation around resampled fire ages of 25 yr. Results using this value were comparable to our more conservative analysis.

We derived the median percentage of sites burned per century from the 50$^{th}$ percentile of 1000 simulations of possible combinations of fire ages, and used the 5$^{th}$ and 95$^{th}$ percentile of these simulations to estimate 90% confidence intervals. We calculated an Alaska-wide version of this metric that reflects each region equally, regardless of the number of sites it included, by taking the 5$^{th}$, 50$^{th}$, and 95$^{th}$ percentiles of the regional values at each time step (i.e., the median and 95$^{th}$ percentile confidence interval of ~4000 percent burned values [4 regions x 1000 simulations]). Results are presented as a LOESS regression with a 100-yr window. For comparison to other fire regime metrics, a value of 50% of sites burned per century is analogous

to a 200-year fire rotation period (FRP) and a 200-yr point-based mean fire return interval (mFRI) (Johnson and Gutsell 1994, Calder et al. 2015).

In addition to the percent of sites burned per century, we also quantified fire event frequency by calculating FRI between every fire event, and the Alaskan-wide mean FRI. FRI were measured as the years between the estimated ages of consecutive fire events in a record, and the Alaska-wide mFRI is a 1000-yr LOWESS smooth of the mFRI calculated form all FRIs in a given 1000-yr period. Finally, we also present the ratio of composite biomass burning to the composite mFRI, interpreted as a metric of total biomass burned per fire event, or fire severity (Kelly et al. 2013).

### 2.3.7 Correlation analysis

To quantify the relationships among our fire and climate proxies, we conducted a pairwise correlation analysis between measure of fire activity and temperature proxies. We calculated a Pearson product-moment correlation coefficient between the Kaufman et al. (2016) composite temperature record and binned 500-year mean composite biomass burning, binned 500-year mFRI, and the percent of sites burned per century from 8000 – 0 yr BP. From 1200 – 0 yr BP we calculated correlation coefficients between decadal mean temperature from the GOA record and all three measures of fire activity.

## 2.4 Results

### 2.4.1 Composite records of biomass burning

Our Alaska-wide composite record of biomass burning showed significant high- and low-frequency variability during the Holocene. Biomass burning generally increased over the Holocene, with elevated periods centered at ca. 8000, 6000, 4000, and 1000 yr BP. Biomass burning increased from ca. 8000 to 6000 yr BP and remained relatively high throughout 6000 –

1000 yr BP, with the 500-year mean reaching its maximum value ca. 1000 yr BP, before declining briefly from ca. 1000-300 yr BP and then increasing through present. The 100-year mean biomass burning record also showed high variability, with four distinct peaks between ca. 6000 and 4000 yr BP, and again at 1000 yr BP. Both the 100-yr and 500-yr means were higher in the most recent decade sampled (centered at -50 yr BP) than at any other time in the Holocene.

Region-specific records of biomass burning likewise showed significant high- and low-frequency variability, both within and among regions (Fig. 4). The Noatak exhibited the greatest variability in biomass burning, with alternating high and low periods approximately every 1000 years. Biomass burning in the Kobuk region increased gradually over the Holocene, with distinct increases at ca. 8000 and 5000 yr BP. After decreasing slightly at ca. 3500 yr BP, biomass burning in the Kobuk region increased again at ca. 300 yr BP, which continued through present. The Yukon Flats composite increased in a similarly gradual fashion over the Holocene, with notable peaks at ca. 5000 and 3000 yr BP. The record reaches its maximum at ca. 1000 yr BP, before decreasing towards present. Biomass burning in the Copper River generally increased from ca. 7000-5000 yr BP and then declined until ca. 1500 yr BP when it temporarily increased, decreased, and then returned to an increasing trend ca. 300 yr BP that continued through present.

### 2.4.2 Fire event frequency

The Alaskan record of centennial-scale fire synchrony shows considerable high-frequency variability, with 0% of sites burned per century ca. 8000 yr BP and up 100% burned periodically throughout the Holocene (Fig. 5D). Fire synchrony had non-significant variability after accounting for radiometric dating uncertainty, with maxima near 100% throughout the Holocene. Region-specific records of fire synchrony also show considerable high-frequency variability through time, with long-term trends apparent only in the Kobuk and Yukon Flats

regions (Fig. S2). In the Kobuk region, synchrony in fire activity generally increased through ca. 5000 yr BP, and decreased after. Synchrony in the Yukon Flats was variable, showing no long-term trend until the mid-Holocene, when synchrony increased ca. 4000 yr BP. Synchrony in the Noatak was highly variable, with no long-term trend throughout the Holocene. The Copper River showed the lowest degree of synchrony with a notable maximum ca. 4000 yr BP, but no long-term trend. The Yukon Flats had the highest average rate of burning ($5^{th}$, $95^{th}$ percentiles) at 86% (0,152) of sites burned per century, while the Copper River had the lowest rate of burning at 42% (0, 100) of sites burned per century. This contrast is consistent with the relative differences between these regions in the modern record, where mean FRPs are 82 yr and 2178 yr respectively (Young et al. 2017). Clearly, however, the Copper River experienced significantly more fire activity throughout the Holocene than during the observational period.

### 2.4.3 Correlation analyses

Relationships between fire and the temperature records varied by proxy. The Alaskan composite mFRI was positively correlated with and temperature ($r = 0.79$, $p < 0.001$), indicating that the time between fires increased with increasing temperature over the Holocene. The percent of sites burned per century was positively correlated to our measure of fire severity ($r = 0.62$, $p = 0.01$). Biomass burning and the percent of sites burned per century both uncorrelated with temperature ($r = -0.43$, $p = 0.058$ and $r = -0.32$, $p = 0.170$, respectively). Over the past 1200 years, the percent of sites burned and fire severity were both positively correlated with decadal mean temperature ($r = 0.54$, $p = 0.006$, and $r = 0.44$, $p = 0.032$, respectively), but biomass burning was only weakly correlated with temperature ($p = 0.045$).

## 2.5 Discussion

We hypothesized that changes in broad-scale drivers of fire activity, like climate change, would facilitate synchronous changes in biomass burning and potentially simultaneous high fire activity among regions. In contrast, spatiotemporal variability in climate change or heterogeneity in landscape-scale drivers of fire would result in variability in biomass burning among regions. Our results complement pervious findings from regional studies and provide evidence that both climate and biome-scale vegetation change drove millennial-scale changes in biomass burning. However, at centennial time scales, we found that synchronous burning across regions was rare during the Holocene, likely due to the muting of broad-scale forcing by local variation in vegetation and ecosystem properties, or high local variability in the signal of broad-scale trends.

### 2.5.1 Direct climatic controls of fire

Our Alaskan composite record highlights significant shifts in biomass burning during the Holocene, occurring in conjunction with millennial-scale changes in climate and vegetation. This record provides a single reference for the average trends in biomass burning across flammable ecosystems of Alaska. Biomass burning increased during relatively warm periods ca. 10,000-9000, and 8000-4000 yr BP, and decreased in conjunction with cooling from ca. 9000-8000 and 4000-2500 yr BP. At Holocene time scales, broad agreement between trends in biomass burning and temperature from ca. 10,000-2500 yr BP, even during a period of substantial vegetation change in the boreal forest biome, suggests that climate and vegetation both exerted substantial controls on biomass burning (Fig. 5A,C), likely through mechanisms of fuel abundance and flammability, from local to landscape scales (Macias-Fauria et al. 2011). At ca. 2500 yr BP the direct relationship between the Alaskan composite record of biomass burning and temperature estimates (Kaufman et al. 2016) degrades, as biomass burning increases and temperature

estimates decrease. Rather than a change in the dominant fire-climate relationship, this divergence may reflect spatial heterogeneity in climate change, or coarsely resolved temperature proxies (Barrett et al. 2013). The 500-year, subcontinental resolution of the Holocene climate record (Kaufman et al. 2016) may not be adequately resolve to capture the centennial-scale climate variability that characterized the late-Holocene. Annual temperature anomalies from tree-ring records (Wiles et al. 2014), in contrast, are generally positively correlated with biomass burning over the past 1200 years, including maxima during the Medieval Climate Anomaly (MCA. ca. 1000-600 yr BP), and subsequent declines in biomass burning with temperature during the Little Ice Age (LIA, ca. 600-300 yr BP), in the Noatak, Yukon Flats, and Copper River. Disagreement between the two paleoclimate records limits our ability to attribute increases in biomass burning from ca. 1500-1000 yr BP to directional climate forcing, but suggests spatial heterogeneity in climate in the study area and the possibility that centennial- to millennial-scale climate variability was less directly linked with fire activity than annual- to decadal-scale variability.

Regional trends in biomass burning were also qualitatively correlated with climate variability, but sensitivity to climate appears to have varied through time. Fire activity in the Copper River and in the Noatak regions showed significant millennial-scale sensitivity to climate, evidence by periods of elevated biomass burning under the relatively warm temperatures of the mid-Holocene thermal maximum centered at ca. 6000 yr BP. The Yukon Flats, Copper River, and Noatak regions showed centennial-scale maxima during the MCA, suggesting sensitivity to MCA warming likely occurred outside of the previously documented response in the Yukon Flats (Kelly et al. 2013). Biomass burning peaked during the MCA a few centuries earlier in the Noatak and Copper River regions, relative to the Yukon Flats, but changes in

biomass burning in all three regions correspond strongly with positive temperature anomalies in the GOA during the MCA and negative anomalies during the LIA.

The Noatak showed the highest variability in biomass burning among regions, with abrupt increases/decreases every ca. 1000 years. This variability may be an artifact of the overall lower charcoal accumulation rates in these records relative to boreal forest records (Higuera et al. 2011a), but it suggests the possibility of high sensitivity of tundra biomass burning to climate variability. Fire-climate relationships estimated from modern observational records in both boreal forest and tundra ecosystems are strongly non-linear, with distinct temperature thresholds to burning (Hu et al. 2015, Young et al. 2017). The high variability in biomass burning in the Noatak relative to the other regions may stem from the region's proximity to a temperature threshold to burning, such that small changes in temperature can results in large changes in the probability of burning (Young et al. 2017). Statistical modeling suggests that regions well above temperature thresholds to burning (+1-2°C) will have high probabilities of fire, regardless of decadal- to centennial-scale climate variability, and may therefore be limited more by landscape flammability or ignitions than by climatic conditions. Conversely, systems that are near temperature thresholds may show greater sensitivity to climatic variability (Young et al., in preparation).

Our regional records of fire synchrony all document short periods of simultaneous fire activity among sites, but when combined into a composite they display little evidence of widespread synchrony in fire activity across Alaska. Furthermore, the coupling between climate and fire suggested by the trends in biomass burning described above do not emerge in the long-term pattern of fire synchrony across Alaska. Abrupt increases in biomass burning during the warm MCA were significant in the Copper River and Noatak regions, but our results do not

show a clear pattern in fire synchrony of mFRI. This pattern suggests that the increases in biomass burning per fire event (i.e., a metric of fire severity) under anomalously warm conditions proposed Kelly *et al.* (2013) may have occurred in other boreal forest and tundra regions as well. Composite paleofire records from the eastern boreal forest display similar patterns, where biomass burning increased over the last 2000 years while frequency (the inverse of mFRI) did not (Ali et al. 2012). There, increases in the ratio of biomass burning to fire frequency were interpreted as reflective of mean fire size, but the authors note the co-varying nature of fire frequency and mean fire size.

The low temporal resolution and proxy-related uncertainty of climate reconstructions for Alaska limit our ability to infer climatic forcing of fire activity throughout the Holocene. Modern observations indicate strong spatial autocorrelation in climate across Alaska, but heterogeneity in local climate could have also contributed to variability in biomass burning and synchrony in fire activity during the Holocene, without being reflected in multi-century, biome-wide anomalies. Such a pattern could potential mask any direct impacts of climate on fire activity. Alternatively, the absence of any prolonged periods of synchronous fire activity across Alaska could indicate that the magnitude of post-glacial climate variability was never extreme enough to initiate synchronous increases in fire activity across multiple regions. Wide uncertainty also reveals the challenges of detecting centennial-scale fire synchrony from paleofire datasets, due to the inherent uncertainty in age-depth models. Our uncertainty estimate is conservative, so a lack of statistically significant periods of fire synchrony across Alaska may indicate a temporal precision to accurately detect synchrony at centennial scales, rather than a true lack of synchrony in fire activity across landscapes or regions.

### 2.5.2 Vegetation-mediated control of fire and limits to synchronous burning

Increased biomass burning in the boreal forest (Kobuk, Yukon Flats and Copper River regions) during the period of black spruce expansion 7000-4000 yr BP supports previous evidence that biome-scale changes in vegetation can initiate widespread shifts in biomass burning (Lynch et al. 2004, Brubaker et al. 2009, Higuera et al. 2009, Kelly et al. 2013). The contrasting trends in biomass burning between the Noatak and boreal forest regions (Kobuk, Yukon Flats, Copper River) suggests that vegetation change was a more important driver of fire-regime variability in boreal forest than in tundra. The Noatak was not characterized gradual increases in biomass burning as in the boreal forest, but punctuated periods of elevated burning lasting ~1000 years. *Picea glauca* and *Alnus* expanded into northwestern Alaska to form a mix of shrub and open woodland ecosystems during in the early Holocene (Anderson 1988, Anderson and Brubaker 1994), so all species present in modern tundra were present 8000-7000 yr BP (Higuera et al. 2011b). This is in contrast with the interior Alaska, where black spruce expanded 6000-4000 yr BP and eventually came to be a dominate tree species (Lynch et al. 2002, 2004, Anderson et al. 2003, Higuera et al. 2009). The change in fire activity after the arrival of black spruce is also evident in the degree of fire synchrony in the Kobuk and Yukon Flats regions, which increase coincident with the biome-scale change in landscape flammability that occurred with the establishment of the modern boreal forest ca. 6000-4000 yr BP in these regions (Fig. S2).

The high-frequency variability in biomass burning (Fig. 4) and absence of widespread fire-event synchrony among regions (Figs. S2, 5D) underscores the significant heterogeneity in fire activity across flammable ecosystems. Our results suggest that periods of high fire synchrony occur within a single or a few regions in any given century, but rarely (or never) in all regions at

once. The broad agreement in fire synchrony between the Kobuk and Yukon Flats regions highlights the impact of broad shifts in species composition on fire activity, but variations in regional weather, vegetation composition, soil moisture, permafrost, and topography likely impose significant limits to the extent of synchronous burning across Alaska. Although synchrony within any given region exceeded 100% for short periods of time, these periods did not occur at the same time across Alaska, resulting in a consistent upper limit to synchrony in fire events across Alaska near 100%. This limit points toward a potential negative feedback to high fire activity, where lower flammability in the decades following fire limits burning until ecosystems redevelop continuous, flammable fuels (Johnstone et al. 2010b, Mann et al. 2012, Kelly et al. 2013). Our findings agree with those from the eastern boreal forest, where drought-induced increases in fire activity over the last 200 years were only sustained for short periods, and the abundance of a young, low-flammability stands imposed a negative feedback to subsequent fire occurrence and spread for decades (Héon et al. 2014). While the self-limiting nature of fire is particularly strong in stand-replacing fire regimes, where live crown fuels are significantly reduced after fire, it has also been documented in mixed-conifer forests of the Rocky Mountains (Parks et al. 2016) and in the Sierra Nevada of California (Collins et al. 2009).

**2.6 Implications and Conclusions**

This synthesis provides a novel comparison of Holocene fire activity among flammable regions of Alaska, revealing the varying controls of fire at multiple spatial and temporal scales. Over millennial timescales, biophysical changes associated with deglaciation imposed key controls on biomass burning indirectly, through broad-scale vegetation shifts. At centennial time scales, however, fire regimes across Alaska were characterized by substantial heterogeneity. Increases in biomass burning were greater than declines in fire return intervals, particularly

during warm periods (Fig. 5C). This dynamic could indicate that increases in biomass burning from direct climate forcing manifest as increases in fire severity rather than increased fire occurrence. Ecosystem models indicate that, together with variability in fire frequency, fire severity accounted for as much as 84% of the variability in total carbon stocks in a boreal forest ecosystem over the past 1200 years, implicating fire, and fire severity, as a major driver of carbon dynamics in boreal forests ecosystems (Kelly et al. 2016). The apparent variability in fire severity over decadal to millennial scales challenges the steady-state initial conditions in fire activity typically used by ecosystem models, and indicates the potential for significantly different outcomes when empirically based fire data are used to drive the timing and characteristics of modeled disturbances.

Projections of fire activity for the 21$^{st}$ century, based on modern fire-climate relationships and GCM ensembles, indicate that climate conditions across Alaska will become more conducive to burning across nearly all of Alaska (Young et al. 2017). However, limits to the magnitude of fire synchrony among regions documented here suggest that regional heterogeneity may prevent synchronous increases in fire activity (Héon et al. 2014). Our results imply that widespread directional increases in fire activity may not manifest in the upcoming decades, but they do not ensure ecosystem resilience. Although negative feedbacks could ultimately dampen fire activity, that magnitude of vegetation change would result in ecosystems with significantly altered structural and functional characteristics at landscape scales. More work to define the "safe operating space" (Johnstone et al. 2016) for fire-regime variability in boreal forests and tundra ecosystems is required to anticipate whether high-latitude systems will retain their historic characteristics and continue to provide globally important ecosystem services into the future.

## 2.7 References


Ali, A. A., O. Blarquez, M. P. Girardin, C. Hély, F. Tinquaut, A. El Guellab, V. Valsecchi, A. Terrier, L. Bremond, A. Genries, S. Gauthier, Y. Bergeron, C. Hely, F. Tinquaut, A. El Guellab, V. Valsecchi, A. Terrier, L. Bremond, A. Genries, S. Gauthier, and Y. Bergeron. 2012. Control of the multimillennial wildfire size in boreal North America by spring climatic conditions. Proceedings of the National Academy of Sciences of the United States of America 109:20966–70.

Anderson, P. M. 1988. Late quaternary pollen records from the Kobuk and Noatak river drainages, northwestern Alaska. Quaternary Research 29:263–276.

Anderson, P. M., and L. B. Brubaker. 1994. Vegetation history of northcentral Alaska: a mapped summary of late-Quaternary pollen data. Quaternary Science Reviews 13:71–92.

Anderson, P. M., M. E. Edwards, and L. B. Brubaker. 2003. Results and paleoclimate implications of 35 years of paleoecological research in Alaska. Development in Quaternary Science 1:427–440.

Balshi, M. S., A. D. McGuire, P. Duffy, M. Flannigan, J. Walsh, and J. Melillo. 2009. Assessing the response of area burned to changing climate in western boreal North America using a Multivariate Adaptive Regression Splines (MARS) approach. Global Change Biology 15:578–600.

Barrett, C. M., R. Kelly, P. E. Higuera, and F. S. Hu. 2013. Climatic and land cover influences on the spatiotemporal dynamics of Holocene boreal fire regimes. Ecology 94:389–402.

Barrett, K., A. D. McGuire, E. E. Hoy, and E. S. Kasischke. 2011. Potential shifts in dominant forest cover in interior Alaska driven by variations in fire severity. Ecological Applications 21:2380–2396.

Bonan, G. B. 2008. Forests and climate change: forcings, feedbacks, and the climate benefits of forests. Science 320:1444–1449.

Bond-Lamberty, B., S. D. Peckham, D. E. Ahl, and S. T. Gower. 2007. Fire as the dominant driver of central Canadian boreal forest carbon balance. Nature 450:89.

Bowman, D. M. J. S., J. K. Balch, P. Artaxo, W. J. Bond, J. M. Carlson, M. A. Cochrane, C. M. D'Antonio, R. S. DeFries, J. C. Doyle, S. P. Harrison, F. H. Johnston, J. E. Keeley, M. A. Krawchuk, C. A. Kull, J. B. Marston, M. A. Moritz, I. C. Prentice, C. I. Roos, A. C. Scott, T. W. Swetnam, G. R. van der Werf, and S. J. Pyne. 2009. Fire in the Earth System. Science 324:481–484.

Brown, C. D., and J. F. Johnstone. 2012. Once burned, twice shy: Repeat fires reduce seed availability and alter substrate constraints on Picea mariana regeneration. Forest Ecology and Management 266:34–41.

Brubaker, L. B., P. E. Higuera, T. S. Rupp, M. A. Olson, P. M. Anderson, and F. S. Hu. 2009. Linking sediment-charcoal records and ecological modeling to understand causes of fire-regime change in boreal forests. Ecology 90:1788–1801.

Bunbury, J., and K. Gajewski. 2009. Postglacial climates inferred from a lake at treeline, southwest Yukon Territory, Canada. Quaternary Science Reviews 28:354–369.

Calder, W. J., D. Parker, C. J. Stopka, G. Jiménez-Moreno, and B. N. Shuman. 2015. Medieval warming initiated exceptionally large wildfire outbreaks in the Rocky Mountains. Proceedings of the National Academy of Sciences of the United States of America 112:13261–13266.

Calef, M. P., A. Varvak, A. D. McGuire, F. S. Chapin, and K. B. Reinhold. 2015. Recent changes in annual area burned in Interior Alaska: The impact of fire management. Earth Interactions:10.1175/EI-D-14-0025.1.

Chapin, F. S., A. D. Mcguire, J. Randerson, R. Pielke, D. Baldocchi, S. E. Hobbie, N. Roulet, W. Eugster, E. Kasischke, E. B. Rastetter, S. A. Zimov, and S. W. Running. 2000. Arctic and boreal ecosystems of western North America as components of the climate system. Global Change Biology 6:211–223.

Chipman, M. L., V. Hudspith, P. E. Higuera, P. A. Duffy, R. Kelly, W. W. Oswald, and F. S. Hu. 2015. Spatiotemporal patterns of tundra fires: Late-Quaternary charcoal records from Alaska. Biogeosciences 12:4017–4027.

Clegg, B. F., R. Kelly, G. H. Clarke, I. R. Walker, and F. S. Hu. 2011. Nonlinear response of summer temperature to Holocene insolation forcing in Alaska. Proceedings of the National Academy of Sciences of the United States of America 108:19299–19304.

Collins, B. M., J. D. Miller, A. E. Thode, M. Kelly, J. W. Van Wagtendonk, and S. L. Stephens. 2009. Interactions among wildland fires in a long-established Sierra Nevada natural fire area. Ecosystems 12:114–128.

Duffy, P. A., J. E. Walsh, J. M. Graham, D. H. Mann, and T. S. Rupp. 2005. Imapcts of Lage-Scale Atmospheric–Ocean Variability on Alaskan Fire Season Severity. Ecological Applications 15:1317–1330.

Flannigan, M., B. Stocks, M. Turetsky, and M. Wotton. 2009. Impacts of climate change on fire activity and fire management in the circumboreal forest. Global Change Biology 15:549–560.

Genet, H., A. D. McGuire, K. Barrett, A. Breen, E. S. Euskirchen, J. F. Johnstone, E. S. Kasischke, A. M. Melvin, A. Bennett, M. C. Mack, T. S. Rupp, A. E. G. Schuur, M. R. Turetsky, and F. Yuan. 2013. Modeling the effects of fire severity and climate warming on active layer thickness and soil carbon storage of black spruce forests across the landscape in interior Alaska. Environmental Research Letters 8:45016.

Grosse, G., J. Harden, M. Turetsky, A. D. McGuire, P. Camill, C. Tarnocai, S. Frolking, E. A. G. Schuur, T. Jorgenson, S. Marchenko, V. Romanovsky, K. P. Wickland, N. French, M. Waldrop, L. Bourgeau-Chavez, and R. G. Striegl. 2011. Vulnerability of high-latitude soil organic carbon in North America to disturbance. Journal of Geophysical Research: Biogeosciences 116:doi:10.1029/2010JG001507.

Héon, J., D. Arseneault, and M.-A. Parisien. 2014. Resistance of the boreal forest to high burn rates. Proceedings of the National Academy of Sciences of the United States of America 111:13888–13893.

Hess, J. C., C. A. Scott, G. L. Hufford, and M. D. Fleming. 2001. El Nino and its impact on fire weather conditions in Alaska. International Journal of Wildland Fire 10:1–13.

Higuera, P. E., J. L. Barnes, M. L. Chipman, and F. S. Hu. 2011a. The burning tundra: a look back at the last 6,000 years of fire in the Noatak National Preserve, northwestern Alaska. Alaska Park Science 10:36–41.

Higuera, P. E., L. B. Brubaker, P. M. Anderson, F. S. Hu, and T. A. Brown. 2009. Vegetation mediated the impacts of postglacial climate change on fire regimes in the south-central Brooks Range, Alaska. Ecological Monographs 79:201–219.

Higuera, P. E., M. L. Chipman, J. L. Barnes, M. A. Urban, and F. S. Hu. 2011b. Variability of tundra fire regimes in Arctic Alaska: Millennial-scale patterns and ecological implications.

Ecological Applications 21:3211–3226.
Higuera, P. E., M. E. Peters, L. B. Brubaker, and D. G. Gavin. 2007. Understanding the origin and analysis of sediment-charcoal records with a simulation model. Quaternary Science Reviews 26:1790–1809.
Hinzman, L., N. Bettez, W. R. Bolton, F. S. Chapin, M. Dyurgerov, C. Fastie, B. Griffith, R. Hollister, A. Hope, H. Huntington, A. Jensen, G. Jia, T. Jorgenson, D. Kane, D. Klein, G. Kofinas, A. Lynch, A. Lloyd, A. D. McGuire, F. Nelson, W. Oechel, T. Osterkamp, C. Racine, V. Romanovsky, R. Stone, D. Stow, M. Sturm, C. Tweedie, G. Vourlitis, M. Walker, D. Walker, P. Webber, J. Welker, K. Winker, and K. Yoshikawa. 2005. Evidence and Implications of Recent Climate Change in Northern Alaska and Other Arctic Regions. Climatic Change 72:251–298.
Hollingsworth, T. N., M. D. Walker, F. S. Chapin, and A. L. Parsons. 2006. Scale-dependent environmental controls over species composition in Alaskan black spruce communities. Canadian Journal of Forest Research 36:1781–1796.
Hu, F. S., L. B. Brubaker, D. G. Gavin, P. E. Higuera, J. A. Lynch, T. S. Rupp, and W. Tinner. 2006. How Climate and Vegetation Influence the fire Regime of the Alaskan Boreal Biome: The Holocene Perspective. Mitigation and Adaptation Strategies for Global Change 11:829–846.
Hu, F. S., P. E. Higuera, P. Duffy, M. L. Chipman, A. V Rocha, A. M. Young, R. Kelly, and M. C. Dietze. 2015. Arctic tundra fires: natural variability and responses to climate change. Frontiers in Ecology and the Environment 13:369–377.
Hu, F. S., P. E. Higuera, J. E. Walsh, W. L. Chapman, P. A. Duffy, L. B. Brubaker, and M. L. Chipman. 2010. Tundra burning in Alaska: Linkages to climatic change and sea ice retreat. Journal of Geophysical Research: Biogeosciences 115:1–8.
Irvine, F., L. C. Cwynar, J. C. Vermaire, and A. B. H. Rees. 2012. Midge-inferred temperature reconstructions and vegetation change over the last ~15,000 years from Trout Lake, northern Yukon Territory, eastern Beringia. Journal of Paleolimnology 48:133–146.
Johnson, E. A. 1996. Fire and vegetation dynamics: studies from the North American boreal forest. Cambridge University Press.
Johnson, E. A., and S. L. Gutsell. 1994. Fire Frequency Models, Methods and Interpretations. Pages 239–287 *in* M. Begon and A. H. Fitter, editors. Advances in Ecological Research. Academic Press.
Johnstone, J. F., C. D. Allen, J. F. Franklin, L. E. Frelich, B. J. Harvey, P. E. Higuera, M. C. Mack, R. K. Meentemeyer, M. R. Metz, G. L. W. Perry, T. Schoennagel, and M. G. Turner. 2016. Changing disturbance regimes, ecological memory, and forest resilience. Frontiers in Ecology and the Environment 14:369–378.
Johnstone, J. F., F. S. Chapin, T. N. Hollingsworth, M. C. Mack, V. Romanovsky, and M. Turetsky. 2010a. Fire, climate change, and forest resilience in interior Alaska. Canadian Journal of Forest Research 40:1302–1312.
Johnstone, J. F., T. N. Hollingsworth, F. S. Chapin, and M. C. Mack. 2010b. Changes in fire regime break the legacy lock on successional trajectories in Alaskan boreal forest. Global Change Biology 16:1281–1295.
Kasischke, E. S., N. L. Christensen Jr., and B. J. Stocks. 1995. Fire, Global Warming, and the Carbon Balance of Boreal Forests. Ecological Applications 5:437–451.
Kasischke, E. S., and J. F. Johnstone. 2005. Variation in postfire organic layer thickness in a

black spruce forest complex in interior Alaska and its effects on soil temperature and moisture. Canadian Journal of Forest Research 35:2164–2177.
Kasischke, E. S., and M. R. Turetsky. 2006. Recent changes in the fire regime across the North American boreal region—spatial and temporal patterns of burning across Canada and Alaska. Geophysical Research Letters 33:doi:10.1029/2006GL025677.
Kasischke, E. S., D. L. Verbyla, T. S. Rupp, A. D. McGuire, K. A. Murphy, R. Jandt, J. L. Barnes, E. E. Hoy, P. A. Duffy, M. Calef, and M. R. Turetsky. 2010. Alaska's changing fire regime — implications for the vulnerability of its boreal forests. Canadian Journal of Forest Research 40:1313–1324.
Kasischke, E. S., D. Williams, and D. Barry. 2002. Analysis of the patterns of large fires in the boreal forest region of Alaska. International Journal of Wildland Fire 11:131–144.
Kaufman, D. S., Y. L. Axford, A. C. G. Henderson, N. P. McKay, W. W. Oswald, C. Saenger, R. S. Anderson, H. L. Bailey, B. Clegg, K. Gajewski, F. S. Hu, M. C. Jones, C. Massa, C. C. Routson, A. Werner, M. J. Wooller, and Z. Yu. 2016. Holocene climate changes in eastern Beringia (NW North America): A systematic review of multi-proxy evidence. Quaternary Science Reviews 147:312–339.
Kelly, R., M. L. Chipman, P. E. Higuera, I. Stefanova, L. B. Brubaker, and F. S. Hu. 2013. Recent burning of boreal forests exceeds fire regime limits of the past 10,000 years. Proceedings of the National Academy of Sciences of the United States of America 110:13055–13060.
Kelly, R. F., P. E. Higuera, C. M. Barrett, and F. S. Hu. 2011. A signal-to-noise index to quantify the potential for peak detection in sediment–charcoal records. Quaternary Research 75:11–17.
Kelly, R., H. Genet, A. D. McGuire, and F. S. Hu. 2016. Palaeodata-informed modelling of large carbon losses from recent burning of boreal forests. Nature Climate Change 6:4–9.
Krawchuk, M. A., M. A. Moritz, M.-A. Parisien, J. Van Dorn, and K. Hayhoe. 2009. Global Pyrogeography: the Current and Future Distribution of Wildfire. PLoS ONE 4:e5102.
Lynch, J. A., J. S. Clark, N. H. Bigelow, M. E. Edwards, and B. P. Finney. 2002. Geographic and temporal variations in fire history in boreal ecosystems of Alaska. Journal of Geophysical Research 108:1–17.
Lynch, J. A., J. L. Hollis, and F. S. Hu. 2004. Climatic and landscape controls of the boreal forest fire regime: Holocene records from Alaska. Journal of Ecology 92:477–489.
Macias-Fauria, M., S. T. Michaletz, and E. A. Johnson. 2011. Predicting climate change effects on wildfires requires linking processes across scales. Wiley Interdisciplinary Reviews-Climate Change 2:99–112.
Mack, M. C., M. S. Bret-Harte, T. N. Hollingsworth, R. R. Jandt, E. A. G. Schuur, G. R. Shaver, and D. L. Verbyla. 2011. Carbon loss from an unprecedented Arctic tundra wildfire. Nature 475:489–92.
Mann, D. H., T. Scott Rupp, M. A. Olson, and P. A. Duffy. 2012. Is Alaska's boreal forest now crossing a major ecological threshold? Arctic, Antarctic, and Alpine Research 44:319–331.
Marcott, S. A., J. D. Shakun, P. U. Clark, and A. C. Mix. 2013. A Reconstruction of Regional and Global Temperature for the Past 11,300 Years. Science 339:1198 LP-1201.
Marlon, J. R., P. J. Bartlein, A.-L. Daniau, S. P. Harrison, S. Y. Maezumi, M. J. Power, W. Tinner, and B. Vanniére. 2013. Global biomass burning: a synthesis and review of Holocene paleofire records and their controls. Quaternary Science Reviews 65:5–25.

Marlon, J. R., R. Kelly, A.-L. Daniau, B. Vannière, M. J. Power, P. Bartlein, P. Higuera, O. Blarquez, S. Brewer, T. Brücher, A. Feurdean, G. Gil-Romera, V. Iglesias, S. Y. Maezumi, B. Magi, C. J. C. Mustaphi, and T. Zhihai. 2016. Reconstructions of biomass burning from sediment charcoal records to improve data-model comparisons. Biogeosciences 13:3225–3244.

McKay, N. P., D. S. Kaufman, and N. Michelutti. 2008. Biogenic silica concentration as a high-resolution, quantitative temperature proxy at Hallet Lake, south-central Alaska. Geophysical Research Letters 35:4–9.

Miller, G. H., R. B. Alley, J. Brigham-Grette, J. J. Fitzpatrick, L. Polyak, M. C. Serreze, and J. W. C. White. 2010. Arctic amplification: can the past constrain the future? Quaternary Science Reviews 29:1779–1790.

Moritz, M. A., M.-A. Parisien, E. Batllori, M. A. Krawchuk, J. Van Dorn, D. J. Ganz, and K. Hayhoe. 2012. Climate change and disruptions to global fire activity. Ecosphere 3:art49.

Nowacki, G. J., P. Spencer, M. Fleming, T. Brock, T. Jorgenson, and S. Geological. 2003. Unified Ecoregions of Alaska: 2001. Page Open-File Report. No. 2002-2.

O'Donnell, J. A., J. W. Harden, A. D. Mcguire, M. Z. Kanevskiy, M. T. Jorgenson, and X. Xu. 2011. The effect of fire and permafrost interactions on soil carbon accumulation in an upland black spruce ecosystem of interior Alaska: Implications for post-thaw carbon loss. Global Change Biology 17:1461–1474.

Parks, S. A., C. Miller, L. M. Holsinger, L. S. Baggett, and B. J. Bird. 2016. Wildland fire limits subsequent fire occurrence. International Journal of Wildland Fire 25:182–190.

Pastick, N. J., M. Rigge, B. K. Wylie, M. T. Jorgenson, J. R. Rose, K. D. Johnson, and L. Ji. 2014. Distribution and landscape controls of organic layer thickness and carbon within the Alaskan Yukon River Basin. Geoderma 230–231:79–94.

Randerson, J. T., H. Liu, M. G. Flanner, S. D. Chambers, Y. Jin, P. G. Hess, G. Pfister, M. C. Mack, K. K. Treseder, L. R. Welp, F. S. Chapin, J. W. Harden, M. L. Goulden, E. Lyons, J. C. Neff, E. a G. Schuur, and C. S. Zender. 2006. The impact of boreal forest fire on climate warming. Science 314:1130–1132.

Rocha, A. V, M. M. Loranty, P. E. Higuera, M. C. Mack, F. S. Hu, B. M. Jones, A. L. Breen, E. B. Rastetter, S. J. Goetz, and G. R. Shaver. 2012. The footprint of Alaskan tundra fires during the past half-century: implications for surface properties and radiative forcing. Environmental Research Letters 7:44039.

Shenoy, A., J. F. Johnstone, E. S. Kasischke, and K. Kielland. 2011. Persistent effects of fire severity on early successional forests in interior Alaska. Forest Ecology and Management 261:381–390.

Sundqvist, H. S., D. S. Kaufman, N. P. McKay, N. L. Balascio, J. P. Briner, L. C. Cwynar, H. P. Sejrup, H. Sepp, D. A. Subetto, J. T. Andrews, Y. Axford, J. Bakke, H. J. B. Birks, S. J. Brooks, A. De Vernal, A. E. Jennings, F. C. Ljungqvist, K. M. Rohland, C. Saenger, J. P. Smol, and A. E. Viau. 2014. Arctic Holocene proxy climate database - New approaches to assessing geochronological accuracy and encoding climate variables. Climate of the Past 10:1605–1631.

Szeicz, J. M., G. M. MacDonald, and A. Duk-Rodkin. 1995. Late Quaternary vegetation history of the central Mackenzie Mountains, Northwest Territories, Canada. Palaeogeography, Palaeoclimatology, Palaeoecology 113:351–371.

Turner, M. G. 2010. Disturbance and landscape dynamics in a changing world. Ecology 91:2833–2849.
Viau, A. E., and K. Gajewski. 2009. Reconstructing Millennial-Scale, Regional Paleoclimates of Boreal Canada during the Holocene. Journal of Climate 22:316–330.
Whitlock, C., P. E. Higuera, D. B. McWethy, and C. E. Briles. 2010. Paleoecological perspectives on fire ecology: revisiting the fire-regime concept. The Open Ecology Journal 3:6–23.
Wiles, G. C., R. D. D'Arrigo, D. Barclay, R. S. Wilson, S. K. Jarvis, L. Vargo, and D. Frank. 2014. Surface air temperature variability reconstructed with tree rings for the Gulf of Alaska over the past 1200 years. The Holocene 24:198–208.
Young, A. M., P. E. Higuera, P. A. Duffy, and F. S. Hu. 2017. Climatic thresholds shape northern high-latitude fire regimes and imply vulnerability to future climate change. Ecography 40:606–617.

## 2.8 Tables and Figures

**Table 1.** Modern climate and fire regimes in each study region. Temperatures are average January and July minimum and maximum values from the nearest meteorological station. Precipitation is the mean annual total. Fire rotation periods statistics are based on observed fire perimeter data from the Alaskan Interagency Coordination Center published by Young et al. (2016) and Rocha et al. (2012).

| Region | January min. (°C) | January max. (°C) | July min. (°C) | July max. (°C) | Annual precip. (mm) | Fire rotation period |
|---|---|---|---|---|---|---|
| Noatak | -26.9 | -17.2 | 7.3 | 19.4 | 391 | 425[a] |
| Kobuk | -29.2 | -20.3 | 9.4 | 20.7 | 361 | 163[b] |
| Yukon Flats | -33.2 | -23.8 | 10.7 | 22.9 | 167 | 82[b] |
| Copper River | -25.7 | -16.4 | 7.9 | 20.2 | 280 | 2178[b] |

[a]Rocha et al. 2012
[b]Young et al. 2017

**Table 2.** Summary of paleofire records used in this synthesis.

| Site | Code | Ecoregion | Median resolution (yr) | Start (yr BP) | End (yr BP) | Latitude | Longitude | Publication | Peak Analysis |
|---|---|---|---|---|---|---|---|---|---|
| Code | CO | Kobuk Ridges and Valleys | 16 | -33 | 7426 | 67.16 | -151.86 | Higuera et al. 2009 | Yes |
| Last Chance | LC | Kobuk Ridges and Valleys | 7 | -52 | 2972 | 67.13 | -150.75 | Higuera et al. 2007 | Yes |
| Rupert | RU | Kobuk Ridges and Valleys | 11 | -50 | 10245 | 67.07 | -154.25 | Higuera et al. 2009 | Yes |
| Wild Tussock | WK | Kobuk Ridges and Valleys | 13 | -12 | 7834 | 67.14 | -151.51 | Higuera et al. 2009 | Yes |
| Xindi | XI | Kobuk Ridges and Valleys | 21 | -52 | 10232 | 67.11 | -152.49 | Higuera et al. 2009 | No |
| Crater | CR | Copper River Basin | 13 | -56 | 7000 | 62.10 | -146.24 | Barrett et al. 2013 | Partial |
| Hudson | HD | Copper River Basin | 9 | -55 | 7000 | 61.90 | -145.67 | Barrett et al. 2013 | Yes |
| Minnesota Plateau | MP | Copper River Basin | 17 | -52 | 7000 | 62.32 | -146.15 | Barrett et al. 2013 | No |
| Super Cub | SC | Copper River Basin | 12 | -57 | 6780 | 62.30 | -145.35 | Barrett et al. 2013 | Yes |
| Little Issac | LI | Kobuk Ridges and Valleys | 13 | -50 | 8552 | 67.94 | -160.80 | Higuera et al. 2011a/b | Yes |
| Poktovik | PO | Kobuk Ridges and Valleys | 9 | -55 | 5296 | 68.03 | -161.38 | Higuera et al. 2011a/b | Yes |
| Raven | RA | Kobuk Ridges and Valleys | 8 | -57 | 6270 | 68.01 | -162.04 | Higuera et al. 2011a/b | Yes |
| Uchugrak | UC | Kobuk Ridges and Valleys | 8 | -56 | 6784 | 68.05 | -161.73 | Higuera et al. 2011a/b | Yes |
| Chopper | CP | Yukon-Old Crow | 4 | -56 | 1560 | 66.00 | -146.28 | Kelly et al. 2013 | Yes |
| Epilobium | EP | Yukon-Old Crow | 9 | -58 | 3704 | 65.97 | -145.57 | Kelly et al. 2013 | Yes |
| Granger | GA | Yukon-Old Crow | 9 | -58 | 4831 | 66.06 | -145.65 | Kelly et al. 2013 | Yes |
| Jonah | JA | Yukon-Old Crow | 5 | -58 | 3216 | 66.07 | -145.08 | Kelly et al. 2013 | Yes |
| Landing | LD | Yukon-Old Crow | 20 | -56 | 7245 | 65.90 | -145.78 | Kelly et al. 2013 | Yes |
| Latitude | LT | Yukon-Old Crow | 6 | -57 | 2887 | 65.93 | -146.14 | Kelly et al. 2013 | Yes |
| Lucky | LU | Yukon-Old Crow | 5 | -58 | 1863 | 66.02 | -145.53 | Kelly et al. 2013 | Yes |
| Noir | NR | Yukon-Old Crow | 2 | -53 | 1113 | 66.00 | -145.93 | Kelly et al. 2013 | Yes |
| Picea | PI | Yukon-Old Crow | 16 | -57 | 10232 | 65.88 | -145.59 | Kelly et al. 2013 | Yes |
| Reunion | RE | Yukon-Old Crow | 8 | -59 | 5394 | 66.01 | -146.11 | Kelly et al. 2013 | Yes |
| Robinson | RO | Yukon-Old Crow | 6 | -57 | 2109 | 65.97 | -145.70 | Kelly et al. 2013 | Yes |
| Screaming Lynx | SL | Yukon-Old Crow | 7 | -56 | 10250 | 66.07 | -145.40 | Kelly et al. 2013 | Yes |
| West Crazy | WC | Yukon-Old Crow | 2 | -56 | 2770 | 65.89 | -145.62 | Kelly et al. 2013 | Yes |
| Windy | WI | Yukon-Old Crow | 7 | -57 | 2803 | 66.04 | -145.75 | Kelly et al. 2013 | Yes |

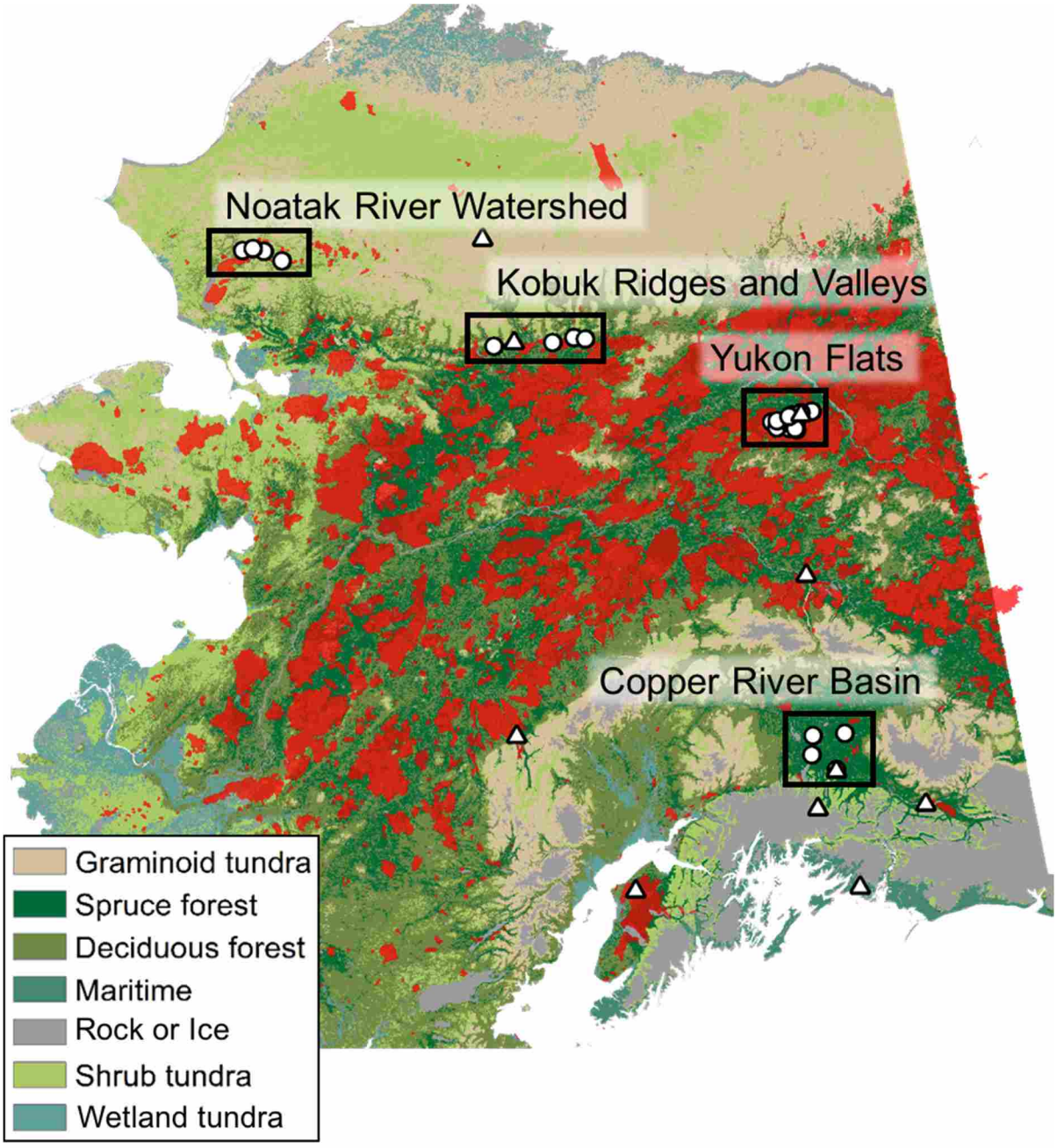


**Figure 1**. Locations of paleofire and paleoclimate component records across Alaska. White circles are paleofire records, white triangles are paleoclimate records, and red areas are observed fire perimeters from 1950-2014. Labels identify four regions of study, and colors represent dominant vegetation type as described in legend (simplified from National Land Cover Dataset 2005).

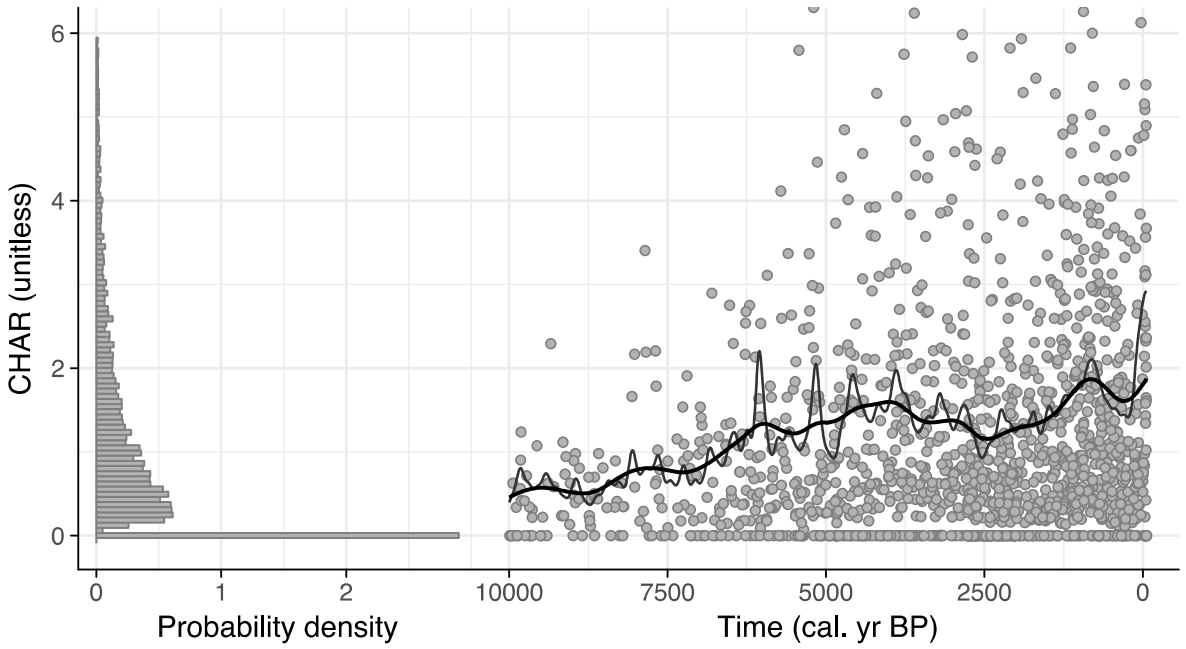


**Figure 2.** Distribution and mean estimation of standardized CHAR. CHAR can be modeled as a zero-inflated log-normal process because they are derived from discrete count data.

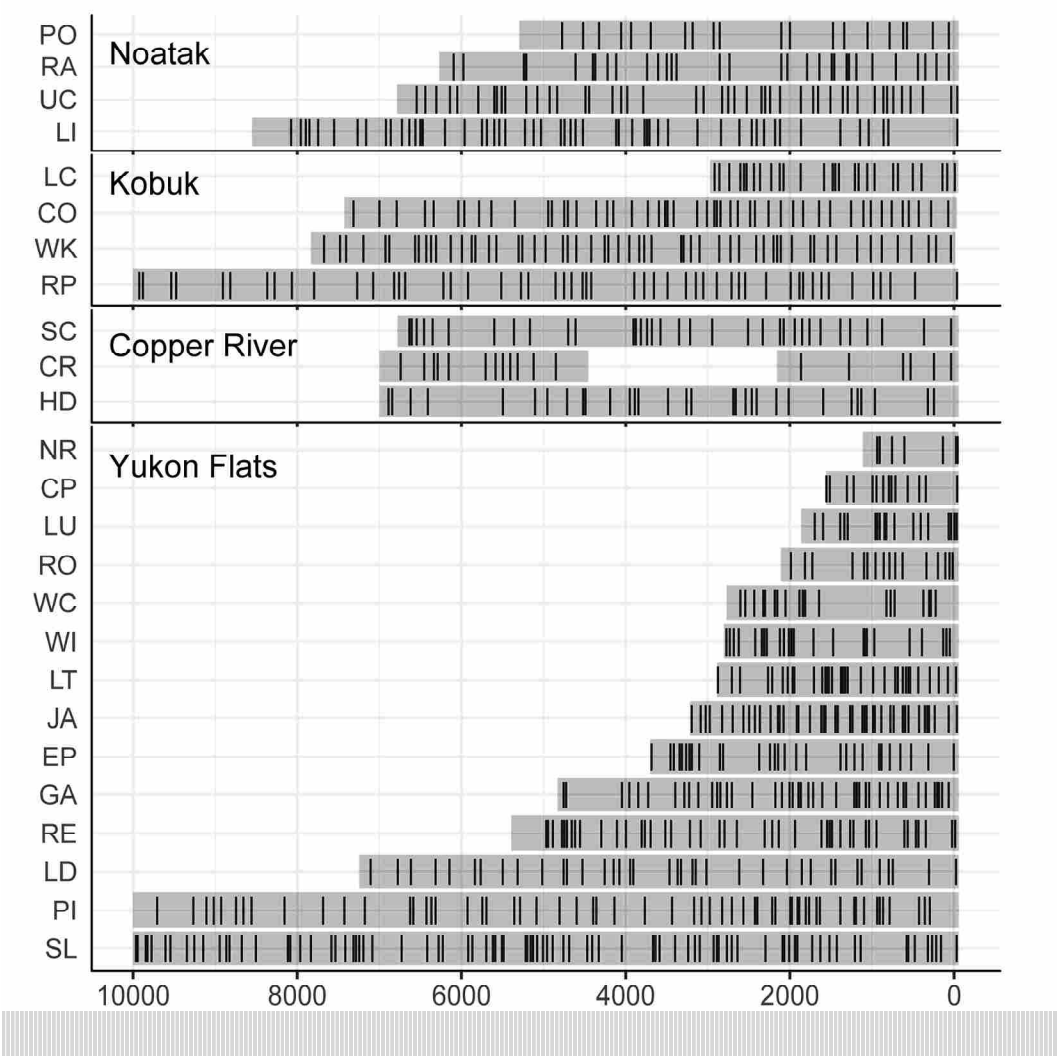


**Figure 3**. Paleofire records used in this synthesis. Each horizontal line represents and individual paleofire record, grouped by region. Gray bars indicate the temporal range of each record, and black vertical ticks indicate the timing of peaks in charcoal accumulation rates, inferred as local fire events. For lake names associated with two-letter code, see Table 1.

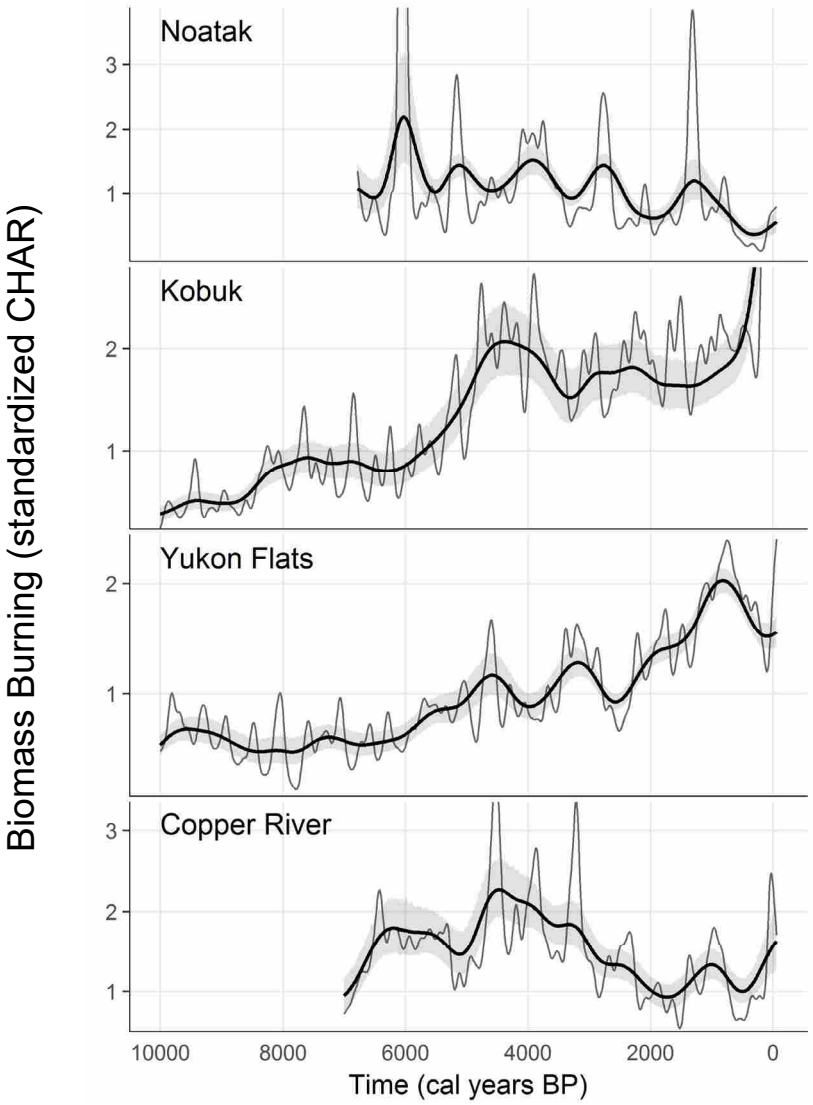


**Figure 4.** Composite records of biomass burning within each study region. The black curves indicate biomass burning at 500-yr timescales, the thin grey lines shows 100-yr mean biomass burning, and the grey band is a bootstrapped 90% CI.

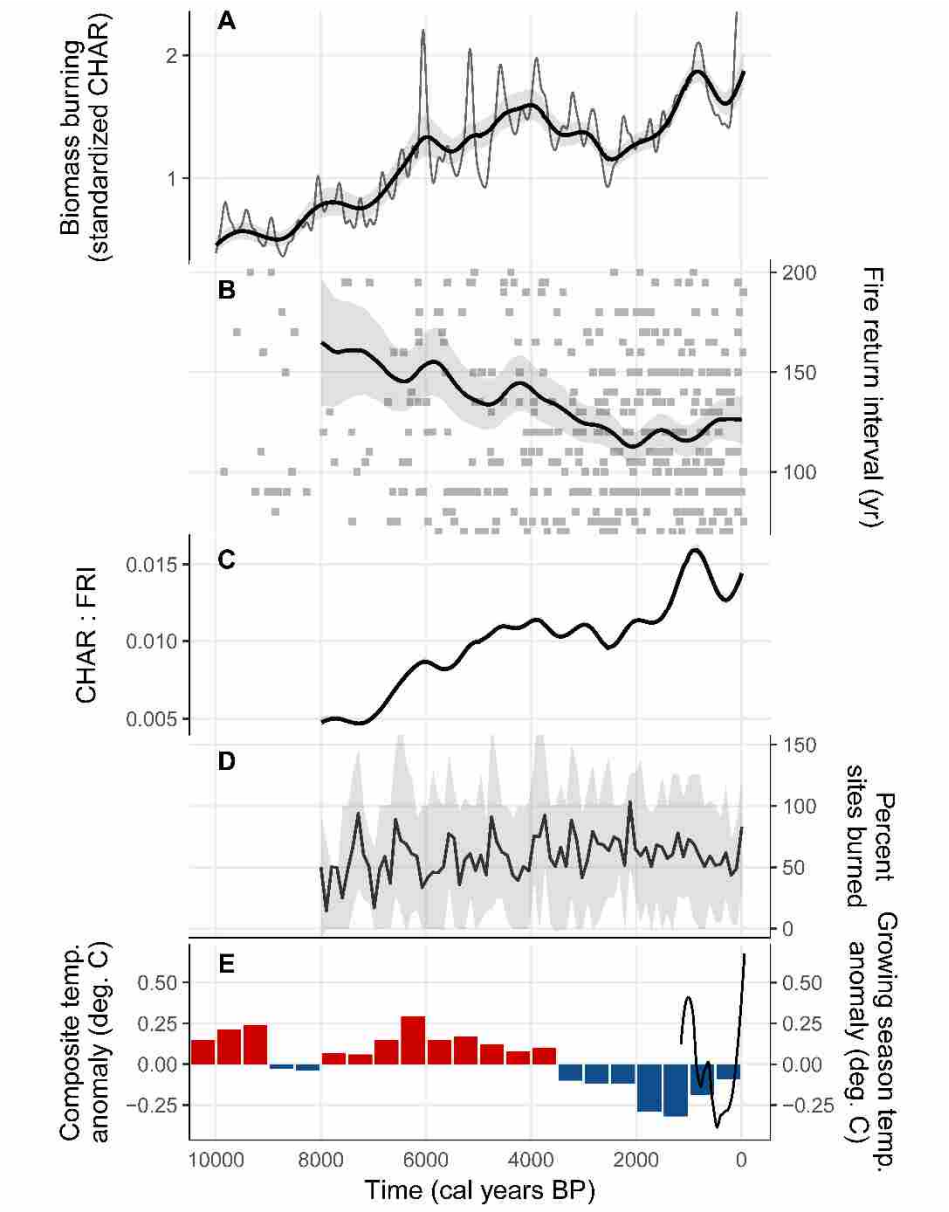


**Figure 5.** Composite fire and climate proxies for Alaska during the Holocene. From top to bottom: thin line shows 100-year mean and thick line shows 500-year mean biomass burning (standardized CHAR), grey band is bootstrapped 90% confidence intervals; grey squares are fire events and time since previous fire (FRI, yr), thick line is 1000-year mFRI and 90% bootstrapped confidence interval; black line is ratio of CHAR to FRI (fire severity); black line is median percent sites burned per century with 90% confidence intervals based on simulated age uncertainty; colored bars are composite proxy air temperature (Kaufman et al, 2016) and line is tree-ring based growing season temperature (Wiles et al 2014).

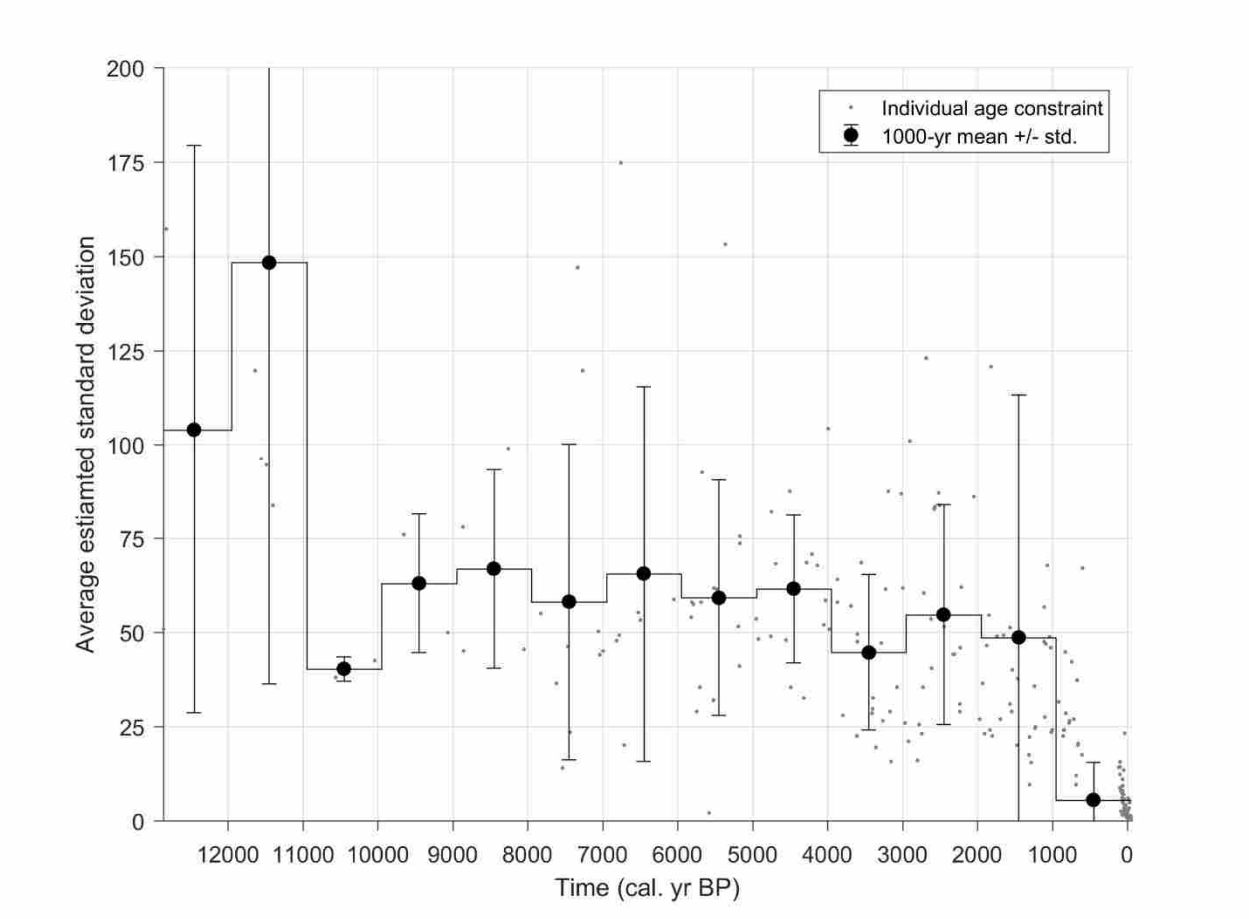


**Figure S1**. Standard deviations around radiometric ages from all published records used in this analysis. Dots represent the standard deviation for each calibrated $^{14}C$ date or $^{210}Pb$-based age estimate, based on the 95% confidence intervals in the published records.

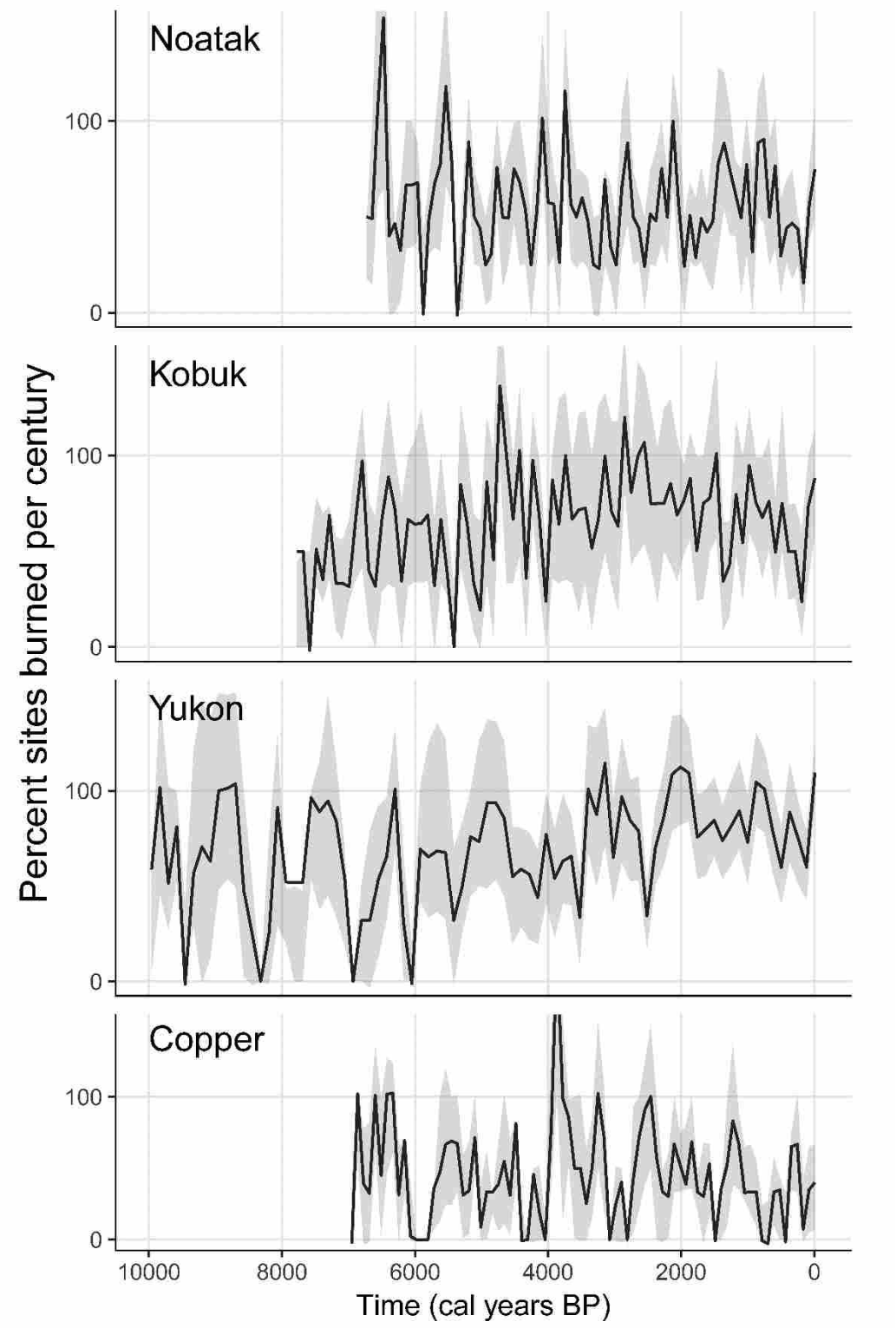


**Figure S2.** Percent of sites burned per century, within each region. The solid line indicates the median of 1000 simulations incorporating age uncertainty, while the dashed line indicates % of sites burned without accounting for age uncertainty.

## 3.0 Appendix

Complete age-depth models corresponding core images for records presented in Chapter 1.

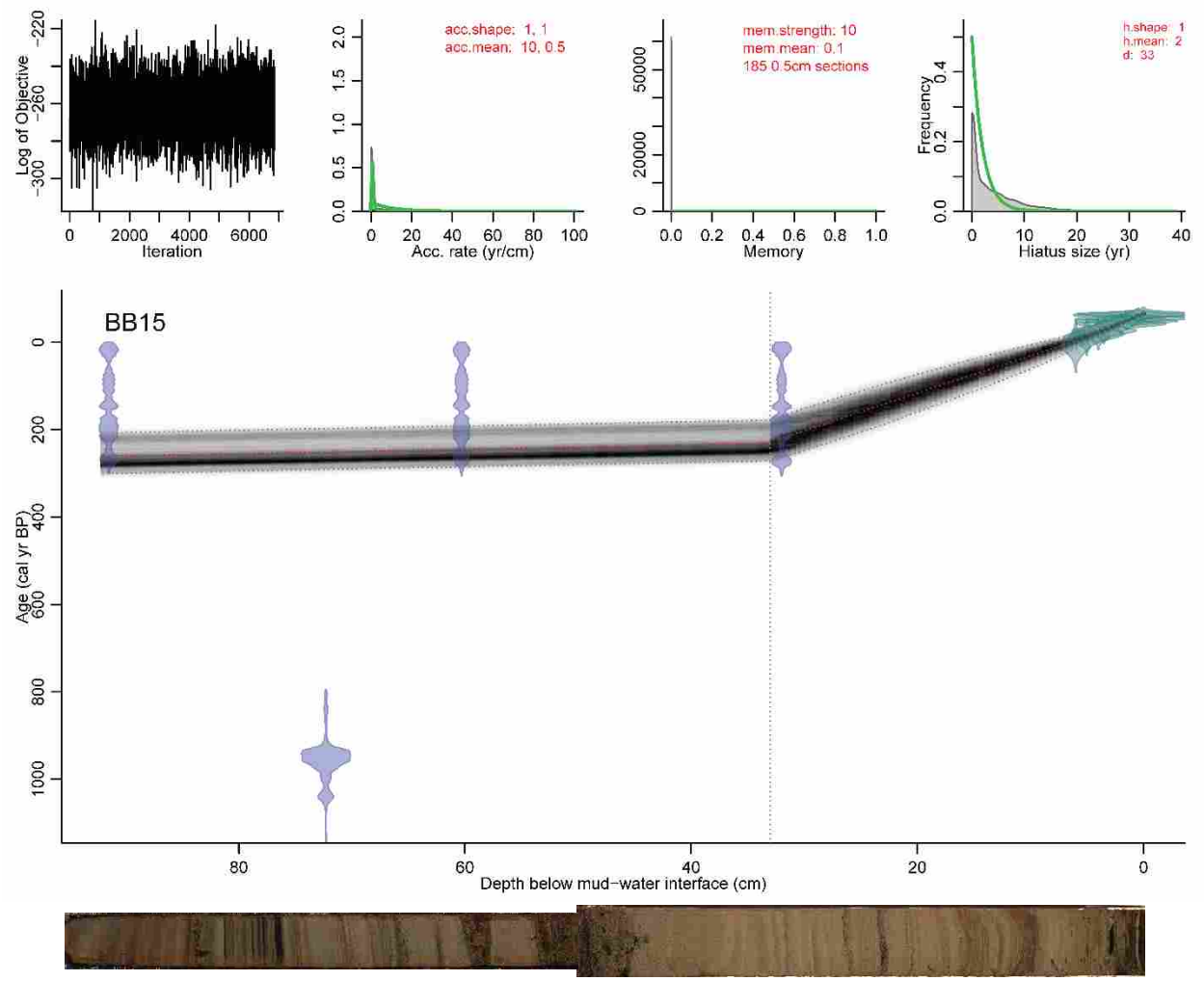


**Figure 1.** Buster Brown Lake (BB15) chronology and core. Hiatus depth is based on radiocarbon ages and distinct change laminated to unlaminated sediment at 32 cm core depth.

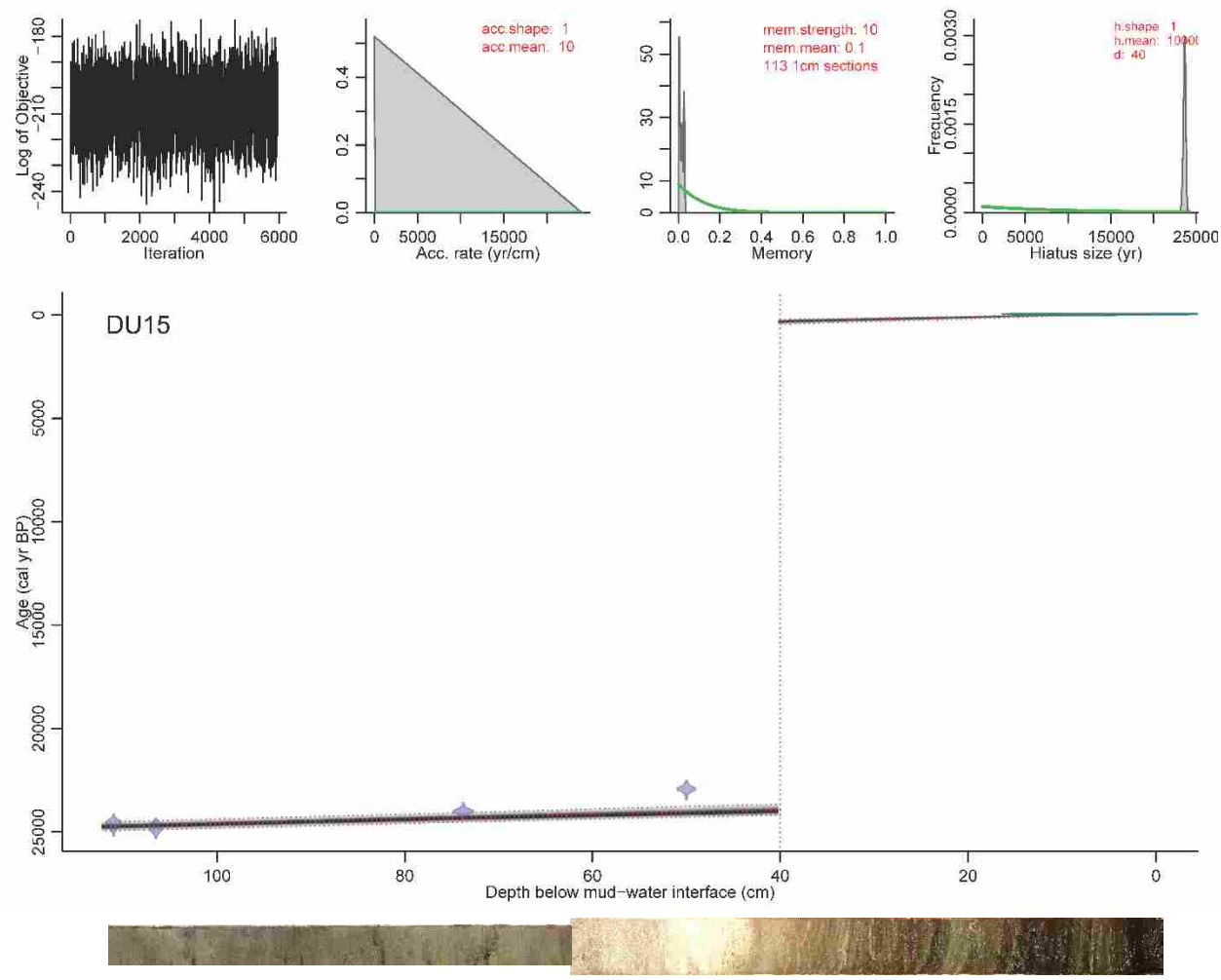


**Figure 2.** Duffy Lake (DU15) chronology and core. Hiatus depth is based on change from laminated to unlaminated sediment at 40 cm core depth.

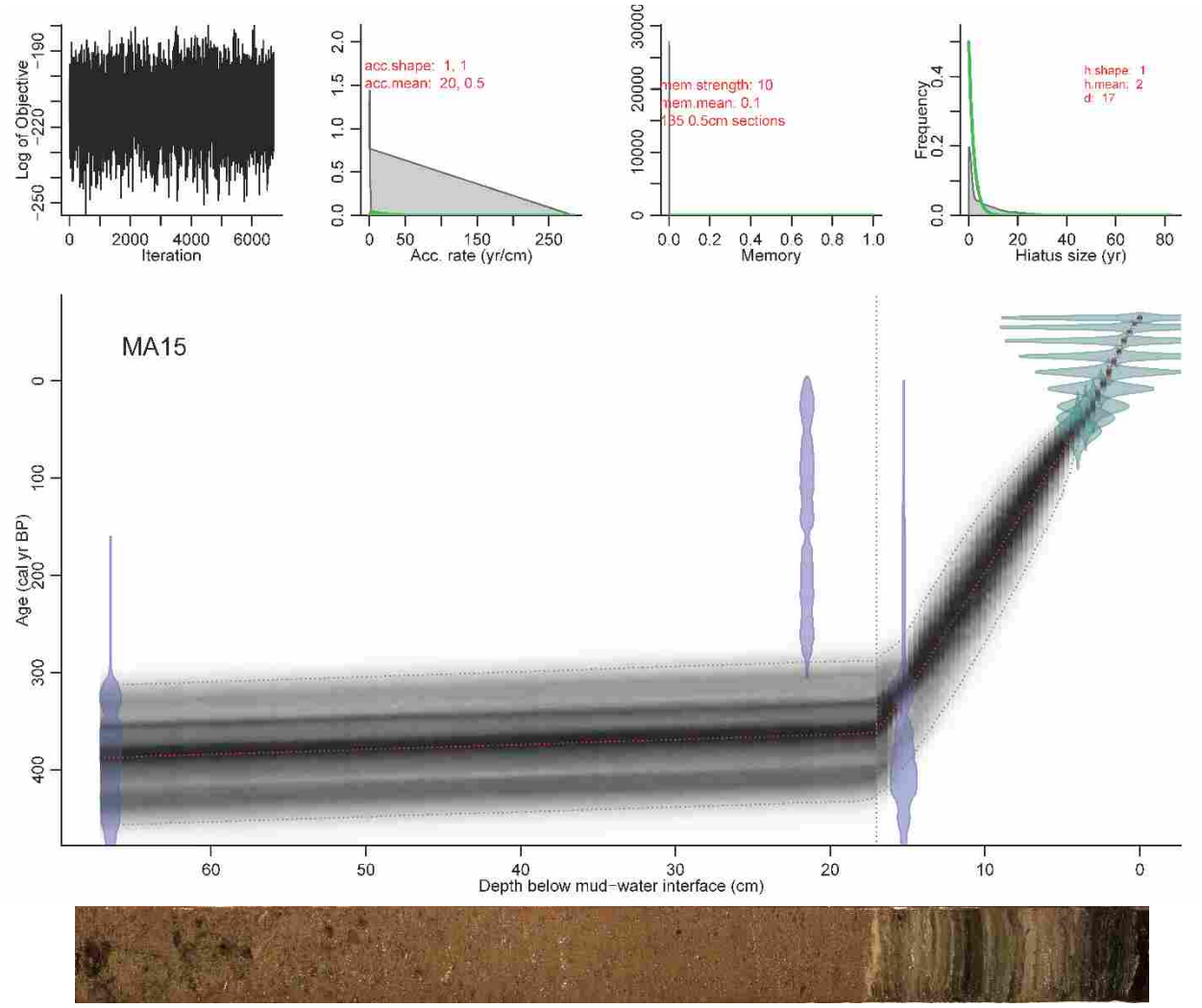


**Figure 3.** Macchiato Lake (MA15) chronology and core. Hiatus depth is based on radiocarbon ages and distinct change from laminated to unlaminated sediment at 16 cm core depth.

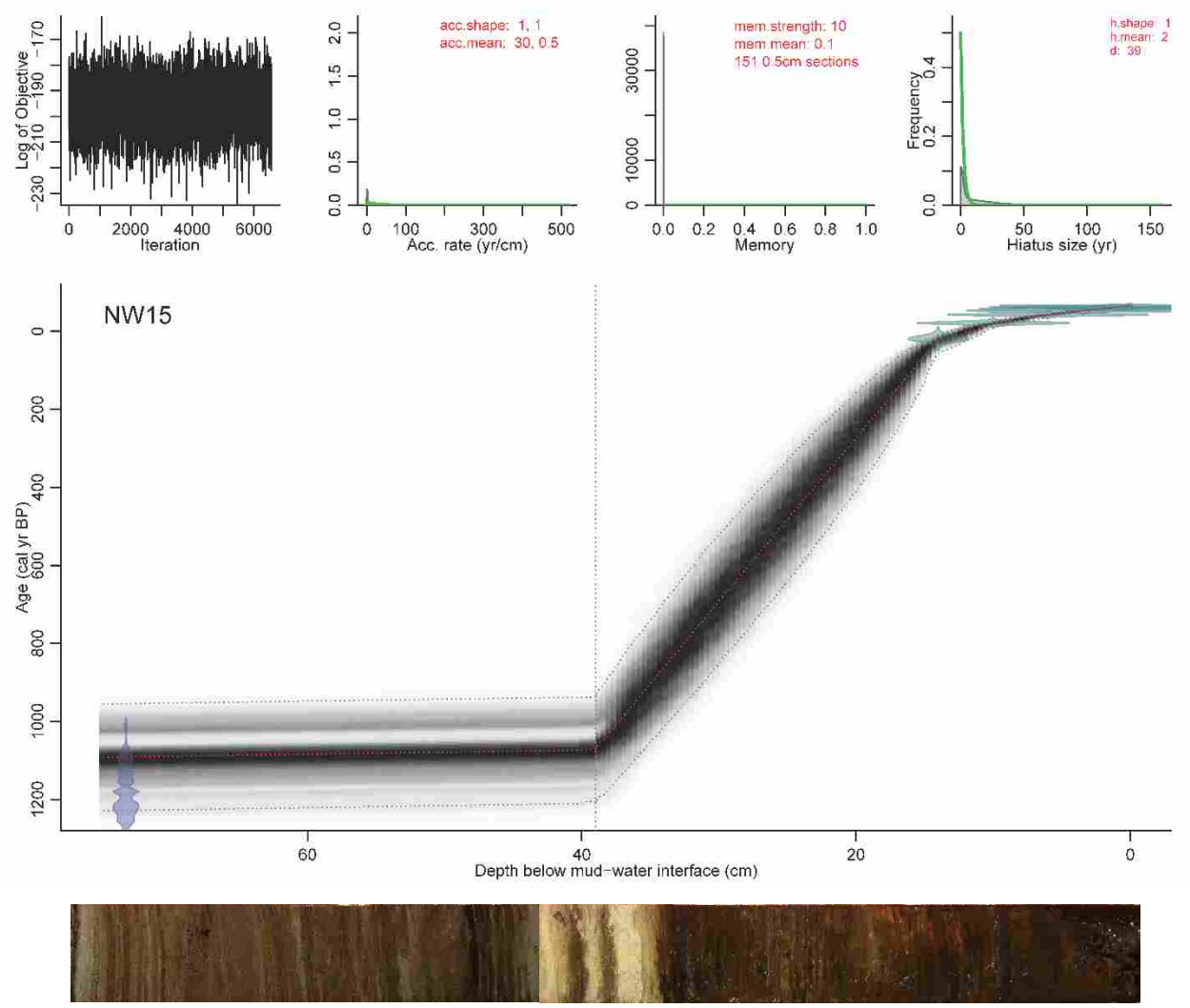


**Figure 4.** Nodwell Lake (NW15) chronology with hiatus at 39 cm based on change in charcoal concentration. This is the chronology presented in Chapter 1.

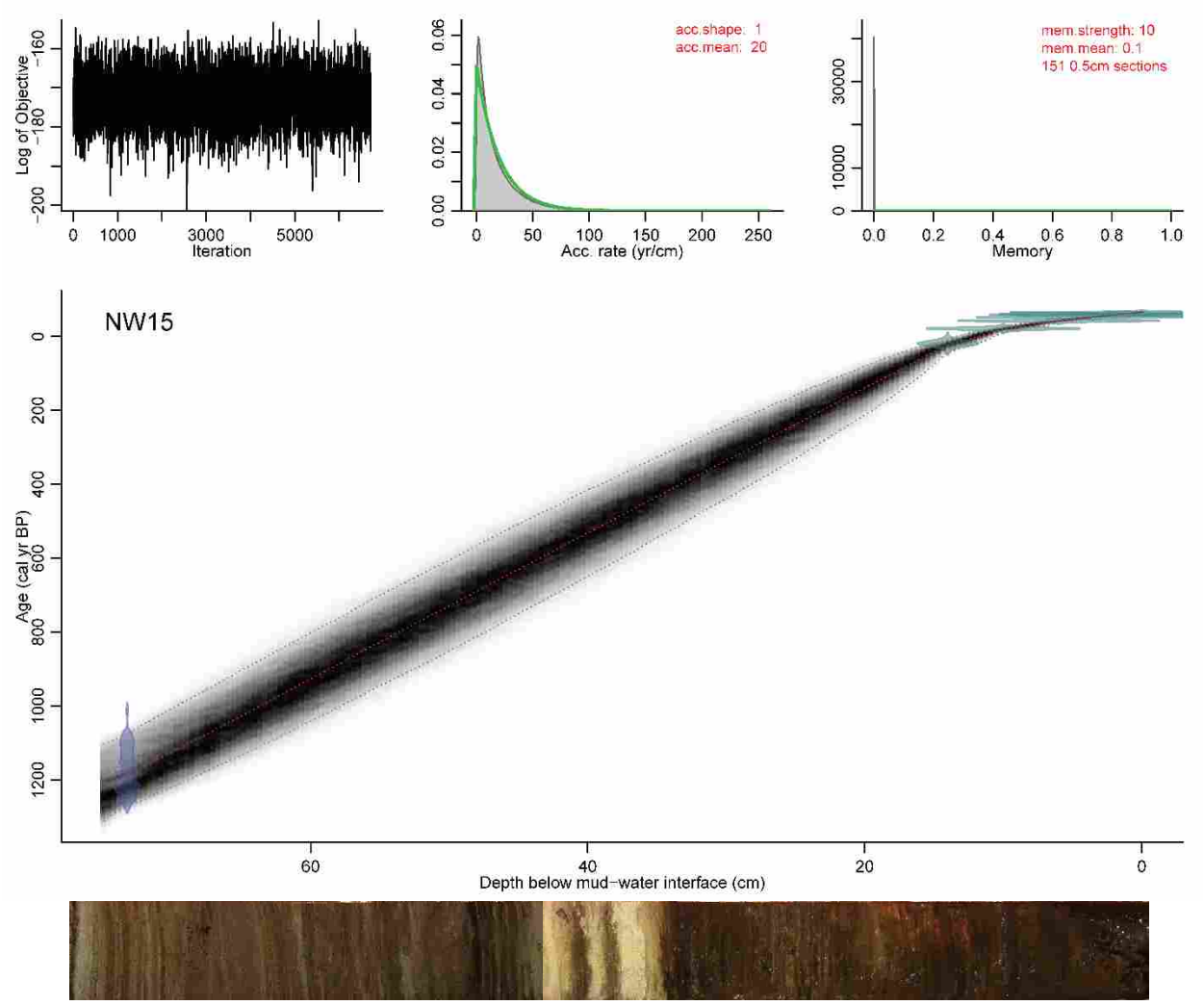


**Figure 5.** Nodwell Lake (NW15) chronology alternative, modeled without a hiaut. Data based on this chronology were not presented.

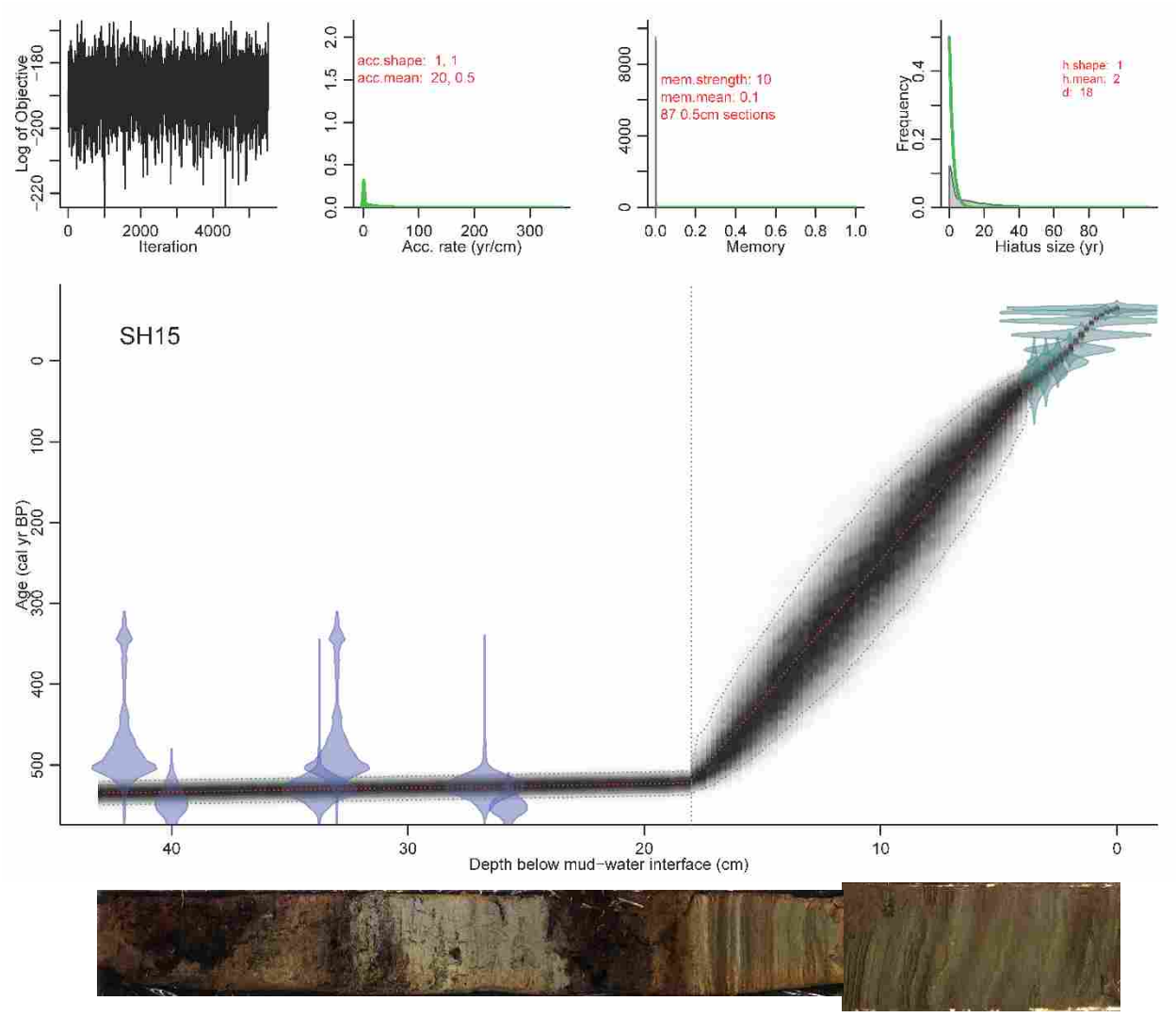


**Figure 6.** Shapiro Lake (SH15) chronology and core. Hiatus is based on distinct change from laminated to unlamented sediment at 18 cm core depth.

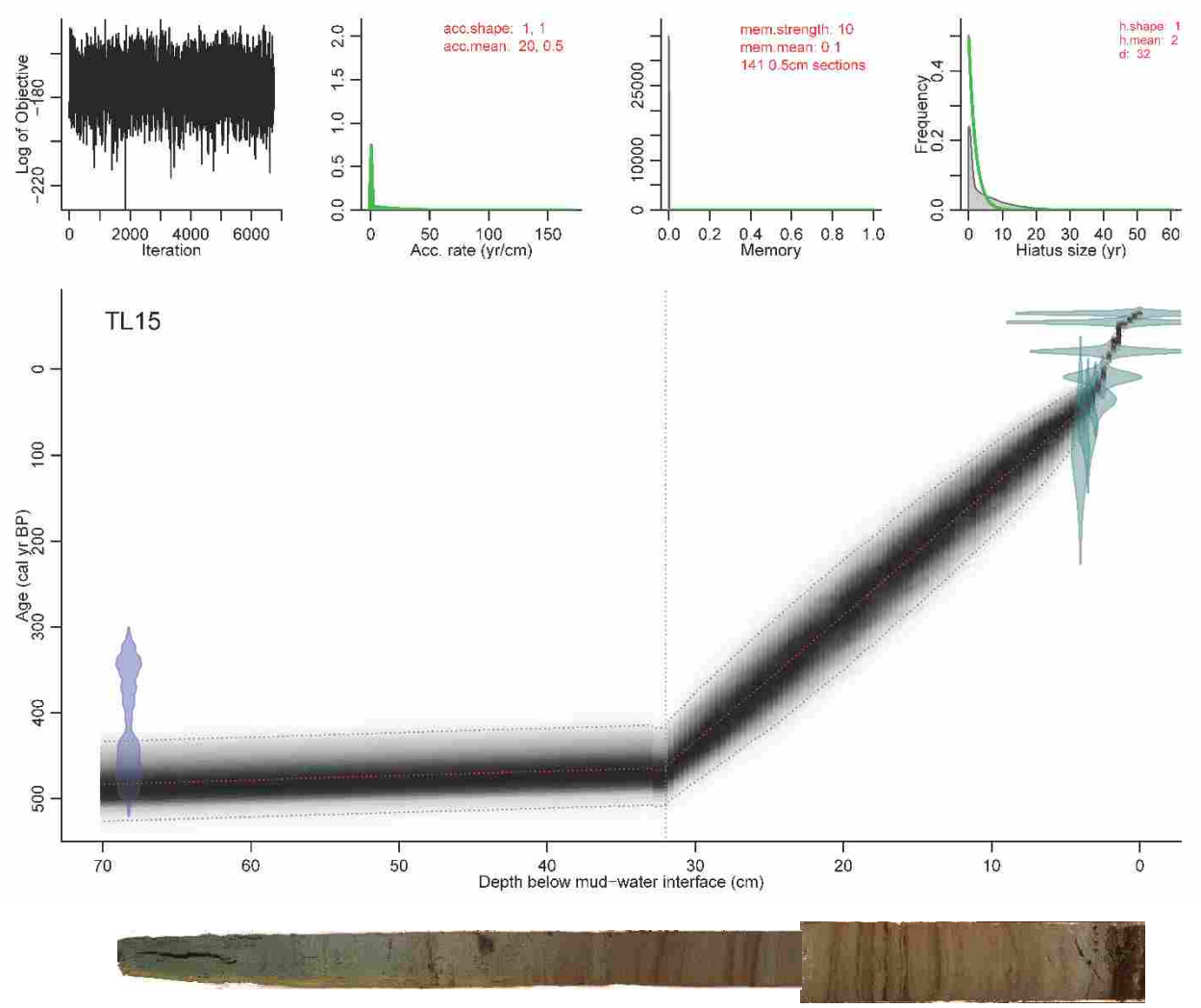


**Figure 7.** Three Lodge Lake (TL15) chronology and core. Hiatus is based on distinct change from laminated to unlamented sediment at 32 cm core depth.

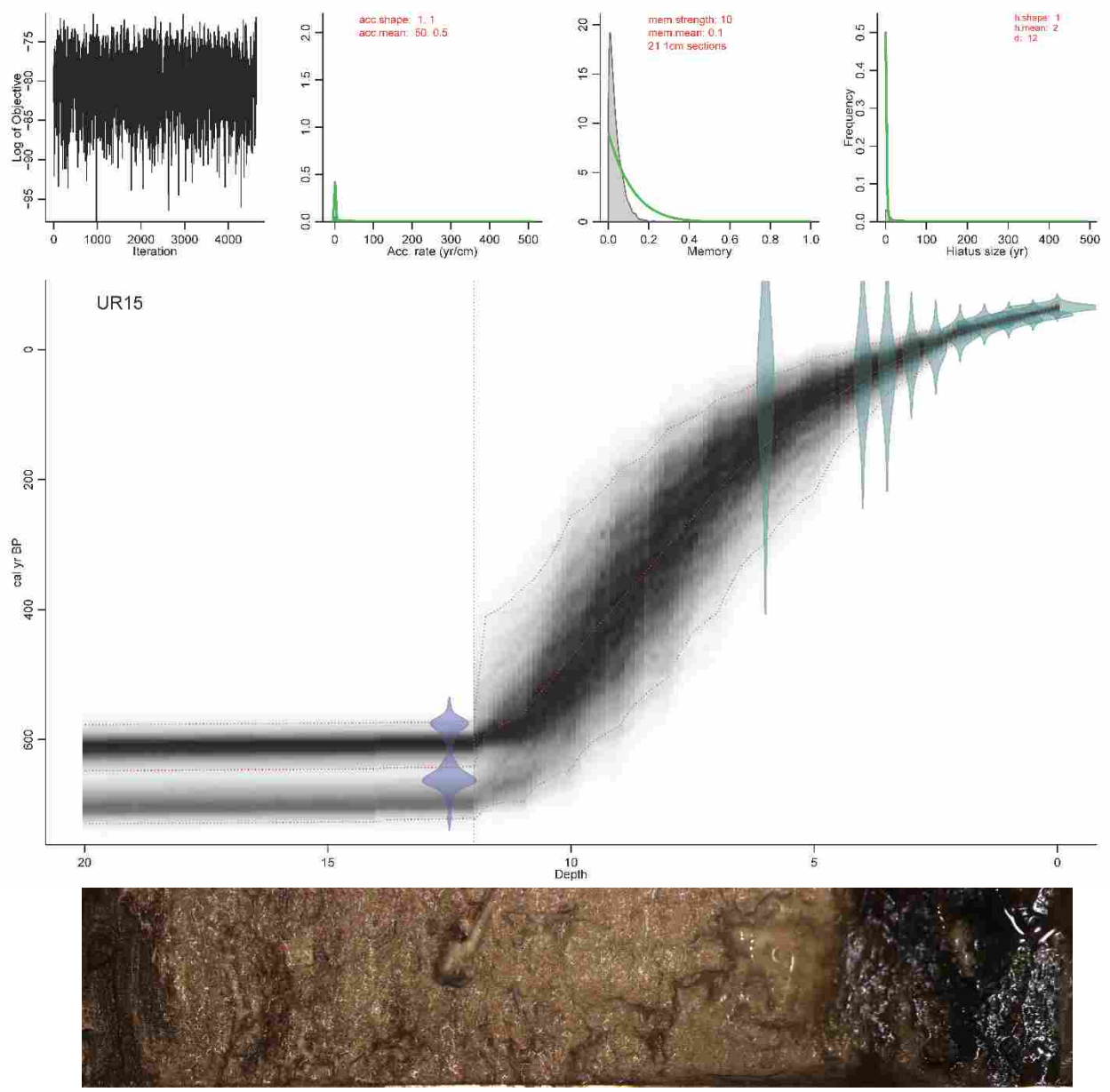


**Figure 8.** Ursa Lake (TL15) chronology and core. Hiatus is based on change in charcoal concentration at 12 cm core depth.